Novel Insights into β-Synuclein and γ-Synuclein Toxicity in a Parkinson's Disease Yeast Model

Federica Bertolotti
Lake Forest College
Lake Forest, Illinois 60045

ACKNOWLEDGEMENTS

First and foremost, I would like to give my gratitude to Dr. Shubhik DebBurman for his unwavering belief in me as a student and researcher over the past three years. Throughout this entire process of being his research student, I have learned invaluable lessons about hard work and mentorship. I learned to grow as a person and a scientist, while developing my love for neuroscience and biochemistry. Under his mentorship, I nurtured my passion for research into a determination to pursue a PhD in the field of neurobiology.

Secondly, I would like to thank my first student mentor at the D-Lab Carris Borland '21. She was a role model in lab, setting good practices and exemplary work that still guides how I approach lab and mentorship. Most importantly, I would like to recognize my initial D-Lab members and my very close friends: Amanda Grassel '23, Ryan Osselborn '23, and Tracey Nassuna '23. We started this process together and amid the challenges and difficulties we faced, we were able to find a way to make it happen and pave the path for others. They were one of the reasons I kept coming back to lab every semester and summer. My deepest gratitude goes to them both as my lab mates and family. Special thanks are due to Amanda, who would always go out of her way to make me feel comfortable and help me in any way. Until this day, I've got guidance from her on quantification of microscopy even when she has graduated and working. To Ryan, who became my biggest support not just in lab but on campus. I wouldn't be able to do my thesis without his novel work on aS, bS, and gS, and expression systems. Lastly, but not less important, my deepest gratitude to Tracey, who became one of the strongest pillars holding the lab together. All the work she did in her senior thesis set the path for what became my senior thesis. I am immensely grateful to Tracey for all her contributions to the subcloning, mutagenesis, substitution projects and her trust in me to continue her work.

Furthermore, I would like to thank all the other D-Lab members that I was lucky to mentor Sebastian Gacek '25, Leslie Casares '26, and Holly Kiernan '26. Especially Leslie for all her work on the gS swaps and Holly with V70M substitutions. They taught me how to effectively communicate and teach the science that has been instrumental throughout my development as a scientist in-training.

My appreciation also extends to my committee members, Dr. Flavia Barbosa, Dr. Erica Schultz, and Dr. Anya Golovkova for believing and supporting my research by agreeing to become part of my committee and making my journey at Lake Forest College better.

I would like to thank the Bartram Family, Nu Rho Psi, and American Society for Biochemistry and Molecular Biology for their recognition of my research potential and their generous funding. I felt honored to be awarded 1st Honorary Mention at the Undergraduate Competition at ASBMB 2024 and be selected as one of only 31 individuals across the country inducted to ASBMB Honor Society.

I also must express my deepest gratitude to my parents and my brother, whose love and care kept me going all these years. No matter how many people would tell me to aim high, I could only achieve it, because I had their support to do so. Even though they have always said they are the proudest regardless of accomplishments, their support fuels my determination to pursue my dreams and ambitions. I will never forget all the sacrifices they had to do to visit during winter break and spend countless hours with me in lab.

*This author wrote this paper as a senior thesis under the direction of Dr. Shubhik DebBurman

LIST OF ABBREVIATIONS

DNA: Deoxyribonucleic acid
RNA: Ribonucleic acid
AD: Alzheimer's disease
ALS: Amyotrophic lateral sclerosis
HD: Huntington's disease
PD: Parkinson's disease
DA: Dopamine/dopaminergic
SNc: Substantia Nigra pars compacta
SNCA: Gene coding for α-Synuclein protein
SNCB: Gene coding for b-Synuclein protein
SNCG: Gene coding for g-Synuclein protein
NAC: Non-amyloid component
aS: α-Synuclein wild-type
bS: b-Synuclein wild-type
gS: g-Synuclein wild-type
Δ: Deletion of indicated gene
A18T: Sporadic PD mutation, Alanine → Threonine at the 18th amino acid
A29S: Sporadic PD mutation, Alanine → Serine at the 29th amino acid
A53V: Familial PD mutation, Alanine → Valine at the 53rd amino acid
A30P: Familial PD mutation, Alanine → Proline at the 30th amino acid
A53E: Familial PD mutation, Alanine → Glutamic acid at the 53rd amino acid
A53T: Familial PD mutation, Alanine → Threonine at the 53rd amino acid
E46K: Familial PD mutation, Glutamic acid → Lysine at the 46th amino acid
H50Q: Familial PD mutation, Histidine → Glutamine at the 50th amino acid
G51D: Familial PD mutation, Glycine → Aspartic acid at the 51st amino acid
A18T-bS: Swap mutant in bS Alanine → Threonine at the 18th amino acid
A29S-bS: Swap mutant in bS Alanine → Serine at the 29th amino acid
A30P-bS: Swap mutant in bS Alanine → Proline at the 30th amino acid
E46K-bS: Swap mutant in bS Glutamic acid → Lysine at the 46th amino acid
G51D-bS: Swap mutant in bS Glycine → Aspartic acid at the 51st amino acid
A53T-bS: Swap mutant in bS Alanine → Threonine at the 53rd amino acid
A18T- gS: Swap mutant in gS Alanine → Threonine at the 18th amino acid
A29S-gS: Swap mutant in gS Alanine → Serine at the 29th amino acid
A30P- gS: Swap mutant in gS Alanine → Proline at the 30th amino acid
V70M- gS: Swap mutant in gS Valine → Methionine at 70th amino acid
V70M-αS-: Swap mutation, Valine → Methionine at 70th amino acid
P128H-αS-: Swap mutation Proline → Histidine at 128th amino acid
V70M-βS: Sporadic PD mutation Valine → Methionine at 70th amino acid
V70A-βS: Substitution mutation Valine → Alanine at 70th amino acid
V70E-βS: Substitution mutation Valine → Glutamic Acid at 70th amino acid
V70N-βS: Substitution mutation Valine → Asparagine at 70th amino acid
V70R-βS: Substitution mutation Valine → Arginine at 70th amino acid
P123H-βS: Familial PD mutation Proline → Histidine at 123rd amino acid
P123A-βS: Substitution mutation, Proline → Alanine at the 123rd amino acid
P123E-βS: Substitution mutation, Proline → Glutamic acid at the 123rd amino acid
P123N-βS: Substitution mutation, Proline → Asparagine at the 123rd amino acid
P123R-βS: Substitution mutation, Proline → Arginine at the 123rd amino acid
ROS: Reactive oxygen species
RNS: Reactive nitrogen species
NO: Nitric oxide
PTM: Post-translational modification
NDD: Neurodegenerative disease
BY4741: Parent budding yeast strain, unaltered
W303: Parent budding yeast strain, unaltered
emGFP: Emerald green fluorescent protein
GFP: Green fluorescent protein
SC-Ura: Synthetic complete supplement mixture minus uracil
LB: Luria Broth

PVDF: Polyvinyl fluoride
PGK: Phosphoglycerokinase
anti-GFP: Antibody for green fluorescent protein
anti-PGK: Antibody for phosphoglycerokinase

ABSTRACT

Synucleinopathies are diverse human neurodegenerative disorders linked to the misfolding and aggregation of proteins of the synuclein family. Unlike intense investigations with α-Synuclein, β- and γ-Synucleins remain understudied. Two β-Synuclein mutants (P123H and V70M) directly cause Dementia with Lewy Bodies (DLB), while γ-Synuclein is associated with Lou Gehrig's disease. α-Synuclein pathogenicity is regulated by familial mutations, post-translational modifications, and several cellular environments altered in synucleinopathies. Here, I use a budding yeast (*Saccharomyces cerevisiae*) model to examine the hypothesis that β- and γ-Synucleins are differentially toxic and regulated by similar factors. I report that 1) High expression is key to β-Synuclein toxicity and aggregation; 2) Basic charge drives P123H-βS toxicity, while hydrophobicity underlies V70M-βS toxicity, and both mutants preserve α-Synuclein's toxicity; 3) Amino acids A29, A30, G51, and A53 in β-Synuclein regulate its toxicity/aggregation, as does nitrative stress, reduced glycation, and increased acetylation; 4) γ-Synuclein is surprisingly non-toxic and cytoplasmically diffuse, and resistant to modifications, except when under nitrative stress.

INTRODUCTION

Molecular Logic of Life's Diversity

All living organisms, from the simplest single cell prokaryote to the most intricate eukaryotes, share the common instruction material vital for cellular functionality. This cornerstone of cellular processes is our genetic material known as DNA. DNA, or deoxyribonucleic acid, serves as the blueprint for proteins contributing to all diversity in life by storing information in a linear code made of four deoxyribonucleotides: Adenine, Thymine, Cytosine, and Guanine (Figure 1A). These nucleobases interact with each other giving DNA its specific structure of antiparallel double-helix. The central dogma delineates the flow of genetic information from DNA to RNA to the expression of traits through proteins (Ostrander, 2023). Additionally, the shape of the protein is what confers function (Figure 1B). As in the case of the proteasome, whose function is to break down and get rid of unwanted proteins, it has similar shape to what we know as a recycling bin (Figure 1B). To unravel the most fundamental organizational principles governing cells, we must conduct a thorough examination at the biochemical level, emphasizing the diverse array of mechanisms, structure, and chemical processes.

For this reason, our inquiry starts with DNA, which undergoes transcription within the nucleus, orchestrated by a multitude of enzymes, such as RNA polymerase III to give a complementary sequence of RNA. Subsequently, RNA leaves the nucleus and gets spliced to yield a mature messenger RNA (mRNA), ready to be translated into proteins at the ribosomes. The ribosomes employ another specialized type of RNA, transfer RNA (tRNA) to selectively bind to codons - three nucleotides coding sequence in the mRNA - to assemble a polypeptide chain comprised of amino acids (Ostrander, 2023). This entire process is interconnected, spanning from the genes that provide with the instructions for the linear sequence of amino acids, to the complex folding and acquisitions of a unique third-dimensional structure in functional proteins that allow for catalytic amino acids to react, see Figure 1 for a depiction of the central dogma.

DNA is susceptible to change

The central dogma controls the flow from our genes in the DNA, which provides instructions for the linear sequence of amino acids, to the folding and unique third-dimensional structure of proteins. The ability of proper and accurate folding determines the functionality of the protein (Figure 2A). Many situations can distort the shape of the protein, as in the case of mutations. As described before, DNA is the blueprint to build proteins, however, DNA is susceptible to change, and these changes are called mutations (Figure 2A). Despite their negative connotations, mutations are not necessarily bad at times. Changes can vary from a single nucleotide insertion to a complete addition of a gene, such as in the case of an opsin gene, which helps primate have an extended and expanded range of color vision (Neitz and Neitz, 2011). This example demonstrates how mutations can be beneficial for the organism. Further studies showed that mutations are also linked to evolution, driving survival and reproduction. For example, antibiotic resistance in bacteria results from the acquisition of multiple copies and changes in protective genes that confer an antibiotic resistance phenotype to bacteria (Martinez and Baquero, 2000).

On the other hand, mutations can also be neutral and detrimental. Heterochromia is a genetically acquired condition characterized by differences in the iris coloration. Mutations in the DNA during cell division result in this condition; however, heterochromia is considered rather harmless, and the eye color causes no differences in the visual system (Stokkermans and Lui, 2023). In contrast, some genetic alterations, like the one in Huntington's Disease (HD), can lead to harmful disorders. In HD, a mutation occurs in the gene coding for the protein Huntingtin,

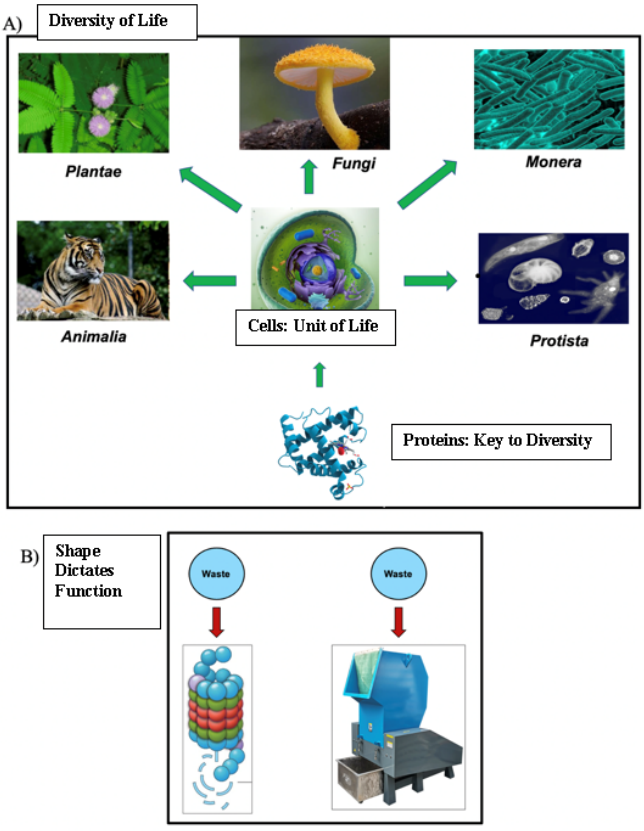

Figure 1. Proteins are the key to life's diversity. A. All five kingdoms show extraordinary diversity on Earth. All these organisms are composed of cells, and within them, they have proteins. Proteins confer the great diversity on the planet. B. Shapes of proteins dictate function. For a protein to be in its healthy state it takes on a three-dimensional structure by folding. This shape is important for function and identify of the protein.

increasing the number of CAG repeats from its normal range of 27 to 35, to 36 or more repeats, consequently synthesizing an abnormally long protein and leading to neuronal degeneration (Jiang *et al.*, 2023). All these conditions highlight and emphasize the extensive variability caused by genetic mutations, and why I find the study of the cause of these genetic mutations' imperative.

Tracing Origins of Disease: Loss of Original Amino Acid

Interestingly, sometimes it only takes a seemingly subtle change,

the loss of the original amino acid in a gene mutation, to trigger a chain of significant and detrimental consequences like protein toxicity. This change is evident in the case of sickle cell anemia (Figure 2B). The loss of glutamic acid in position 6 of the beta-globin chain, replaced by valine, causes this disease, by making the sickle cell hemoglobin (hemoglobin S) have an extra hydrophobic residue (valine) on the surface of the protein (Nelson & Cox, 2017). This leads to deoxygenated hemoglobin S to become insoluble and polymerize into aggregation, producing the elongated, rigid shape, and consequently, a changed of function of the (Steinberg, 1998). When examining the molecular structure of each of these amino acids, we observe that glutamic acid – which is negatively charged - is a polar residue with the capability to participate in hydrogen bonding. In contrast, valine is a nonpolar amino acid containing only carbon and hydrogen. The switch from being acidic to being hydrophobic, aiding and causing aggregation, produces the detrimental changes observed in the loss of structure underlying the disease (Nelson & Cox, 2017).

Tracing Origins of Disease: Gain of New Amino Acid

Another explanation for protein toxicity is the result of gaining a particular amino acid through a gene mutation (Figure 2C). This is the case with the autosomal dominant condition

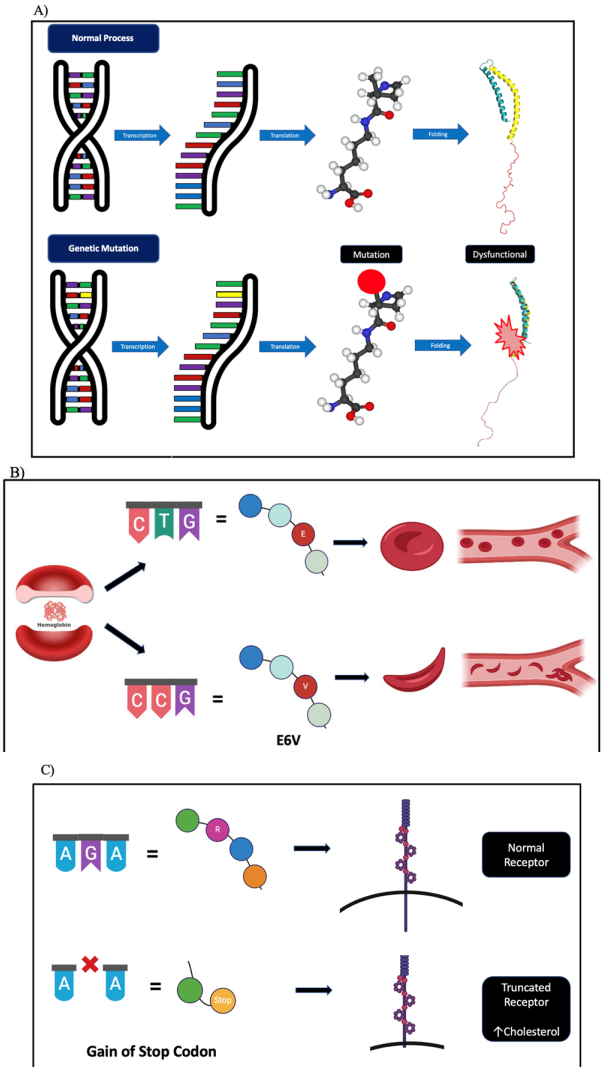

Figure 2. Mutations in amino acid sequences. A) Central Dogma of Biology. B) Loss of original amino acid led to sickle cells changing the structure of red blood cells, and thus, producing hemoglobin to form inflexible chains. C) When gain of new amino acid due to deletion mutation can lead to premature stop codon, truncating the protein, and thus rendering the LDLR receptor unfunctional. Their DNA sequence will have 5′ to 3′ ends for each.

Familial Hypercholesterolemia (FH). Its pathology comprises a high concentration of low-density lipoprotein cholesterol (LDL-C) in the bloodstream and the inability to remove it from the blood.

The reason for the change is a mutation in the LDL receptor gene, which is responsible for metabolizing the "bad" cholesterol in the bloodstream (Callis *et al.*, 1998). Researchers discovered a novel G deletion at codon 185 on chromosome 19 of the LDL receptor gene. This deletion leads to a gain of a premature stop codon, resulting in a truncated receptor that impairs the regulation of cholesterol. The accumulation of unwanted cholesterol is strongly linked to the buildup of fatty acid deposits in the blood vessels, and associated with cardiovascular diseases (Callis *et al.*, 1998). This thesis delves into studying further changes due to the absence or presence of a single amino acid. Understanding the intricate interplay between mutations and protein dysfunction is key to shedding light on the molecular mechanisms of toxicity (Figure 2A).

Neurodegenerative Disease

Neurodegenerative diseases (NDDs) are the group of disorders characterized by the misfolding and aggregation of proteins in the nervous system (Wilson *et al.*, 2023). As the name indicates, the progressive neuronal death overtime causes the pathological aggregation of proteins. These are two out of eight hallmarks of NDDs, which also include: inflammation, synaptic and neuronal network dysfunction, altered energy homeostasis, DNA and RNA defects, cytoskeletal abnormalities, and aberrant proteostasis (Wilson *et al.*, 2023). Even though all NDDs share the same hallmarks, the symptoms are linked to which protein is aggregated and the region in which is located. For example, AD, the most prevalent neurodegenerative disease, pathology is amyloid plaques of aggregate β-amyloid and neurofibrillary tangles of tau protein found in the cholinergic neurons in the hippocampus and amygdala, among other limbic areas (Selkoe & Lansbury, 1999; Wilson *et al.*, 2023). In AD symptoms, a deterioration to these structures exists, which are the areas controlling and regulating social cognition, long-term, spatial, and emotional memory (Rajmohan, & Mohandas, 2007). HD arises from the expansion of the *HTT* gene, resulting in a gain of function for the huntingtin protein (Jiang *et al.*, 2023). These CAG repeats induce the accumulation of *HTT* protein and subsequent degeneration of the putamen and caudate nucleus. These structures play pivotal roles in processes such as decision-making, reward processing, and motor control, all of which manifest behavioral impairments in individuals afflicted with HD (Jiang *et al.*, 2023). *This thesis will focus on a specific subset of NDDs, referred to as Synucleinopathies, characterized by the shared pathology of a-Synuclein (aS) protein aggregation.*

Synucleinopathies

The Synucleinopathies constitute a subset of NDDs distinguished by the presence of aggregated αS in neuronal and/or glial inclusions (Koga *et al.*, 2021). They are categorized into two primary disease entities: MSA and Lewy body disease, which encompass DLB and PD (Koga *et al.*, 2021; Figure 3). All these diseases demonstrate the presence of Lewy Bodies (LBs), which are round inclusions mostly composed of aggregated αS, as well as some damaged mitochondria, lysosomes, and vesicles (Koga *et al.*, 2021). They are found in neuronal and glial cell bodies and neurites, such as the dendrites and axons. MSA, is a rare, but fatal sporadic NDD that primarily affects oligodendrocytes, which oversee producing myelin in the brain and spinal cord (Flabeau *et al.*, 2010). The two subtypes of MSA are Parkinsonian type (MSA-P) with striatonigral degeneration pathology and Cerebellar type (MSA-C) characterized by olivopontocerebellar (olivary nuclei, cerebellar peduncles, and cerebellum) atrophy (Jellinger & Wenning, 2005). These classifications separate according to their symptomatology, having MSA-P manifest Parkinsonism with rigidity, bradykinesia, and abnormalities in the autonomic nervous system, whereas MSA-C displays more ataxic symptoms, marked by challenges in coordination and balance (Flabeau *et al.*, 2010). Furthermore, cerebral dysfunction is also observed more in MSA-C rather than in MSA-P. Differentiation between MSA-C and MSA-P is not always clear, they have overlapping. This is attributed to the shared core pathology, namely the progressive loss of oligodendrocytes causing a decrease of neuronal myelination, thereby degrading myelin sheath, and affecting neuronal functioning (Flabeau *et al.*, 2010).

Another synucleinopathy is DLB, also a progressive NDD affecting emotional and thinking patterns to behavioral and movement coordination. Similarly, to MSA, DLB has Lewy bodies, but also shows evidence for Lewy neurites (LNs), which are the misfolded and aggregated αS forming abnormal filamentous inclusions in dendrites and axons. DLB shows similar pathology to AD, having in some cases β-amyloid plaques, and having a 29-89% of cases being able to be diagnosed for both DLB and AD (Koga *et al.,* 2021). DLB consists of cognitive symptoms, such as visual hallucinations, alertness, and loss of logical and organized thinking, movement symptoms (bradykinesia), and psychological symptoms like depression, anxiety, and restlessness (National Institute on Aging, 2021). Moreover, DLB Lewy bodies are in different areas of the brain having a higher density in the substantia nigra, followed by the entorhinal cortex, then the cingulate gyrus, insula, frontal cortex, hippocampus, and occipital cortex, respectively (Gómez-Tortosa *et al.*, 1999). DLB clinical diagnosis is further challenged by the similarities and associations to PD.

PD, the second most prevalent NDD after AD, affecting more than 10 million people worldwide (Parkinson's Foundation, n.d.). As a global source of disability, the fast increase in mortality rate and prevalence led researchers declare a Parkinson Pandemic (non-infectious) based on the doubling of cases in the last decades, with expected cases increasing over 12 million by

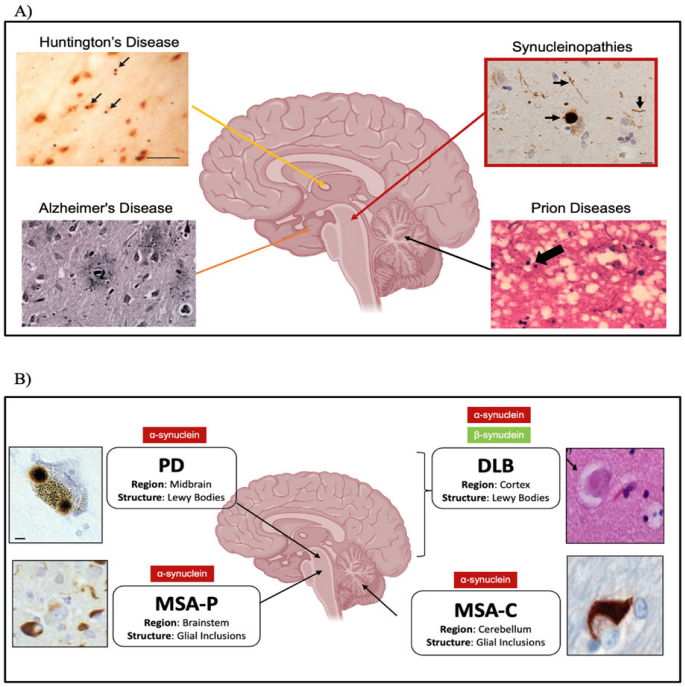

Figure 3. Neurodegenerative Disease. A) Neurodegenerative diseases are characterized by the misfolding and aggregation of specific proteins within the brain. Some of the most known and studied ones are AD, HD, PD, and prion disease. The former one is characterized by the progressive cell death of memory cells, whereas the latter three are characterized by the neuronal death of movements cells. The cells that get affected are linked with the types of symptoms, and thus, why in AD is linked to memory loss. For the other three movement regulation problems. B) Synucleinopathies are NDD that their pathology consists of misfolding of the synucleins, specifically of aS in all of them. βS mutants in DLB. Depending on where the misfolding and aggregation is found, it leads to the diagnosis of the different synucleinopathies.

2040 (Dorsey *et al.*, 2018). It has a variable age of onset, but like most NDDs, typically present symptoms in mid-to-late adulthood, with no known cure. In terms of treatments, the emphasis lies in enhancing quality of life by mitigating motor and non-motor symptoms. The former, often attributed to PD due to its relatively more apparent and faster manifestation, encompasses the following cardinal symptoms: Rigidity, bradykinesia (slowness of movement), postural instability, and resting tremors (Dickson, 2012). The latter, non-motor symptoms, are equally significant and encompass factors such as depression, visual and auditory hallucinations, impaired communication, and sleep disturbances, among others (Dickson, 2012).

While PD presents a diverse range of symptoms, the condition initiates its development much earlier, often in an asymptomatic state. The absence of discernible symptoms prior to onset adds an additional layer of complexity to the challenging diagnostic process for PD. Most patients' symptoms express later in the disease, doctors find a significant decline in striatal dopamine (DA) and substantia nigra pars compacta (SNc) neurons in patients with 70%-80% and almost a third of each of these, respectively, already lost by the time symptoms appear (Wu *et al.*, 2011). Even until today, PD is not studied clinically using a neuropathological method, the closest invention is the Dopamine Transporter Imaging (DaTscan). The DaTscan, a 2011 FDA-approved imaging technique uses a radioactive isotope (Ioflupane-123) injected to the patient veins, that circulates through the bloodstream until uptake by dopamine transporters – the radiotracer is designed to bind specifically to these in the brain. Using a single-photon emission computed tomography scanner (SPECT scanner) a doctor is capable to visualize dopamine transporters in the brain and assess the condition of the dopamine system in the nigrostriatal pathway. PD patients show evidence for an abnormal image as a result of the loss of dopamine-producing neurons (Catafau & Tolosa, 2004). Overall, this technique is accompanied by the patients' medical and symptom-history records by trying to aid in better clinical diagnosis.

PD Causes: Familiar and Sporadic Types

Looking more in depth to PD, the neuropathology is characterized by the misfolding and aggregation of αS forming LBs in the dopaminergic neurons of the SNc in the midbrain, leading to neuronal death. Therefore, producing a reduction in dopamine in the dopaminergic projections from the SNc to the striatum (structure in the basal ganglia), all referred as the nigrostriatal pathway (Sonne *et al.,* 2023). PD can be both monogenic and environmentally determined, contributing to familiar and sporadic PD types (Figure 4A). Starting with sporadic, even though less understood sporadic PD consists of 80-90% of cases. Sporadic PD is more aggressive and has a later onset as compared to familiar PD (Inzelberg *et al.,* 2004). Furthermore, Sporadic PD is the consequence of environmental stressors such as high levels of air pollutants like nitrogen dioxide – from combustion of fossil fuels - as a risk in PD development (Jo *et al.*, 2021; Ritz *et al.*, 2012), exposure to places with large use of pesticides, multiple studies have recorded a few that increase the risks including paraquat, dieldrin, and rotenone (Breckenridge *et al.*, 2016; Pouchieu *et al.*, 2018; Tangamornsuksan *et al.,* 2019), even mining workers are considered at possible risk due to exposure to manganese, a heavy metals (Gorell *et al.,* 1997; Racette *et al.*, 2017). Environmental stressors do not operate in isolation either. Studies using genome-wide association assays in PD researchers found that αS-encoding gene locus, *SNCA*, polymorphisms contribute to Sporadic PD (Nalls *et al.*, 2014), as well as random mutations (Kasten & Klein, 2013; Figure 4C).

Familiar PD was established with the discovery of an inherited cause for PD, supported by an autosomal dominant mutation in the *SNCA* gene coding for αS in three independent Greek families and an Italian family (Polymeropoulos *et al.*, 1997; Figure 4B). Multiple other genes now linked with PD, such as *LRRK2*, also autosomal dominant, *PARK2, PINK1*, and *DJ-1* are autosomal recessive mutations (Konovalova *et al.,* 2015). Lastly, the *GBA* gene is linked to PD, but it does not follow the conventional Mendelian inheritance, for this the mutation ought to cause a loss-of-function, usually in the case of autosomal-recessive (two alleles needed carrying mutation), and a gain-of function for autosomal dominant (one allele needed carrying mutation). However, *GBA* produces a gain and a loss-of-function in parkinsonism (Sidransky & Lopez, 2012).

Synucleinopathies: A Family Tale

The current literature provides substantial compilation of information pertaining to αS and its role in synucleinopathies; however, αS forms part of a larger synuclein family. This family is composed of αS, β-Synuclein (βS), and g-Synuclein (γS). All of these proteins are homologs with

a considerably similar flexible structure with high levels of evolutionary conservation in the nervous system, and they are only found in vertebrates (Surguchev & Surguchov, 2017). αS is the longest out of the three, consisting of 140 amino acids, followed by βS with 134 amino acids, and γS having 127 amino acids; the proteins get made by 5 coding exons that are similar in all three. Their evolutionary conserved sequence indicates a significant role of these proteins that in the case of αS and βS share 61% similarities, and with γS 55.9% similarities (Lavedan, 1998); this homology increases if the focus is the amino terminal which has 76% similarities between αS and βS, and 67% with αS and γS (Burré *et al*., 2018; Jakes *et al*., 1994). Refer to Figure 4 for a comparison between αS, βS, and γS amino acid sequence alignment.

a-Synuclein Protein

αS encoded by the *SNCA* gene, is a small, flexible, yet abundant presynaptic protein within the nervous system (Figure 4B). αS is present in the central and peripheral nervous system involved in neuronal function, with high concentrations found in the substantia nigra, thalamus, hippocampus, neocortex, and cerebellum (Emamzadeh, 2016). The N-terminus (amino acid 1 to 60) has membrane-binding capabilities because of its amphipathic properties. The KTKEGV motifs are seven repeats of 11 residues that encompass a combination of acidic, basic, polar, and nonpolar amino acids (Dettmer *et al*., 2015). Notably, this motif is unique to the synuclein family, despite being highly conserved across all three synucleins. Although many studies using techniques like NMR spectroscopy, X-ray fiber diffraction, and EM reconstruction identified the protein's native state, most biochemical assays indicate a combination of α-helical structures formation (Eliezer *et al*., 2001; Ulmer *et al*., 2005; Wang *et al*., 2011), disorder after dissociation from the cell membrane (Fauvet *et al*., 2012), and various combinations of both (Burré *et al*., 2013).

Conversely, the NAC domain (amino acids 61-95) exhibits higher hydrophobicity compared to the other two domains, and it also encompasses the previously described unique motif (Burré *et al*., 2018; Figure 5A). This region facilitates aggregation by promoting protein polymerization (Burré *et al*., 2018). Lastly, the negatively charged carboxy-terminus (C-terminus), spanning from amino acid 96 to the last 140, has many polar residues. The C-terminus contains the least conserved sequences among the synucleins, and its function is not as well understood as the others. Nevertheless, within this domain, αS undergoes various post-translational modifications, including phosphorylation (Fujiwara *et al*., 2002), glycation (Padmaraju *et al*., 2011), ubiquitination (Nonaka *et al*., 2005), acetylation (Maltsev *et al*., 2012; Dikiy & Eliezer, 2014), nitration (Giasson *et al*., 2000), among others. Some of these modifications serve a protective role against toxicity, as in the case of the first three, while others induce structural changes and altered functionality. In the case of nitration, some of the toxicity observed in αS is attributed to the change of properties due to the addition of the nitro group. This chemical group gets added to the tyrosine residues in αS (Y39, Y125, Y133, Y136, and others) and the change causes a shift on the residues' pKa from their normal 10 to 7.50 (Corpas *et al*., 2009; Sano *et al*., 2021). Additionally, the nitro group presents steric hindrance, affecting the charge distribution, and the bonding with other residues, since tyrosine is a fundamental amino acid for aromatic stacking and hydrogen bonding necessary for protein folding (Sano *et al*., 2021). These alterations to the protein structure can influence the propensity of αS to polymerize and aggregate, and thus, why higher nitration is categorized as an enhance or αS toxicity.

The role of αS is still being elucidated, with a common consensus that αS is involved in vesicle budding with presynaptic membrane, aiding in neurotransmitter release, and thus, in synaptic trafficking (Chandra *et al*., 2003; Varkey *et al*., 2010; Sharma & Burré, 2023). αS is repeatedly linked with NDDs because of its NAC domain tendency to adopt a β-sheet conformation, promoting misfolded αS to form fibrils and aggregate (Tuttle *et al*., 2016). These fibrils are insoluble, and the ones found primarily in LBs. Moreover, through the aggregation process of this protein, αS changes from monomeric unit to form small oligomers that then become and grow into fibrils (Goldberg & Lansbury, 2000; Cookson, 2009).

a-Synuclein Mutations

The synucleinopathies pathology of αS fibrils in LBs needs to be biochemically described by the molecular interaction of the protein. The structure of αS fibrils is established due to the salt-bridges, H-bonding, and steric zippers that form and can be elicited by mutations in the *SNCA* gene. Six old known familiar mutations are highly implicated in aggressive early onset PD. All of these are in the amphipathic N-terminus suggesting the importance of membrane-binding from this domain on αS toxicity.

These six mutants associated with familiar PD are: A30P, E46K, Q50H, G51D, A53E, and A53T (Figure 4C). As well as three newer mutants that are linked with novel familiar PD – A53V – and sporadic PD – A18T and A29S. In the lab, we focus on all these mutants compared them to wildtype (WT) forms of the synucleins and analyze their recipe for toxicity.

Older mutants

A53T

The first mutation in αS' sequence to be discovered was A53T. Researchers identified it in 1997 in a Greek family and using GWAS, in other three Greek unrelated families, Sicilian kindred, in a Swedish, and Korean family (Whittaker *et al*., 2017). This mutation involves the change from the nonpolar (hydrophobic) amino acid alanine in position 53 to the uncharged polar, larger amino acid threonine. This mutation is an autosomal dominant mutation that gives early onset PD, with an average age of 48 years old (Whittaker *et al*., 2017). When the mutation A53T is present in αS in transgenic mice, the protein binds to the membrane similarly to αS (Sharon *et al*., 2001) and in budding and fission yeast (Brandis *et al*., 2006; Sharma *et al*., 2006).

A30P

The second mutation discovered is A30P in a German family during 1998 (Whittaker *et al*., 2017). The mutation involves a change from nonpolar (hydrophobic) amino acid alanine in position 30th to another nonpolar (less hydrophobic) cyclic amino acid proline. In contrast with A53T, A30P αS's toxicity is not explained by aggregation. A30P in αS makes the protein not bind to the membrane when present, it stays diffuse in the cytosol (Jensen *et al*., 1998).

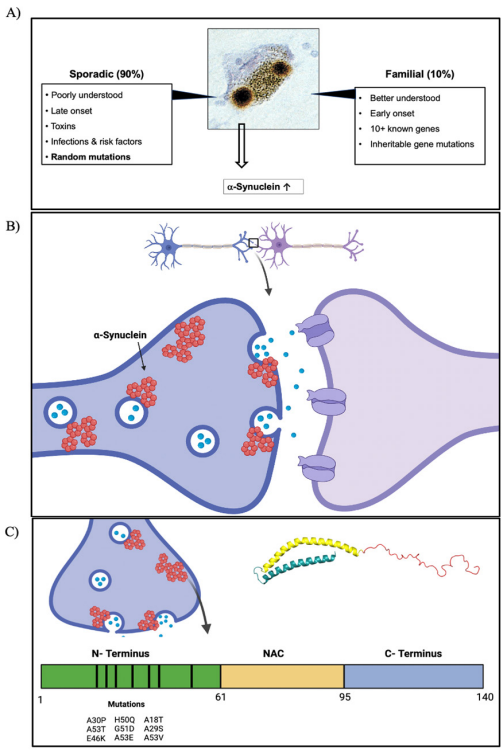

Figure 4. Molecular Biology of PD. A) PD is categorized into two types, one is sporadic (90% of cases) and the other is familiar (10% of cases). B) aS pathology. aS is a synaptic protein that is commonly found helping in vesicle trafficking, regulation, and SNARE complex fusion with membrane. C) aS protein has three domains, N-terminus (amphipathic domain linked with lipid and membrane binding properties), NAC region (hydrophobic domain linked with aggregation), and C-terminus (Acidic domain regulating solubility). The nine known mutations from early-onset PD patients occur in the N-terminus. These are A18T, A29S, A30P, E46K, Q50H, G51D, A53T/E/V.

Moreover, studies of A30P mutation using fluorescence resonance energy transfer showed an induced conformational change of αS preventing it from forming its secondary α-helix structure (McLean *et al,* 2000; Jo *et al*., 2002). This alteration shows the dominance of the proline, which has a cyclic structure impairing the correct folding and membrane-binding ability, rendering the protein more prone to misfolding which is a hallmark of PD. The two different mutations A30P and A53T both contribute to early onset PD but through different unique mechanisms.

E46K

The next mutation to be discovered was E46K, changing the negatively charged (acidic) glutamic acid to a positively charged (basic) lysine at the 46th position. This mutation was found in a Basque Country family in 2004 with severe neuronal loss in the substantia nigra, locus coeruleus, and dorsal nuclei of the vagus (Whittaker *et al.,* 2017). The mutation's position is in the KTKEGV motifs mentioned before. *In vitro* studies have revealed that with this mutation, αS forms and polymerizes into insoluble fibrils quicker than αS, and these fibrils are like amyloid fibrils similar to the ones that form in presence of the A53T mutation (Greenbaum *et al*., 2005; Fredenburg *et al.,* 2007). Furthermore, αS shows high affinity for liposomes and phospholipid binding (Choi *et al*, 2004), this property combined with the high propensity to polymerize are the cause of toxicity for the E46K mutation.

H50Q, G51D, A53E

The less characterized familial mutants of αS are H50Q, G51D, and A53E. These were discovered in an English and a Canadian patient (Appel-Cresswe *et al.,* 2013), a French patient (Lesage *et al*, 2013), and a Finish patient (Pasanen *et al*., 2014), respectively. The H50Q involves a change in the basic amino acid histidine for the polar amino acid glutamine in the 50th site. H50Q- αS has faster aggregation than αS due to having two forms of protofilaments as compared only one (Boyer *et al.,* 2019). H50Q-αS has faster fibril formation activity as compared to all other mutations, promoting, and accelerating αS aggregation (Guan, *et al*., 2020).

G51D involves the change from the nonpolar Glycine amino acid in position 51st to the negatively charged (acidic) amino acid aspartic acid. And A53E involves the change from nonpolar (hydrophobic) alanine to acidic glutamic acid in position 53rd. G51D with A53E and A53T give rise to the earliest age of onset of PD, but contrary to A53T, G51D and A53E are similar to A30P in which they reduce αS aggregation and binding to the membrane (Goedert *et al.,* 2017). Literature shows these mutants such as G51D are present with non-toxic traits, however, contribute to the misfolding and aggregation of αS (Fares *et al.,* 2014). One explanation is other modifications such as post-translational/covalent modifications in specific sites or altered cellular environments (Fares *et al*., 2014).

Newer mutants

A18T, A29S, and A53V

These two sporadic mutations were each identified in a Polish family and linked have different onsets, with A18T showing an earlier onset of symptoms than A29S (Hoffman- Zacharska *et al.,* 2013). And A53T was identified in a Japanese patient with late onset PD in an autosomal dominant inheritance (Yoshino *et al.,* 2017). These genetic mutations are fairly new, and thus, heavily understudied. Our lab started assessing if these genetic mutations are toxic in yeast which led to two senior theses in the last three years by Carris Borland '21 and Amanda Grassel '23, who I helped collecting data for. They showed the three newer mutants are less toxic than αS in yeast, however, many factors and modifications regulate their toxicity. Grassel reported that to unlock the newer mutants' toxicity, they needed different recipes. She saw that A18T and A53V were particularly sensitive and more toxic with high levels of nitrative stress, whereas A29S was more sensitive in environments where specific PD genes were knocked out, and sensitive to altered SUMOylation levels (Grassel, Thesis, 2023). Even though these genetic mutations need further work, Borland and Grassel started assessing and characterizing them in yeast.

β-Synuclein Protein in NDDs

The second member of the synuclein family is βS consisting of 134 amino acids and coded for by the *SNCB* gene. Like αS, βS has an N-terminus expanding from amino acid M1 to K60, an NAC domain (E61-V95), and a C-terminus (K96-A134). Its sequence is high in number of the nonpolar amino acid alanine making 13.4% of the sequence, and the acidic glutamic acid forming 18.7% of its sequence; and contains no cysteine nor tryptophan residues (Hayashi & Carver, 2022a). The body expresses βS in the central nervous system, specifically in astrocytes, myelin, olfactory epithelium, skeletal muscle, and basal forebrain (Hayashi & Carver, 2022a). Unlike αS, βS is slightly dispersed in the substantia nigra and striatum (Li *et al*., 2002). The biggest difference in sequence between βS and αS is the deletion in the NAC region of amino acids 53-63, which is the domain related to aggregation (Figure 5B). This deletion of a piece of the NAC region led to researchers believe βS to be unable to form the fibrils seen in LBs in a variety of physiological conditions (Uversky *et al.,* 2002; Leitao *et al*., 2018; Van de Vondel *et al*., 2018). Researchers believed βS to be nontoxic and protective against αS toxicity. However, multiple recent studies report that βS protective role is not entirely true. βS shows a high degree of intrinsically disordered structure, capable of changing and adapting conformation to the necessary function. Using a vibrational spectroscopic technique called Raman optical activity (ROA), researchers were able to show that βS undergoes a conformation change to take on a polyproline type-II (PP-II) helical conformation, and that this conformation can serve as a template for amyloid fibrils (Syme *et al.,* 2002).

Since βS has a disordered structure, it has many distinct functions within the cells. For example, βS is implicated in lipid binding, similar to αS. Since βS has five conserved repeats of the KTKEGV motif, such as those in class apolipoproteins A2, suggesting lipoprotein lipase activity regulation (Sharon *et al*., 2001; Westphal & Chandra, 2013). Despite its disordered structure, βS can do this function by changing and rearranging its conformation when in contact with lipoproteins to adopt an α-helical shape (Brown *et al.,* 2016). Furthermore, based on its ability to bind to lipids with high affinity, βS regulates synaptic functioning and is in charge of neurotransmitter release, specifically of the Nigrostriatal Dopaminergic System. βS is found to be necessary for dopamine regulation in the projecting axons from the substantia nigra to the dorsal striatum. One group of researchers discovered using mice that those that lack βS had significantly less dopamine uptake by the vesicular monoamine transporter-2 (VMAT-2; Ninkina *et al*., 2021). Another study done in transgenic mice reported a different outcome of lack of βS. They saw those mice lacking βS had symptoms of motor discoordination, decreased sensorimotor function, and strength (Synucleinopathies-like symptoms) as compared to WT, providing more evidence to support the claim that βS aids in the regulation of DA uptake (Connor-Robson *et al*., 2016).

β-Synuclein Mutations in DLB

Recent studies report two βS missense mutations in the *SNCB*, V70M and P123H, that are implicated in NDDs (Figure 5B). The former one was first reported by Ohtake *et al*. (2004) in an 83-year-old Japanese man that had DLB. This genetic mutation was found in the NAC region and produced a change from the hydrophilic amino acid valine in position 70th to another less hydrophobic amino acid methionine. Researchers believe this change involves a substitution of an amino acid with a residual branch to a linear sulfur-containing amino acid. The presence of sulfur and the methyl group allows formation of a thioether functional group which can contribute to conformational changes and low solubility. This change in

amino acid is believed to have created the conformational changes seen in pathological condition of βS. Researchers used transfected rat neuroblast cells with βS-V70M to analyze pathology and found aggregations and inclusions in the cytosol while using markers for lysosomal dysfunction (e.g.: Cathepsin and BLAMP-2; Wei *et al*., 2007). Recently, studies done using yeast expressing βS-V70M shows double the percentage of yeast with inclusions as compared to βS demonstrating a significant molecular effect of this mutation in pathology, specifically related to impairments in the trafficking of vesicles and lysosomal impairments (Tenreiro *et al.,* 2016).

The second genetic mutation, βS-P123H involves the substitution in position 123 of proline, a rigid cyclic amino acid, to histidine, a basic, hydrophilic amino acid. It was found in a familiar autosomal dominant case of DLB. Similarly, using transgenic mice, βS-P123H can form insoluble aggregates in cytosol *in vitro* with lysosomal dysfunction pathology (Fujita *et al*., 2010). Expression of βS-P123H also led to axonal swelling, dependent on age, and astrogliosis – reaction of astrocytes to neuronal damage - in the globus pallidus and striatum (Fujita *et al.,* 2010). Mice also presented cognitive deficits investigated by behavioral tests using the water maze and target quadrant tests for memory and learning, which were both significantly lower as compared to non-tg mice; this was followed by motor deficits after six months. Furthermore, using immunohistochemistry it was found that 14-months-old transgenic mice expressing βS-P123H had a significant decrease of biomarkers involved with mature granule cells, and a high expression of biomarkers related to immature granule cells, microglia, and neuroinflammation in the dentate gyrus of the hippocampus (Hagihara *et al.,* 2018). All of these studies provide a gain-of-function mechanism of toxicity produced by βS-P123H.

To understand the difference in toxicity potential between βS and βS-P123H biochemists looked at their conformational structure by using heteronuclear single quantum coherence profiles (HSQC) and electrospray ionization mass spectrometry (ES-IMS). HSQC analysis yielded these two proteins remarkably similar structurally, but βS-P123H shows more compact conformational ensembles than βS (Janowska & Baum, 2016); and βS-P123H has more conformation similarities to αS as compared to βS in terms of the distribution of population of conformations. αS showed to have compact conformation 49% and extended 51%, while βS-P123H showed 51% compact conformation and 49% extended, and βS with the lowest similarity of 46% being compact and 54% extended (Janowska & Baum, 2016). These differences are caused by the changes in the C-terminus of each protein. As stated, the C-terminus is the least conserved between the synuclein families, and the P123H substitution is found in this domain. Furthermore, sequence analysis shows a repetition of proline in amino acids 122 and 123 (mutation site), not found in αS (P122, S123). The loss of the second proline provides a much more flexible C-terminus, triggering self-aggregation, and the gain of P123H allows H-bonding properties similar to the interactions of αS S123 (Janowska & Baum, 2016).

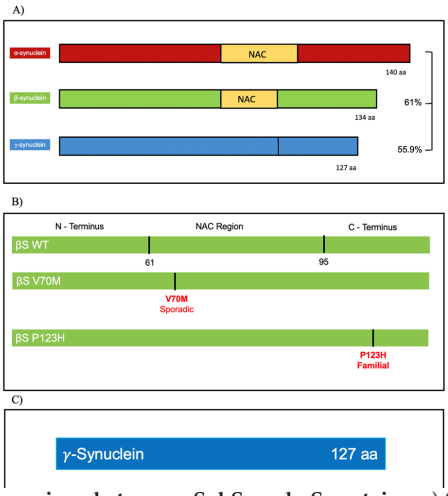

Figure 5. Comparison between aS, bS, and gS proteins. a) Sequence homology between the synuclein protein family, percentages are in relation to aS. b) βS sequence and the two known mutants. c) gS sequence, it does not contain an NAC region.

γ-*Synuclein in NDDs*

The smallest protein in the synuclein family is γS with 127 amino acids, and no NAC domain (Figure 5C). γS is expressed by the gene *SNCG*, mostly in the peripheral nervous system, in glia and in dopaminergic neurons in the substantia nigra, red nucleus, and anterior commissure (Brenz Verca *et al.,* 2003; Galvin *et al.,* 20011). γS is not highly implicated in synucleinopathies, however, novel studies with transgenic mice show γS accumulation into inclusions leads to the hallmarks of amyotrophic lateral sclerosis (ALS) patients producing cell death and motor dysfunction symptoms (Peters *et al*., 2012). ALS is a progressive fatal neurodegenerative disease characterized by motor neuron death weaking and stiffing muscles, distorting speech patterns, and more (Peters *et al*., 2012). Similarly, to αS, γS is naturally unfolded but in solution it can rapidly form and self-associate into oligomers (Golebiewska *et al.,* 2014). Moreover, γS is present in the presynaptic axons of the hippocampus of PD and DLB pa-tients but not found in healthy control group's brains (Galvin *et al.,* 1999). In DLB and in other NDDs such as AD, γS inclusions are found in the amygdala and the substantia nigra, interestingly, the aggregation of this protein is aided by the oxidation at the methionine in position 38, and colocalize with phosphorylated αS at position 129 (Surgucheva *et al*., 2014). Importantly, the oxidation of γS at M38, or

Y39 (two of the easiest residues to oxidize in γS), create oligomers that can rapidly form oligomers and contribute to aggregation, and furthermore, seed aggregation of αS (Surgucheva *et al.,* 2012). All these cases provide evidence to pursue a deeper analysis into the nature of γS and its potential for toxicity, investigating post-translation modified γS, which shows prion-like properties of seeding aggregation of the other synuclein. γS is also implicated in different cancers such as colon, pancreas, and breast contributing to progression of tumors acting through a variety of mechanisms (Pan *et al*., 2002; Inaba *et al*., 2005; Hua *et al*., 2009).

Emily Ong's Thesis Inspired Substitution Mutants

Emily Ong in her senior thesis studied the familiar αS mutations, H50Q, G51D, and A53E, and the cause of their toxicity (See Appendix A). Different mutations can render a protein toxic. One way could be due to the loss of the original amino acid or the gain of the new one conferring pathology hallmarks of PD. Using both the budding and fission yeast model system, she created substitution mutants of these mutations in αS by switching the original amino acid with a new one from the four distinctive functional groups of amino acids. In the case of H50Q, she synthetized H50G (glycine, nonpolar), H50N (asparagine, polar), H50R (arginine, basic), and H50D (aspartic acid, acidic). Her results showed that the loss of the original histidine was conferring toxicity, presenting all substitutions toxic (Ong, Thesis, 2017). For the A53E, loss of the original amino acid was key to toxicity and was further supported by the presence of two other mutations in position 53 (A53T and A53V). On the other hand, G51D seemed to be toxic due to the gain of the aspartic acid, which showed similar toxicity to the substitution mutant G51E, also acidic (Ong, Thesis, 2017). This analysis inspired my first aim because she designed the substitution mutants to gain insights on what is driving toxicity. *I learned how important the substitution idea was to understand better the mutants, and thus, I wanted to apply the same project design to the understudied βS mutants.*

Ryan Osselborn's Senior Project and My Contributions

Ryan Osselborn in his senior project he comparatively evaluated WT αS, βS, and γS in both low and high expression models using the budding yeast (See Appendix B). His senior project work started with contributions from myself in the tool making process. I helped Ryan and Tracey get all the necessary synuclein constructs and contributed data for their theses. From his work, he reported that αS and βS are differentially toxic, with the former being more, whereas γS is nontoxic in a high expression model. In a low expression model, no differences in toxicity were reported for any of the synuclein proteins. Even though no cytotoxicity is achieved with a low expression model, this system is still powerful too study what properties or altered cellular environments can enhance toxicity. Similarly, with a high expression system, we are able to study what elements de-

crease or provide a protection against toxicity.

In his senior project, Osselborn also reports βS the protein to have higher than expected molecular weight through western blot analysis. The change in size could be due to post translational modifications that the protein undergoes after being synthetized, specifically SUMOylation Nonetheless more information is needed to understand its size. *In my thesis I aim to investigate what drives toxicity of βS and if I can make γS toxic. For this reason, all my senior thesis work is done in the high expression system.*

Tracey Nassuna's Thesis and My Contributions

Tracey Nassuna, in her senior thesis studied the molecular underlying of toxicity for the βS mutation P123H (See Appendix C). Using the budding yeast model system, Tracey Nassuna, and I, using the same strategy as Emily Ong, created substitution mutants for P123H βS following the same functional groups to investigate if the loss or the gain of the new amino acid is key to toxicity. We created in βS P123E (glutamic acid, acidic), P123R (arginine, basic), P123A (alanine, nonpolar), and P123N (asparagine, polar). For her thesis, I collected all the data with the high expression system. Nassuna and I reported that for P123H βS the gain of the new amino acid is the cause of the mutant toxicity since no other substitution mutant showed similar toxicity than the mutant. I am interested in continuing collecting data for the P123H mutant and expanding this work by also analyzing the second βS mutant V70M, by also creating substitution mutants with the same amino acids.

Furthermore, Tracey Nassuna in her thesis also studied the initial effects of swapping the known βS mutants (V70M and P123H) for αS. With my help, we created the swap mutant αS-V70M and αS-P128H, following sequence alignments and corresponding conserved sequences. She found that V70M αS showed similar toxicity that αS, whereas P128H αS showed less toxicity when compared to the former two, but similar to βS. *I am interested in furthering this research by expanding on this work and creating swap mutants of known aS mutations into βS and γS, and βS mutations into γS.*

Post translational modifications in synucleins

One way a protein can change function, structure, and localization after being synthetized is through post-translational modifications (PTM). PTM occur at specific sites where different chemical groups, such as methyl, are added to the protein. PTM are necessary for certain cellular processes such as ubiquitination, in which a ubiquitin molecule is added to a protein's lysine residues and creates a signal for degradation in the proteasome (Ramazi & Zahiri, 2021). Another especially important type of PTM is methylation, attaching a methyl group to a protein producing an epigenetic regulator of gene expression (Ramazi & Zahiri, 2021). aS has many PTM sites linked to either facilitating or preventing formation of fibrils and membrane interactions (Ellis *et al*., 2001). PTM are classified as beneficial or harmful in the context of aS toxicity. Many studies *in vivo* and *in vitro* report that aS can get phosphorylated by kinases (CKI and CKII among others) at S87-P (Okochi *et al.,* 2000), S125 -P (Ellis *et al.,* 2001; Nakamura *et al.,* 2001), and S129-P (Okochi *et al.,* 2000; Anderson *et al*., 2006). Phosphorylation is considered a harmful event, increasing aS toxicity. Similarly, to αS, βS also gets phosphorylated at the C-terminus, S118-P (Hayashi, & Carver, 2022b). Based on sequences alignments the phosphorylation at position S118 is comparable to the one for aS at position S129 (Hayashi, & Carver, 2022b). No known serine residue is known to get phosphorylated in γS.

aS has high susceptibility to get nitrated, increasing oxygen and nitric stress, at the tyrosine residues in positions Y39, Y125, Y133, and Y136 (Sevcsik *et al*., 2011; Burai *et al*., 2015). Like phosphorylation, nitration is a harmful PTM. These tyrosine residues are critical in intermolecular interactions and cross-linking of the protein mediating oligomerization, which is not seen when these sites are blocked by replacing the tyrosine residue with a hydrophobic phenylalanine (Y39F, Y125F, Y133F, and Y136F; (Burai *et al*., 2015). Many of these tyrosine residues are conserved also in βS and γS, however, PTM in βS and γS are less studied and understood than those in αS.

Nonetheless, some PTM can be beneficial such as SUMOylation and acetylation. αS can get sumoylated at the SUMO accepting lysine residues sites, K96 and K102 (Krumova *et al.,* 2011), and acetylated at K6 and K10 (de Oliveira *et al*., 2017). For SUMOylation, studies using mutants to block SUMO sites (K95R and K102R) showed that αS was more propense to aggregate and had higher cytotoxicity in the substantia nigra dopaminergic neurons (Hassanzadeh *et al*., 2023). Acetylation also decreases progression, propensity to aggregate, and the morphology of the aggregates, which had lower content of β-sheet content (Bell *et al*., 2022). Given the notable conservation of amino acid sequence between αS, βS, and γS, it follows that they share analogous PTM sites. *The focus of my senior thesis pertains to the potential impact of the PTM described before in aS, in the context of βS and γS.*

Gap in Knowledge

All literature in synucleinopathies and Lewy body diseases focuses on αS and its mutations, which are well characterized. Until recently, βS was believed to protect against αS toxicity, however, studies provided new links between βS and γS with NDDs. Two βS mutations, V70M and P123H, are causative agents in DLB. Nonetheless, the mechanisms behind toxicity are not well understood. γS also shows promising potential for being a causative candidate of toxicity, however, the nature of its potential to be toxic is unknown. Their toxicity potential and neurodegeneration mechanisms are worth evaluation more fully. *I am eager to ask what drives the toxicity of the two b-Synuclein mutants: The loss of the original amino acid (V70, P123) or gain of the mutants (70M, 123H)?* Secondly, six/four amino acids linked with the nine aS genetic mutations are conserved in βS and γS, respectively, as is βS V70 in both aS and γS, and βS P123 in aS (P128). I wonder about the effect of introducing the aS mutations into βS and γS, and βS mutations into aS and γS. *Gaining this knowledge will illuminate the molecular determinants of the bS* and *γS' elusive toxicity.*

Furthermore, like aS, βS is modified post-translationally, however the effect of disrupted cellular environments (mitochondrial stress, nitrative stress, lysosomal dysfunction) and post-translational site mutations remain unassessed**.** Even less is known about γS post-translational modifications and these other disruptions. I am interested in exploring these in βS and γS for the known aS' phosphorylation, SUMOylation, and glycation sites for those that are conserved in βS and γS. The gaps in knowledge of this thesis are represented in Figure 6.

Yeast as a Model Organism

Many labs around the world use different model organisms to study synucleinopathies and PD, such as Drosophila, C. elegans, rodents, neuronal cell cultures. All of these provide benefits and disadvantages to study synucleinopathies. Some of the most popular models such as rodents or neuronal cells which have easier translation into humans present many obstacles such as difficult to manipulate and difficult for high/low-throughput screening and genetic analysis. For the purpose of this thesis, the DebBurman lab and many others choose to use an unconventional and powerful model organism: Budding Yeast (Saccharomyces cerevisiae, S. cerevisiae).

S. cerevisiae have a fast reproduction time, only taking between 1.5 to 3 hours to replicate being a single-celled organisms belonging to the fungus eukaryotes. Yeast has a small, sequenced genome (approximately 6,000 genes), with high similarities between humans and yeast sharing an overlapping 32% between amino acid sequences (Leslie, 2015). Many human genes linked with NDDs have yeast homologs, such as PARK2 that codes for the Parkin protein, which is the cytosolic ubiquitin-E3-ligase, involved in ubiquitination and where mutations of PARK2 lead to PD (Konovalova et al., 2015). Other yeast homologs and orthologs from human genes are SCA2 associated with spinocerebellar ataxia type 2, SOD1 in ALS, and ATP7B mutations leading to transporter dysfunction linked to Wilson Disease (Allendoerfer et al., 2008). Yeast also has a highly conserved stress response, protein folding, modification, and degradation pathways as humans (Allendoerfer et al, 2008). All these similarities allow for yeast to be used as a powerful and insightful model organism to study the neuropathology and protein interactions these diseases are characterized by. Almost half of the yeast genes have human counterparts, which

make it easier to use yeast as a genetic tool. Yeast is amazingly easy to manipulate the yeast genome and introduce human genes without losing functionality, as well as having knock-out knock-in techniques (Allendoerfer et al, 2008). In the case of this thesis, we use aS, βS, and γS, but have no yeast homolog. Outeiro and Lindquist were the first to establish a PD yeast model in 2003 by reproducing the characteristics of aS toxicity in pathology seen in patients (Outeiro & Lindquist, 2003).

Since then, many labs use yeast for a PD model including the DebBurman lab, which used both the budding yeast and the fission yeast (Schizosaccharomyces pombe) to contribute to a larger community. The DebBurman lab uses a high copy 2-micron plasmid in which aS, βS, or γS genes can be inserted and expressed in the yeast. Many past members used this system to study the familial older and newer mutants such as Brandis et al., 2006; Fiske et al., 2011; Sharma et al, 2006; Emily Ong (Thesis, 2017), Amanda Grassel (Thesis, 2023), and Tracey Nassuna (Thesis, 2023).

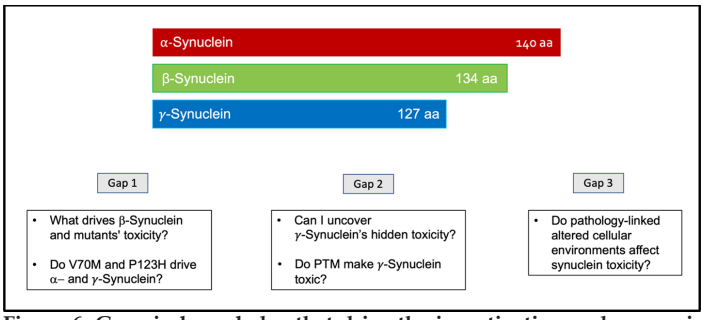

Figure 6. Gaps in knowledge that drive the investigation and comparison between the synuclein proteins. Gap 1 is to understand what drives the bS and the bS mutants' toxicity. As well as understand how critical are the mutations V70M and P123H for toxicity by looking at them in aS and gS. Gap 2 is to investigate if I can uncover gS hidden toxicity, by showing toxicity, and study how post-translational modifications might affect gS. Gap 3 is to understand the effects of disease-linked altered cellular environments on the synucleins' toxicity.

Hypotheses and Aims

I propose to add insight into three hypotheses:

1) Either the loss of the original amino acid or gain of the mutant is key to V70M and P123H βS toxicity.

2) At least some of the known aS and βS mutations when swapped onto each other (aS, βS, and γS) will increase their toxicities.

3) Finally, post-translational modifications and altered neurodegeneration-related environments will regulate βS and γS toxicity.

Chapter 1

The goal for chapter 1 was to create all the 30 mutants necessary for all aims in my thesis. For Aim 1, my goal was to create eight substitution mutations. For Aim 2 to create swap mutants. For Aim 3, to evaluate covalent modifications with PTM site mutants. For my project, I was able to successfully create 25 of the mutants necessary in budding yeast, as described in chapter 1 of results. All plasmids used in this thesis use a high expression system, having GFP in p426 vector.

Chapter 2

The goal of this chapter is to answer Aim 1 and Hypothesis 1 by characterizing the βS substitution mutants for both V70M and P123H. I am examining toxicity, localization, and expression of the synuclein as compared to WT βS using three assays: Serial dilution spotting, GFP fluorescent microscopy, and Western blot, in two control strains W303 and BY4741.

I predicted for V70M substitutions, the mutant that conserved the hydrophobicity properties of WT βS and the V70M mutant will show similar toxicity, while the other substitution mutants would have non-toxic properties. For P123H, I predicted all mutants would show toxicity because of proline loss. My findings support the first hypothesis, and I found position 70th is critical for toxicity and aggregation, while for P123H, the polar and basic residues matter.

Chapter 3

My goal for this chapter was to investigate if the presence of specific amino acids are crucial toxicity regulators. I created swap mutants by introducing the disease-linked mutations from aS and bS into each other and γS. For aS mutations into bS and γS, I predicted that bS toxicity would be aggravated by aS mutations, and γS will show potential for toxicity. I also predicted aS toxicity would also be aggravated by bS mutants. I was to show that aS swaps had differential toxicity, aS-V70M showed similar toxicity to WT aS, whereas aS-P128H to WT bS. Contrary to my hypothesis, γS swaps showed no toxicity or aggregation.

Chapter 4

My aim was to study covalent modifications of bS and γS by creating PTM site mutants. Based on previous literature of oxidization of γS, I predicted that the mutant that mimics nitration would make γS toxic, while those mutants that block nitration and mimic SUMOylation and acetylation will conserve the non-toxic properties of γS. As for bS, I predicted increased pathogenicity when nitration and phosphorylation are mimicked, but a protective phenotype when acetylation, SUMOylation are mimicked, but nitration and phosphorylation, are blocked. My findings are preliminary data that shows that toxicity in bS is not affected, and the PTM do not make γS toxic.

Chapter 5

For my last chapter, my goal is to continue answering aim 3 by studying bS and γS in yeast strains altered for different cellular environments. In particular, for altered levels of nitrative stress, decreased glycation, and increased acetylation. These strains will be compared to the control strain BY4741. I used cox5AΔ for elevated levels of nitrative stress and cox5BΔ for low levels of nitrative stress. Then, I used sirt2Δ for high levels of acetylation, and glo1Δ for decreased levels of glycation. This work was done with Leslie Casares '26. Our findings show that high nitrative stress can aggregate bS and its mutants' toxicity, and even make γS toxic. While decreasing glycation and increasing acetylation is protective to the synucleins.

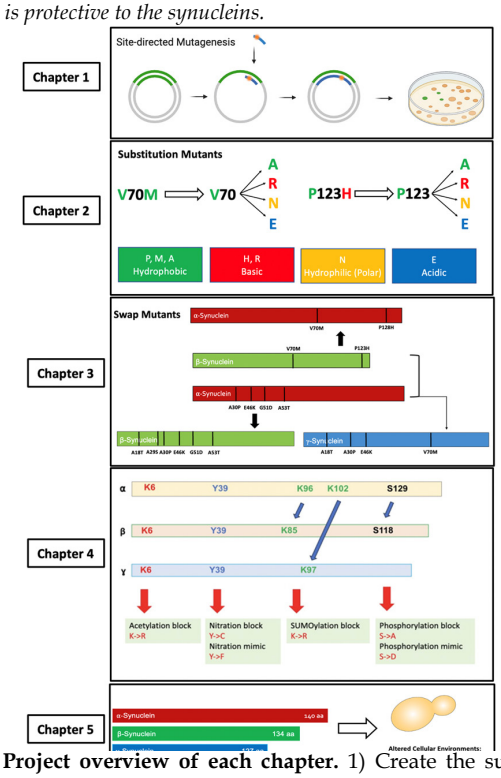

Figure 7. Project overview of each chapter. 1) Create the substitution, swap, and PTM site mutants by introducing the mutations into αS, βS,

of the original amino acid (V70 or P123) or the gain of a new amino acid (70M or 123H) is the determinant of the βS mutants' toxicity. 3) Examine the impact of swap mutants of αS, βS, and γS to investigate if these would aggravate αS, βS, and make γS toxic. 4) Characterize and study if PTM site mutants for βS and γS show similar toxicity properties than αS. 5) Use different yeast strain modelling altered neurodegeneration-related cellular environments and their effects on βS and γS 's potential toxicity.

MATERIALS AND METHODS

The methods used in this thesis were adapted from Outeiro and Lindquist (2003), Brandis et al. (2006), Sharma et al. (2006), and Fiske et al. (2011).

β- and γ-Synuclein Constructs

The goals of my thesis were to evaluate the molecular reason of βS mutant toxicity, as well as the pathological properties of swap and post translational site mutants in yeast. To carry out this work, different constructs of mutants were used each aim. For aim 1, I designed four substitutions mutations on both βS-V70M and P123H, to represent the four functional classes of amino acids: hydrophobic (V70A/P123A), basic (V70R/P123R), polar (V70N/P123N), and acidic (V70E/P123E). For aim 2, I introduced six αS mutations (A18T, A29S, A30P, E46K, G51D, and A53T) into βS and three of them (A18T, A30P, E46K) into γS. Similarly, the βS-V70M will be inserted into both αS and γS and just βS-P123H in αS (but at P128H). Lastly, for aim 3, to evaluate covalent modifications on βS and γS toxicity, I designed β-mutations to mimic or block phosphorylation (S118D/A, respectively), block SUMOylation (K85R), mimic or block nitration (Y39F/C, respectively), and block acetylation (K6R). I designed for γS mutants on K97R to block SUMOylation, Y39C to block or Y39F mimic nitration, and K6R to block acetylation. All the mutants I created were tagged with Green Fluorescent Protein (GFP) and transformed into S. cerevisiae budding yeast. This project consisted of designing, successfully making, and assessing 30 mutants, using the methods below.

Site-Directed Mutagenesis

To produce the 30 mutations in αS, βS, and γS, the Quick Change II mutagenesis kit was used following the protocol by GENEART Site-Directed Mutagenesis System from Invitrogen Life Technologies. Designed complementary forward and reverse primers with the desire mutation were used to introduce single-/double-nucleotide changes in the synuclein WT sequence. After PCR and recombination reaction the amplified product was transformed into One Shot Max Efficiency DH5α-T1R competent E. coli cells. The template DNA used was αS, βS, and γS tagged with GFP that we received from our collaborators at the Outeiro Lab (Germany). After all plasmids were successfully transformed and isolated from E. coli using the Qiagen Mini-prep kit, the purified plasmids DNA were sent to the Sequencing Facility Core at the University of Chicago for Sanger sequencing to confirm desired mutations were successful. See Chapter 1 for full details.

Yeast Strains

For all experiments, budding yeast, Saccharomyces cerevisiae (S. cerevisiae), was used as the model organism. For chapters 1 to 3, all wild-type and mutant synucleins were analyzed in two control strains of yeast: BY4741 (haploid) and W303 (diploid), which have no gene deletions. For chapter 4, I transformed the WT synucleins and the two βS mutants (V70M and P123H) into modified strains of yeast (glo1Δ and sirt2Δ) for low glycation and high acetylation, respectively, to assess pathological properties in a PD modelled cellular environment.

Yeast Transformations

All mutants used are in the p426 yeast-expressing vector that were transformed into budding yeat. This vector is used because of its powerful selective marker, the URA3 gene. During DNA plasmid transformations, it allows for positive selection in a media lacking external the nucleotide uracil (SC-Ura). The vector also has a GAL1 promoter, that acts as an on/off switch of the designed synuclein gene by simply providing galactose media (SC-Ura galactose_. In contrast, SC-Ura glucose represses the gene expression. Table 1 summarizes all synuclein constructs and yeast strains used for each chapter.

Serial Dillution Spotting Assay

To investigate the toxicity of the synuclein mutants, yeast cells were inoculated and grown in liquid SC-Ura, overnight at 30 °C, and shaking at 200 rpm. Cells are washed three times with 5 mL of deionized water and counted using a hemocytometer with a dilution of 100-fold. Cell dilution is calculated to reach a final volume of 5.0x106 cells/mL. The cells were then further diluted 5-fold in a 96-well plate 5 times. The cells were spotted onto SC-Ura glucose and galactose plates using triplicates and incubating these for 3 days at 30 °C. Plates were imaged at each day using an Epson Perfection V600 photo scanner and Adobe Photoshop CS3 software. Generally, five independent trials were done for each set of spotting.

GFP Fluorescent Microscopy
A close-up of a green cell

Description automatically generatedTo localize where the GFP-tagged synuclein protein is within the yeast cells, they are grown in SC-Ura glucose overnight, washed three times with 5 mL of deionized water, and transferred to inductive SC-Ura galactose for 6, 12, and 24 hours. At each time, 1 mL was pelleted out of the cells and taken to the TE2000-U Nikon Fluorescent microscope at a magnification of 60X. Blue light was used to make the GFP glow bright green. At least three independent trials were done for each set, counting 1000 cells for each time point. The phenotypes were classified according to the established phenotypes for budding yeasts associated with the diseased or healthy states of the protein, these are pictured below, and the ones used for characterizing phenotypes.

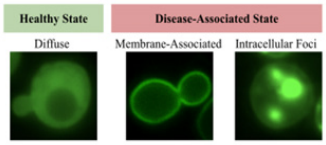

Statistics for Microscopy Quantification

For each mutant synuclein trial of microscopy, the 1000 cells were classified based on observed phenotype, as pictured before. To compare the mutant yeast to synuclein yeast, the phenotypes observed were quantified using Prism one-way ANOVA with Bonferroni post-hoc analysis. Since multiple comparisons were made, the alpha level (significance threshold) was adjusted from $\alpha = 0.05$ to α/n (n = number of comparisons) in each case. The results were presented in graphs made in Microsoft Excel.

Western Blot Assay

A close-up of a blue line

Description automatically generatedTo assess expression of synuclein protein in the budding yeast, the cells were grown in 5 mL of repressive SC-Ura glucose overnight at 30 °C, then pelleted and washed three times with deionized water, and transferred to 20 mL of SC-Ura inductive galactose. After 12 hours of induction of gene expression, 1 mL of the cells was pelleted and using a hemocytometer the cells were counted and diluted to reach a final volume of 2.5x10^7 cell/mL. To prepare the cell lysate, the cells were then washed with 1 mL of 50 mM Tris and 10 mM NaN3. The cells were lysed by adding an electrophoresis sample buffer (ESB) with protease inhibitor and 40 g of microbeads followed by 2 min vortexing and incubating at 100 °C for 1 min. 20 µl of each sample were loaded on 8-16% Tris-Glycine gel (Invitrogen, #XP08165BOX) using the SeeBlue Plus2 Pre-Stained Protein Standard (Invitrogen, LC5925) as control ladder. Then the proteins were transferred to a polyvinyl fluoride membrane (PVDF); Millipore Sigma) using a semi-dry transfer at 15 V for

50 min for western blotting. The synuclein proteins were detected by GFP anti-mouse monoclonal primary antibody (Thermo), followed by goat anti-mouse secondary antibody from WesternBreeze Chromogenic kit (Thermo). To ensure same number of cells were present in each sample, phosphoglycerokinase (PGK) was used as a loading control, probing with primary antibody for PGK from Molecular Probes. At least three independent trials were done for each set of samples.

Chapter 1
Creation of Synuclein Mutants
RESULTS

The first step in my thesis was to create all the molecular tools I needed to carry out all the studies detailed in subsequent Chapters 2-5. For Chapters 2-4, I needed to create point mutations on the various synucleins and transform them into relevant yeast strains (BY4741 and W303). For Chapter 5, I had to transformed bS and its two familial mutants (V70M and P123H) into relevant yeast strains (BY4741, which served as control, and four gene deletion strains).

For Chapter 2, I set to create eight substitution mutants in all, four for each bS mutant (V70M and P123H). I chose one amino acid substitution mutation to represent each functional amino acid class: hydrophobic (A), hydrophilic (N), basic (R), and acidic (E). Therefore, they were V70A, V70R, V70E, V70N, P123A, P123R, P123E, and P123N.

For Chapter 3, I set to create twelve swap mutants in all: i) five point mutations on bS to swap in each familial mutant of aS on amino acids that were conserved in bS (specifically, A18T, A29S, A30P, E46K, G51D, A53T); ii) two point mutations on aS to swap in both familial mutants of bS since both amino acids were conserved in aS (V70M, P128H); and, finally, iii) four point mutations on gS cDNA to swap in the three familial mutants of aS (A18T, A30P, E46K) and one familial mutant of bS (V70M) because those amino acids were conserved in gS.

For Chapter 4, I set to create a total of ten post-translational modification mutants on those amino acids of bS and gS that were conserved with aS and were known to be post-translationally modified on it. Specifically, six on bS cDNA (K96R to block acetylation, Y39C and Y39F to mimic and block nitration, K85R to block SUMOylation, and S118A and S118D to block and mimic phosphorylation) and four on bS cDNA: K6R to block acetylation, Y39C and Y39F to mimic and block nitration, K97R to block SUMOylation.

To make each mutation, I used site-directed mutagenesis which has seven key steps. Table 1 summarizes the progress towards creating all 30 mutants note above, chronicling the main steps of the seven-step mutagenesis process I used. I successfully mutagenized 25 of the 30 planned mutations (including all eight substitution mutants for Chapter 2), allowing me to make considerable progress in all my studies. I am still working to complete the five mutagenesis reactions that did not come out successful despite multiple tries. These were two swap mutants for Chapter 3 (A18T-bS, E46K- bS), and three post-translational modification mutants for Chapter 4 (Y39C- bS, K85R- bS, K97R- gS).

The data for the mutagenesis process is represented in Figure 8. Detailed below I only describe the process and that data for creating the swap mutation aS-V70M, but the same mechanism and similar data were obtained for the rest of the mutants I made.

Isolation of Template DNA

I first isolated and purified template DNA for aS tagged with GFP from E. coli using Life Technologies' MiniPrep kit. After isolating the plasmid, I conducted a 1.0% agarose gel electrophoresis to confirm successful extraction. Figure 8A presents evidence confirming the successful extraction and isolation of the plasmid. The observed DNA band measured approximately 6,810 base pairs, consistent with expectations. This size is from the synuclein length of 420 base pairs, the GFP tag of 790 base pairs, and the p426 vector used for gene insertion, which contributes 5600 base pairs. The results depicted in Figure 8A display a robust DNA band at the anticipated 6000 bp.

Creation of PCR Primers

Next, I designed primers that were 100% complementary to the synuclein sequence, except for the site of the mutation wanted (Figure 8B). In the case of aS-V70M, I changed the codon 5′ – GTG – 3′ for 5′ – ATG – 3′, creating the mutation valine to methionine. For the primers, I designed them to be 30-40 nucleotides long with a melting temperature in between 60 and 75°C and a %GC content above 55%, as indicated by the mutagenesis protocol for more successful amplification. Table 1 shows all the primers I designed for each chapter and Figure 8B shows the designed primers for aS-V70M.

PCR Mutagenesis Reaction

The third step was the site-directed mutagenesis, I conducted a PCR reaction incorporating the isolated aS, the forward and reverse primers, and essential components such as 25x SAM, 10x enhancer, DNA methylase, and PCR water. Following the guidelines outlined in the manual, I meticulously set the PCR timings. Once the reaction concluded, I proceeded to conduct gel electrophoresis on the samples to assess amplification. To establish a baseline, I compared these samples with a background sample containing identical volumes of template DNA utilized in the PCR reaction. The results, shown in Figure 8C, revealed a band at approximately 1,200 base pairs showing I successfully amplified the template DNA for αS-V70M.

Transformation of plasmid into E. coli

Fourthly, I recombined and transformed the amplified amplicon from step 3 into E. coli cells. For this purpose, I utilized DH5α T1R competent cells. Figure 8D depicts the transformation plates after 16 hours of incubation, showcasing the sample plates alongside a positive control—marked by blue colonies indicating successful mutagenesis and transformation. Additionally, I included a negative control, revealing no growth and thus confirming the absence of contamination. Notably, I plated two volumes: 20 µL and 80 µL for the sample. As for the negative control, I plated only 80 µL in LB Broth + Ampicillin. I used the Ampicillin (Amp) as the selective marker, since the p426 vector in which I inserted the synuclein possess an Amp resistance gene, and thus, only the transformed cells with the desired plasmids would grow in the LB+Amp agar plates.

Isolation of Amplified Mutant DNA

I carefully selected four colonies of E. coli and isolated and purified DNA from them using the same Miniprep kit as in step 1. After the process, I ran the plasmids on a gel using gel electrophoresis to check for extraction. Figure 8E illustrates that isolation was successful for all samples, evident in the thick dark bands at around 6,000 base pairs.

Sanger Sequencing at the University of Chicago

Afterward, I sent the extracted plasmids to the DNA Sequencing Facilities at the University of Chicago to obtain the plasmids' sequences through Sanger sequencing and analyzed them using ApE software. I obtained correct sequences for all samples. This result means the mutation was present, and the rest of the synuclein sequence aligned 100% with the template αS-V70M (Figure 8F).

Transformation of Mutant Plasmid into Yeast

In the seventh and final step, after I successfully isolated the DNA and confirmed their sequence for the desired mutation, I proceeded to transform αS-V70M into budding yeast (S. cerevisiae). The data for the mutagenesis process is represented in Figure 8G. To accomplish this, I employed the Cold Spring Harbor Yeast Transformation protocol (Amberg et al., 2006). The budding yeast I utilized in the lab possess a selective marker, the Ura gene. Therefore, I plated the transformations on YPD media as a positive control to confirm the presence of cells in the samples, along with glucose plates lacking uracil.

This strategy ensured that only the transformed yeast containing the new plasmid with the Ura gene could survive, as they could produce their own uracil. Consequently, the yeast that grew on these plates were the ones harboring the plasmid. I am pleased to report that all transfor-

mations were successful into both control yeast strains BY4741 and W303. Table 2 shows all the progress I made for all the mutants in each chapter.

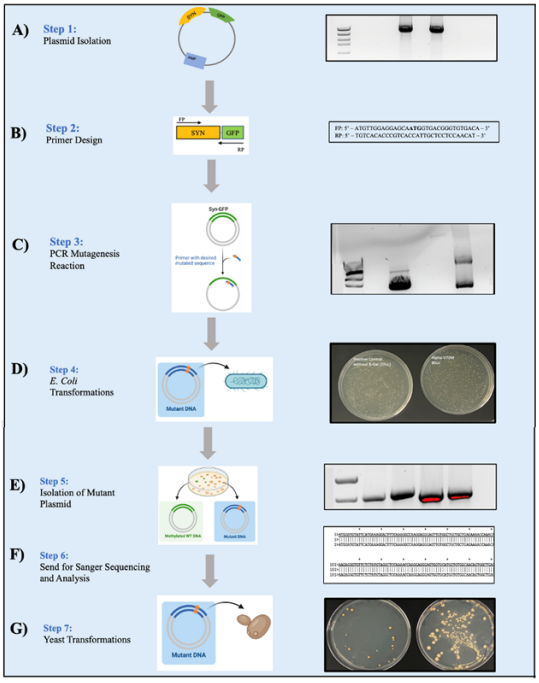

Figure 8. Creation of Mutants Process for αS-V70M. Depiction of steps needed to create the mutant αS-V70M. Same process for all other mutants created in the thesis. A) Steps 1 is the isolation of template DNA. B) Primer design for forward and reverse primers with the wanted mutation sites. C) Step 3 is the mutagenesis reaction, and then recombination reaction. D) Step 4 is the transformation into E. coli using mutated and methylated original DNA. E) Step 5 is the isolation and purification of the mutated plasmid from four E. coli colonies. F) Step 6 involves sending the purified plasmid DNA for sequencing at the University of Chicago. G) After sequence confirmation of the desired mutation, the plasmids are transformed into the budding yeast by yeast transformations.

A. **Chapter 2**

Synuclein Mutant	Primer Sequence Complements
V70A β-Synuclein	FP: 5' - ATCTGGGAGGAGCTGCGTTCTCTGGGGCAGG – 3' RP: 5' – CCTGCCCCAGAGAACGCAGCTCCTCCCAGAT – 3'
V70R β-Synuclein	FP: 5' – CATCTGGGAGGAGCTCGGTTCTCTGGGGCAGG – 3' RP: 5' – CCTGCCCCAGAGAACCGAGCTCCTCCCAGATG – 3'
V70E β-Synuclein	FP: 5' – ATCTGGGAGGAGCTGAGTTCTCTGGGGCAGG – 3' RP: 5' – CCTGCCCCAGAGAACTCAGCTCCTCCCAGAT – 3'
V70N β-Synuclein	FP: 5' - ACATCTGGGAGGAGCTAACTTCTCTGGGGCAGGGA–3' RP: 5' – TCCCTGCCCCAGAGAAGTTAGCTCCTCCCAGATGT – 3'
P123R β-Synuclein	FP: 5' – AGTTATGAGGACCCACGCCAGGAGGAATATCAG – 3' RP: 5' – CTGATATTCCTCCTGGCGTGGGTCCTCATAACT – 3'
P123E β-Synuclein	FP: 5' – GAGTTATGAGGACCCAGAGCAGGAGGAATATCAGG – 3' RP: 5' - CCTGATATTCCTCCTGCTCTGGGTCCTCATAACTC – 3'
P123N β-Synuclein	FP: 5' – GGAGAGTTATGAGGACCCAAACCAGGAGGAATATCAGGAG – 3' RP: 5' – CTCCTGATATTCCTCCTGGTTTGGGTCCTCATAACTCTCC – 3'
P123A β-Synuclein	FP: 5' – GAGTTATGAGGACCCAGCCCAGGAGGAATATCA – 3' RP: 5' – TGATATTCCTCCTGGGCTGGGTCCTCATAACTC – 3'

B. **Chapter 3**

Synuclein Mutant	Primer Sequence Complements
V70M α-Synuclein	FP: 5' – ATGTTGGAGGAGCAATGGTGACGGGTGTGACA – 3' RP: 5' – TGTCACACCCGTCACCATTGCTCCTCCAACAT – 3'
P128H α-Synuclein	FP: 5' – GGCTTATGAAATGCATTCTGAGGAAGGG – 3' RP: 5' – CCCTTCCTCAGAATGCATTTCATAAGCC – 3'
A18T β-Synuclein	FP: 5' – GGAGGGCGTTGTGGCAACCGCGGAGAAAACCAA – 3' RP: 5' – TTGGTTTTCTCCGCGGTTGCCACAACGCCCTCC – 3'
A29S β-Synuclein	FP: 5' – CAGGGGGTCACCGAGTCGGCGGAGAAGACCA – 3' RP: 5' – TGGTCTTCTCCGCCGACTCGGTGACCCCCTG – 3'
A30P β-Synuclein	FP: 5' – GGGGTCACCGAGGCGCCGGAGAAGACCAAGG – 3' RP: 5' – CCTTGGTCTTCTCCGGCGCCTCGGTGACCCC – 3'
E46K β-Synuclein	FP: 5' – GTCGGAAGCAAGACCCGAAAAGGTGTGGTACAAGGTG – 3' RP: 5' – CACCTTGTACCACACCTTTTCGGGTCTTGCTTCCGAC – 3'
G51D β-Synuclein	FP: 5' – GAAGGTGTGGTACAAGATGTGGCTTCAGTGGCT – 3' RP: 5' – AGCCACTGAAGCCACATCTTGTACCACACCTTC – 3'
A53T β-Synuclein	FP: 5' – AAGGTGTGGTACAAGGTGTGACTTCAGTGGCTGAAAAAACC – 3' RP: 5' – GGTTTTTTCAGCCACTGAAGTCACACCTTGTACCACACCTT – 3'
A18T γ-Synuclein	FP: 5' – GGAGGGCGTGGTGGGTACGGTGGAAAAGACCAA – 3' RP: 5' – TTGGTCTTTTCCACCGTACCCACCACGCCCTCC – 3'
A30P γ-Synuclein	FP: 5' – CAGGGGGTGACGGAAGCACCTGAGAAGACCAAGGAGG – 3' RP: 5' – CCTCCTTGGTCTTCTCAGGTGCTTCCGTCACCCCCTG – 3'
E46K γ-Synuclein	FP: 5' – GTGGGAGCCAAGACCAAGAAGAATGTTGTACAGAGCG – 3' RP: 5' – CGCTCTGTACAACATTCTTCTTGGTCTTGGCTCCCAC – 3'
V70M γ-Synuclein	FP: 5' – CGCCGTGAGCGAGGCTATGGTGAGCAGCGTCAA – 3' RP: 5' – TTGACGCTGCTCACCATAGCCTCGCTCACGGCG – 3'

C. **Chapter 4**

Synuclein Mutant	Primer Sequence Complements
K6R β-Synuclein	FP: 5' – TGGACGTGTTCATGAGGGGCCTGTCCATGGC – 3' RP: 5' – GCCATGGACAGGCCCCTCATGAACACGTCCA – 3'
Y39C β-Synuclein	FP: 5' – AGGAGGGCGTCCTCTGCGTCGGAAGCAAGAC – 3' RP: 5' – GTCTTGCTTCCGACGCAGAGGACGCCCTCCT – 3'
Y39F β-Synuclein	FP: 5' – AGGAGGGCGTCCTCTTCGTCGGAAGCAAGAC – 3' RP: 5' – GTCTTGCTTCCGACGAAGAGGACGCCCTCCT – 3'
K85R β-Synuclein	FP: 5' – GCCACAGGACTGGTGAGGAGGGAGGAATTCCCT – 3' RP: 5' – AGGGAATTCCTCCCTCCTCACCAGTCCTGTGGC – 3'
S118A β-Synuclein	FP: 5' – GGAGCCAGAAGGGGAGGCTTATGAGGACCCACC – 3' RP: 5' – GGTGGGTCCTCATAAGCCTCCCCTTCTGGCTCC – 3'
S118D β-Synuclein	FP: 5' – GAGCCAGAAGGGGAGGATTATGAGGACCCACCC – 3' RP: 5' – GGGTGGGTCCTCATAATCCTCCCCTTCTGGCTC – 3'
K6R γ-Synuclein	FP: 5' – TGGATGTCTTCAAGAGGGGCTTCTCCATCGC – 3' RP: 5' – GCGATGGAGAAGCCCCTCTTGAAGACATCCA – 3'
Y39C γ-Synuclein	FP: 5' – AGGAGGGGGTCATGTGTGTGGGAGCCAAGAC – 3' RP: 5' – GTCTTGGCTCCCACACACATGACCCCCTCCT – 3'
Y39F γ-Synuclein	FP: 5' – AGGAGGGGGTCATGTTTGTGGGAGCCAAGAC – 3' RP: 5' – GTCTTGGCTCCCACAAACATGACCCCCTCCT – 3'
K97R γ-Synuclein	FP: 5' – CCGGGGTGGTGCGCAGAGAGGACTTGAGGCCA – 3' RP: 5' – TGGCCTCAAGTCCTCTCTGCGCACCACCCCGG – 3'

Table 1. Mutations Primer Sequences. Designs of each primer used for substitution mutants in chapter 2 (A), swap mutants in chapter 3 (B), and post-translational site modifications in chapter 4 (C).

A) Chapter 2

Synuclein Mutant	Yeast Strain	Vector Used	Fluorescent Tag
WT β-Synuclein	BY4741 and W303	p426	GFP
V70M β-Synuclein	BY4741 and W303	p426	GFP
V70A β-Synuclein	BY4741 and W303	p426	GFP
V70R β-Synuclein	BY4741 and W303	p426	GFP
V70E β-Synuclein	BY4741 and W303	p426	GFP
V70N β-Synuclein	BY4741 and W303	p426	GFP
P123H β-Synuclein	BY4741 and W303	p426	GFP
P123R β-Synuclein	BY4741 and W303	p426	GFP
P123E β-Synuclein	BY4741 and W303	p426	GFP
P123N β-Synuclein	BY4741 and W303	p426	GFP
P123A β-Synuclein	BY4741 and W303	p426	GFP

B) Chapter 3

Synuclein Mutant	Yeast Strain	Vector Used	Fluorescent Tag	Still in Progress
WT α-Synuclein	BY4741 and W303	p426	GFP	
V70M α-Synuclein	BY4741 and W303	p426	GFP	
P1238H α-Synuclein	BY4741 and W303	p426	GFP	
WT β-Synuclein	BY4741 and W303	p426	GFP	
A18T β-Synuclein	BY4741 and W303	p426	GFP	X
A29S β-Synuclein	BY4741 and W303	p426	GFP	
A30P β-Synuclein	BY4741 and W303	p426	GFP	
E46K β-Synuclein	BY4741 and W303	p426	GFP	X
G51D β-Synuclein	BY4741 and W303	p426	GFP	
A53T β-Synuclein	BY4741 and W303	p426	GFP	
WT γ-Synuclein	BY4741 and W303	p426	GFP	
A18T γ-Synuclein	BY4741 and W303	p426	GFP	
A30P γ-Synuclein	BY4741 and W303	p426	GFP	
E46K γ-Synuclein	BY4741 and W303	p426	GFP	
V70M γ-Synuclein	BY4741 and W303	p426	GFP	

C) Chapter 4

Synuclein Mutant	Yeast Strain	Vector Used	Fluorescent Tag	Still in Progress
WT α-Synuclein	W303	p426	GFP	
WT β-Synuclein	W303	p426	GFP	
K6R β-Synuclein	W303	p426	GFP	
Y39C β-Synuclein	W303	p426	GFP	X
Y39F β-Synuclein	W303	p426	GFP	
K85R β-Synuclein	W303	p426	GFP	X
S118A β-Synuclein	W303	p426	GFP	
S118D β-Synuclein	W303	p426	GFP	
WT γ-Synuclein	W303	p426	GFP	
K6R γ-Synuclein	W303	p426	GFP	
Y39C γ-Synuclein	W303	p426	GFP	
Y39D γ-Synuclein	W303	p426	GFP	
K97R γ-Synuclein	W303	p426	GFP	X

D) Chapter 5

Synuclein Mutant	Yeast Strain	Vector Used	Fluorescent Tag
WT α-Synuclein	*sirt2Δ, glo1Δ, cox5AΔ, cox5BΔ*, BY4741	p426	GFP
WT β-Synuclein	*sirt2Δ, glo1Δ, cox5AΔ, cox5BΔ*, BY4741	p426	GFP
WT γ-Synuclein	*sirt2Δ, glo1Δ, cox5AΔ, cox5BΔ*, BY4741	p426	GFP
V70M β-Synuclein	*cox5AΔ, cox5BΔ*, BY4741	p426	GFP
P123H β-Synuclein	*cox5AΔ, cox5BΔ*, BY4741	p426	GFP

Table 2. Summary of synuclein constructs. All chapters have the synuclein and the mutants transformed into unmodified control strains. All constructs are within the p436 vector, which was used as a control in chapters 2-5; and were tagged with GFP A) These constructs were used to evaluate substitution mutants. B) The swap mutants were compared to their WT synuclein. C) These were post-translational modification sites mutants. D) Chapter 5 evaluated yeast strains altered for various environmental conditions, glycation, acetylation, and nitration.

Chapter 2

CHARACTERIZATION OF γ-SYNUCLEIN SUBSTITUTION MUTANTS IN YEAST

Part of the V70M spottings in this chapter were obtained in collaboration with Holly Kiernan '26

Experimental set-up

The genetic mutations V70M-βS and P123H-βS play a role in toxicity in patients with DLB. Tracey Nassuna '23 analyzed the βS mutants and their substitution in low expression and found no differences in toxicity or expression (See Appendix C). One of my goals for my thesis was to further analyze if the gain or the loss of the original amino acid is key for toxicity, and thus, I created substitution mutants with high expression. I created the substitution mutants as indicated in Figure 9A. I changed the original amino acid one in each of the amino acid classes; non-polar (V70A/P123A), basic (V70R/P123R), polar (V70N/P123N) and acidic (V70E/P123E), through mutagenesis, tagged with GFP, and compared them to βS and the natural mutant βS-P123H. My hypothesis is that if the gain of the new amino acid is the cause of toxicity, V70M would be the most toxic. V70A would show similar toxic as V70M since A (alanine) and M (methionine) belong to the same class of non-polar amino acids. Similarly, P123H would be the most toxic, with P123R possibly too, since R (arginine) and H (histidine) are from the basic amino acid class.
On the other hand, if loss of the original amino acid is the cause of toxicity for the natural mutant, then all the substitution mutants would be toxic as well as the V70M and P123H since V (valine) and P (proline) are lost, respectively. Starting with V70M and then P123H, I evaluated the substitution mutants in yeast control strains, using 1) serial dilution spotting 2) Western blots 3) live-cell fluorescent microscopy.

Findings

V70M: Hydrophobicity is key for V70M toxicity

Firstly, I characterized the toxicity of the V70M substitution mutants by serial dilution spotting assay in BY4741 and W303 control strains. I serial diluted and spotted the cells onto plates with glucose (suppresses the synuclein expression) and galactose (promotes synuclein expression). First, when I focused on BY4741, refer to Figure 9B for data, the glucose plates grew similarly across samples indicating that I spotted an equal number of cells, and thus, any differences in galactose plates are due to the effects of the synucleins on the yeast.
When I expressed βS and the mutants (on galactose plates), yeast with βS, βS-V70M, and βS-V70A shows low levels of growth when compared with those with the mutants βS-V70R, βS-V70N, and βS-V70E (Figure 9B). Furthermore, βS-V70M showed the least growth out of the three. This finding was expected considering the hypothesis that the gain of the new amino acid is key to toxicity, and moreover, that the hydrophobicity of the residue matter for toxicity. In this case, βS-V70M (natural mutant), βS-V70A, as well as the βS (Valine) all have a nonpolar amino acid residue in position 70th. Additionally, another finding is that βS-V70M mutant also shows to be more toxic than the βS.
In W303, I found similar results, but βS seems to have the highest toxicity, followed by the natural mutant βS-V70M. βS-V70A seems to be slightly less toxic than these. The other mutants show less levels of toxicity βS-V70M, βS, and βS-V70A (Figure 10A).

Aggregation is linked to toxicity

To capture the localization of the synuclein withing the yeast, I looked at the cells at three different time points, 6, 12, and 24 hours after inducing synuclein expression through galactose media using live-cell fluorescent microscopy. βS, βS-V70M, and βS-V70A in both BY4741 and W303 have a distinct localization pattern as compared to βS-V70R, βS-V70N, and βS-V70E (Figure 9D, 10C). Initially at 6 hours, I found that all the mutants and βS showed a diffuse phenotype, followed by membrane-association and foci formation for βS, βS-V70M, and βS-V70A at 12 hours, whereas βS-V70R, βS-V70N, and βS-V70E displayed a diffuse phenotype. Lastly at 24 hours, I found they all localized at the cytoplasm showing a diffuse phenotype.

To quantify and investigate any significant differences in foci phenotypes between the mutants at 6 and 12 hours, two one-way analyses of variance using Bonferroni were performed (Figure 9D, 10D). The a value was adjusted to 0.0083 ($a = 0.5/n$; n = number of groups compared). These analyses revealed that there were significant differences in the foci phenotypes observed at 6 and 12 hours for W303 and BY4741. At 6 hours, analyses showed that for BY4741, $F(5,12) = 8.67$, $p < 0.0001$, but no significant differences were found across groups for foci. For W303 at 6 hours, $F(5,12) = 71.93$, $p < 0.0001$. Even though the most prominent phenotype for all mutants was diffuse, Bonferroni post-hoc reveled that bS, βS-V70M, βS-V70A presented significantly more foci at 6 hours than βS-V70R, βS-V70N, and βS-V70E. For 12 hours in W303, $F(5,12) = 262.33$, $p < 0.0001$, and for BY4741, $F(5,12) = 305.79$, $p < 0.0001$, with the same classification showing that all mutants that had a hydrophobic residue at position 70th showed significantly more foci than the other substitution mutants. These findings highlight the differential localization seen from substitution mutants and provide further connection to the toxicity seen in the spotting patterns. The aggregation of bS, βS-V70M, βS-V70A is linked with toxicity; while the non-toxic ones show diffuse phenotype, commonly associated with a healthy state.

No expression differences between substitution mutants

Since in PD αS excessively accumulates, linked to cell death and disease, I found protein expression to be essential within the yeast cells for both BY4741 and W303 (Figure 9B, 10B). I analyzed expression using Western blots with GFP antibody to detect the synuclein proteins and PGK antibody as a loading control in BY4741 and W303. Firstly, the PGK protein bands appeared sufficiently even indicating that equal number of cells were present in all samples, and thus, I could assess the expression levels of βS and the βS mutant proteins. Secondly, I found that the synuclein proteins were successfully expressed and identified as the bands were at the correct size. βS, βS-V70M, and the substitution mutants showed similar levels of expression in both control strains. As such, I report that the substitution mutants an WT form have no expression differences that relate to the toxicity patterns seen in the serial dilution spotting.

P123H

Basic residues important for toxicity

I characterized the toxicity of the P123H substitution mutants by serial dilution spotting assay in BY4741 and W303 control strains.
After I analyzed the growth across the samples in the glucose plates, I found that it was fairly similar for both BY4741 and W303 (Figure 11A, 12A). For BY4741, when WT βS and the mutants were expressed on galactose plates, yeast with the βS-P123H mutation exhibited lower levels of toxicity compared to the βS. This discovery suggests that the natural mutant was more toxic than the WT form as well as any other substitution mutant. Additionally, both the substitution mutants βS-P123R and βS-P123N

showed comparable growth to βS-P123H and less growth than all others in the control strain BY4741. This finding supports the hypothesis that the gain of the new amino acid is crucial for toxicity. In this scenario, the gain of a basic residue, H (histidine) or R (arginine), resulted in less growth for the yeast, indicating higher toxicity. For βS-P123N, it appears that polar residues, N (asparagine), also play a key role in toxicity in a strain-dependent manner (Figure 11A, 12A). For W303, I found that the βS-P123H mutation exhibited lower levels of toxicity compared to the βS, and all other substitutions. . In contrast to BY4741, both the substitution mutants P123R and βS-P123N showed no differences in growth to the other substitution-

mutants. In this strain, the gain of a basic residue, H (histidine), resulted in less growth for the yeast, indicating higher toxicity, but no similar with the other basic residue. I concluded that βS-P123N and βS-P123R play a key role in toxicity in a strain-dependent manner (Figure 12A).

Aggregation is linked to toxicity

To capture the localization of the synuclein withing the yeast, I looked at the cells at three different time points, 6, 12, and 24 hours after inducing synuclein expression through galactose media using live-cell fluorescent microscopy. Initially at 6 hours, βS-P123H and βS-P123R are the only two showing foci-formation, while the others show a diffuse phenotype, followed by membrane-association and foci formation for βS, βS-P123H, βS-P123R, and βS-P123N at 12 hours (Figure 11C, 12C). Whereas βS-P123A, and βS-P123E displayed a diffuse and membrane-association phenotype. Lastly at 24 hours, most of them localized at the cytoplasm showing a diffuse phenotype, however, βS-P123H kept on showing foci-formation phenotype for some cells. With the foci-formation I provided further connections to the toxicity patterns in the serial dilution spotting. Basic and polar residues are key for aggregation seen across 24 hours. I confirmed this result with quantification.

Two one-way ANOVAs were performed across groups for foci formation at 6 and 12 hours (Figure 11D, 12D). The a value was adjusted to 0.0083, and Bonferroni post-hoc was performed in cases of statistical significance across the means of the samples. At 6 hours, analyses showed that for BY4741, $F(5,12) = 3.75$, $p = 0.03$, with the only significant difference between groups appearing with βS-P123N having significantly more foci than βS-P123A ($p = 0.04$), all other group comparisons were not significant. Differently, for W303, $F(5,12) = 18.11$, $p < 0.0001$, with higher expression in the W303 strain, more differences in presence of foci phenotype were seen across groups, despite the difference in toxicity patterns as compared to BY4741. Post-hoc showed βS-P123H having significantly more foci than bS, βS-P123A, and βS-P123E (Figure 11D, 12D).

The analysis revealed at 12 hours a significant difference between groups for BY4741, $F(5,12) = 59.16$, $p < 0.0001$, and W303 $F(5,12) = 62.08$, $p < 0.0001$. Further analysis demonstrated that for both strains there were significantly more foci on mutants βS, βS-P123H, βS-P123R, and βS-P123N (no statistical differences between these) as compared to βS-P123A and βS-P123E. Foci was also the dominant phenotype for the former samples at 12 hours, whereas for the latter two diffuse was more prominent (Figure 11D, 12D).

Expression does not influence toxicity

After identifying the PGK protein bands sufficiently even, I assessed the expression levels of βS and the βS-P123H substitution mutant proteins, which they were all expressed at the right band size (Figure 11B, 12B). I report that the βS-P123H substitution mutant synuclein proteins expression levels are unrelated to toxicity seen in the serial dilution spotting for the βS-P123H, βS-P123R, and βS-P123N. The toxicity and aggregation of the mutants is linked, the reason must be accounted for by a different mean.

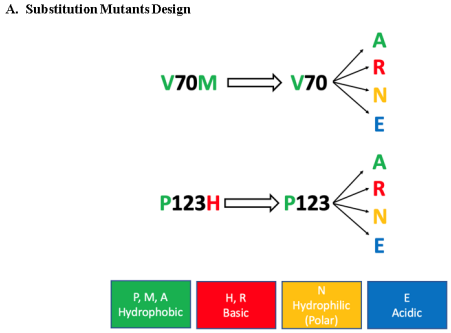

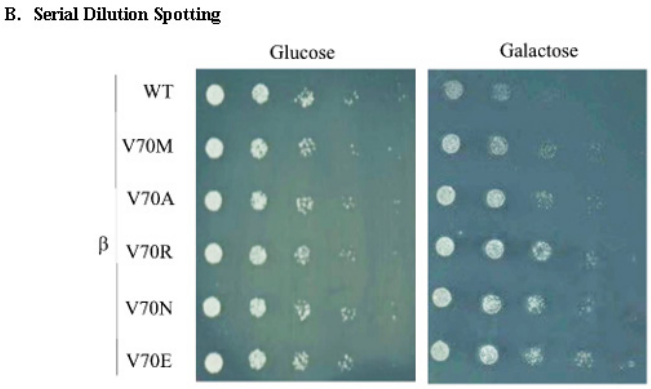

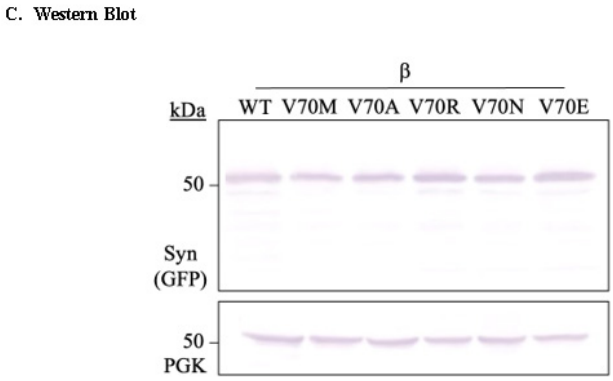

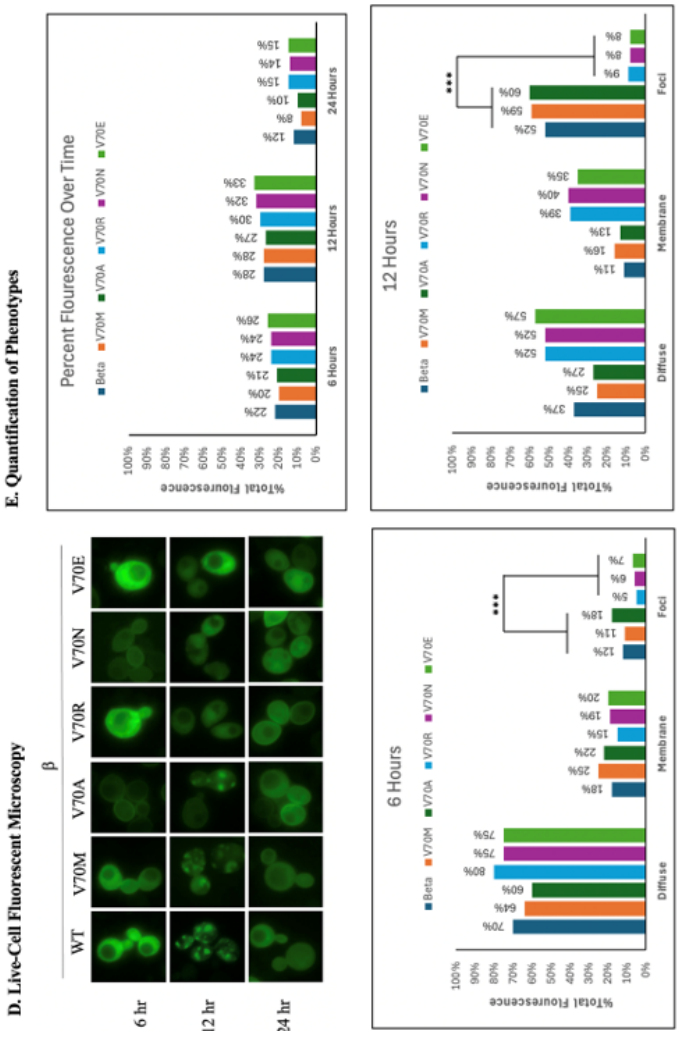

Figure 9: Characterization of V70 substitution mutants in BY4741
Substitution mutant Design. Four substitution mutants for each V70 and P123. When the amino acids are the same color, belonging to the same functional class, they conserved similar properties. When the amino acids are different colors, they lose each other properties.
Serial Dilution Spotting. Five-fold serial dilution spotting assay in BY4741 control yeast strain, expressing βS, V70M-βS, V70A-βS, V70R-βS, V70N-βS, and V70E-βS tagged with GFP. Each sample is spotted in plates containing SC-Ura Glucose (left, not expressing synuclein), and SC-Ura Galactose (right, inducing synuclein expression). The βS is used as positive control to compare growth with natural and substitution mutants. The natural mutant V70M-βS showed the most toxicity, followed by βS, and V70A-βS. In contrast, mutants V70R-βS, V70N-βS, and V70E-βS showed little toxicity compared to βS and the others. (n = 5 each in triplicates).
Western Blot. Trials were done at 12 hours after induction of the synuclein tagged with GFP through expressing media (SC-Ura Galactose). Expression was probed using GFP and PGK (loading control) antibodies. No differences in expression were seen across samples. (n = 3).
Live-Cell Fluorescent Microscopy. Images were taken 6 hr, 12 hr, and 24 hr after induction of the synuclein through expressing media (SC-Ura Galactose). The images are representative of the dominant phenotypes at these three timepoints for all samples. βS, V70M-βS, and V70A-βS form aggregates by 12 hours. Mutants V70R-βS, V70N-βS, and V70E-βS remain diffuse throughout all times. (n = 3).
Quantification of Phenotypes. The percentage of cells fluorescing cells was measured at 6, 12 and 24 hours by counting 1000 cells for each synuclein. These counts were analyzed by calculating total percentage of fluorescing, and if the counts passed a threshold of 20%, then they were analyzed using one-way ANOVA with an adjusted a, and Bonferroni post-hoc correction when needed. The phenotypes to classify were cytoplasmic diffuse, membrane bound, and foci (inclusions).

A. Serial Dilution Spotting

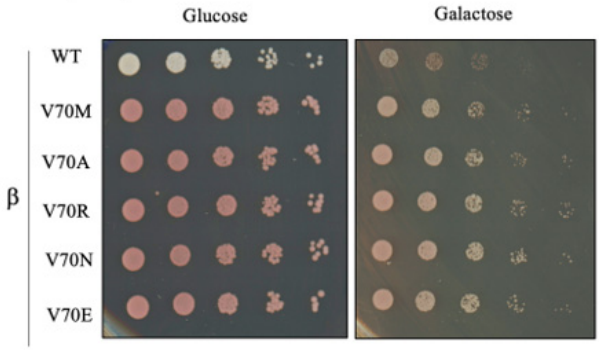

B. Western Blot

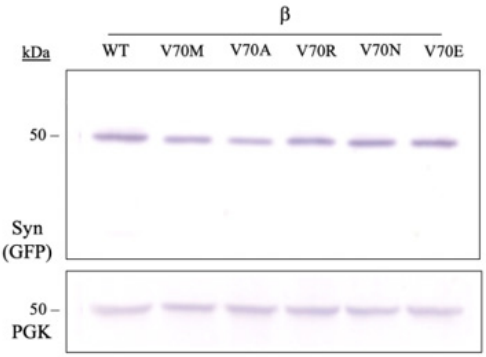

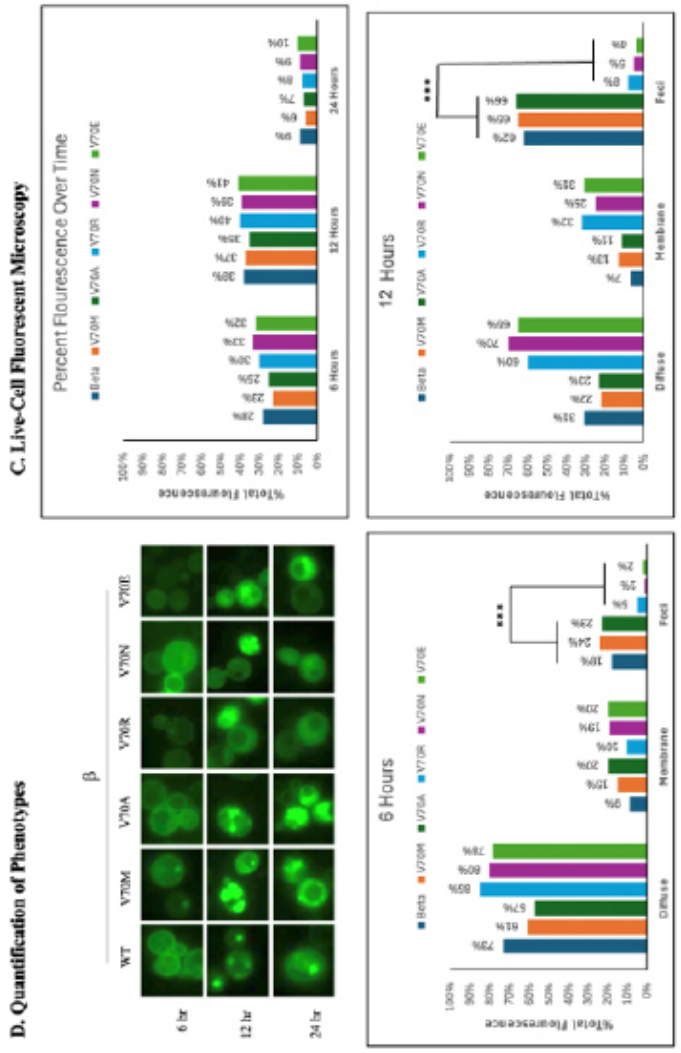

Figure 10: Characterization of V70 substitution mutants in W303
A) Serial Dilution Spotting. Five-fold serial dilution spotting assay in W303 control yeast strain, expressing βS, V70M-βS, V70A-βS, V70R-βS, V70N-βS, and V70E-βS tagged with GFP. Each sample is spotted in plates containing SC-Ura Glucose (left, not expressing synuclein), and SC-Ura Galactose (right, inducing synuclein expression). The βS showed the most toxicity followed by the natural mutant V70M-βS. V70A-βS shows less toxicity more similar to the other mutants V70R-βS, V70N-βS, and V70E-βS. (n = 5 each in triplicates).
B) Western Blot. Trials were done at 12 hours after induction of the synuclein tagged with GFP through expressing media (SC-Ura Galactose). Expression was probed using GFP and PGK (loading control) antibodies. No differences in expression were seen across samples. (n = 3).
C) Live-Cell Fluorescent Microscopy. Images were taken 6 hr, 12 hr, and 24 hr after induction of the synuclein through expressing media (SC-Ura Galactose). The images are representative of the dominant phenotypes at these three timepoints for all samples. βS, V70M-βS, and V70A-βS form aggregates by 12 hours. Mutants V70R-βS, V70N-βS, and V70E-βS remain diffuse throughout all times. (n = 3).
D) Quantification of Phenotypes. The percentage of cells fluorescing cells was measured at 6, 12 and 24 hours by counting 1000 cells for each synuclein. These counts were analyzed by calculating total percentage of fluorescing, and if the counts passed a threshold of 20%, then they were analyzed using one-way ANOVA with an adjusted a, and Bonferroni post-hoc correction when needed. The phenotypes to classify were cytoplasmic diffuse, membrane bound, and foci (inclusions).

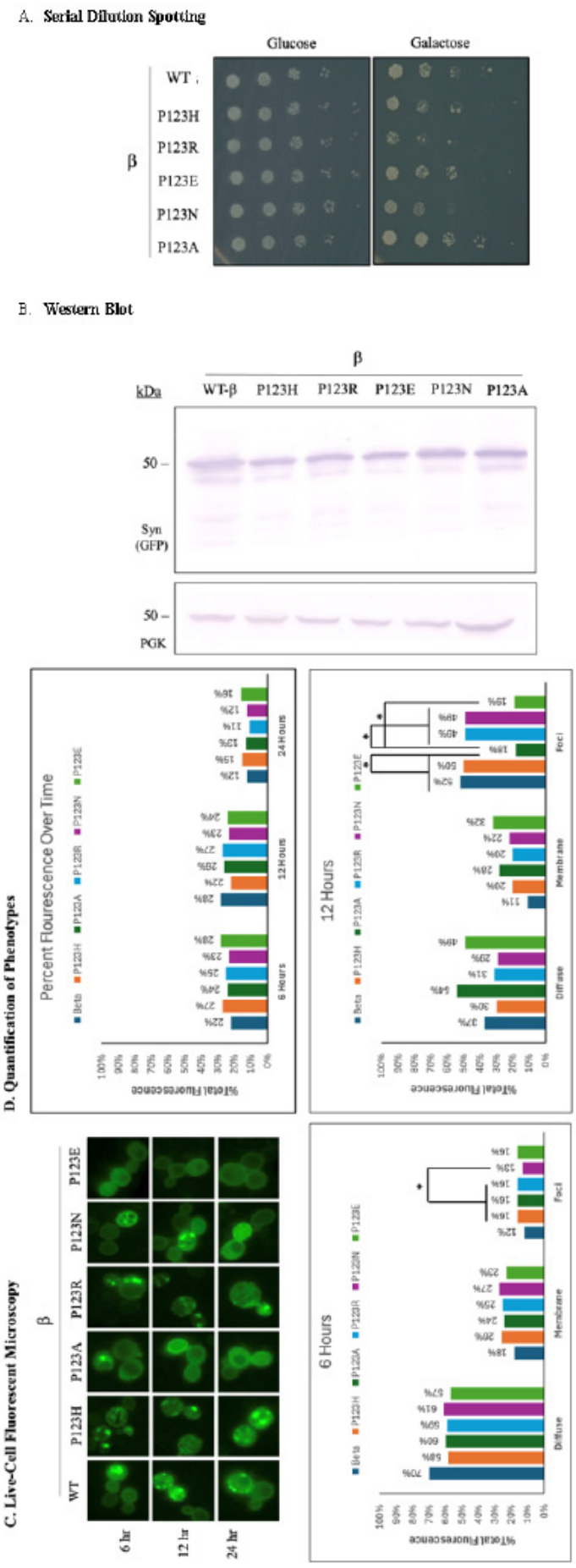

Figure 11: Characterization of P123 substitution mutants in BY4741

A) Serial Dilution Spotting. Five-fold serial dilution spotting assay in BY4741 control yeast strain, expressing βS, P123H-βS, P123R-βS, P123E-βS, P123N-βS, and P123N-βS tagged with GFP. Each sample is spotted in plates containing SC-Ura Glucose (left, not expressing synuclein), and SC-Ura Galactose (right, inducing synuclein expression). The natural mutant P123H-βS showed the most toxicity, with P123R-βS, and P123N-βS. In contrast, mutants P123E-βS showed similar toxicity profile as βS, and P123A-βS showed little toxicity compared to βS and the others. (n = 5 each in triplicates).

B) Western Blot. Trials were done at 12 hours after induction of the synuclein tagged with GFP through expressing media (SC-Ura Galactose). Expression was probed using GFP and PGK (loading control) antibodies. No differences in expression were seen across samples. (n = 3).

C) Live-Cell Fluorescent Microscopy. Images were taken 6 hr, 12 hr, and 24 hr after induction of the synuclein through expressing media (SC-Ura Galactose). The images are representative of the dominant phenotypes at these three timepoints for all samples. βS, P123H-βS, and P123R-βS form aggregates by 6 hours and continue across 24 hours. Mutant P123N-βS also shows aggregates by 12 hours, whereas mutants P123E-βS, and P123A-βS remain diffuse throughout all times. (n = 3).

D) Quantification of Phenotypes. The percentage of cells fluorescing cells was measured at 6, 12 and 24 hours by counting 1000 cells for each synuclein. These counts were analyzed by calculating total percentage of fluorescing, and if the counts passed a threshold of 20%, then they were analyzed using one-way ANOVA with an adjusted a, and Bonferroni post-hoc correction when needed. The phenotypes to classify were cytoplasmic diffuse, membrane bound, and foci (inclusions).

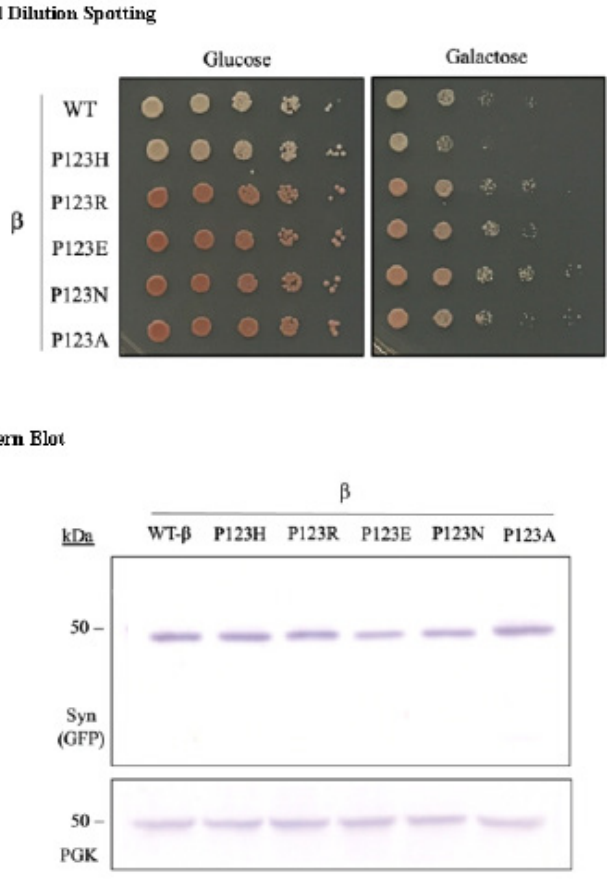

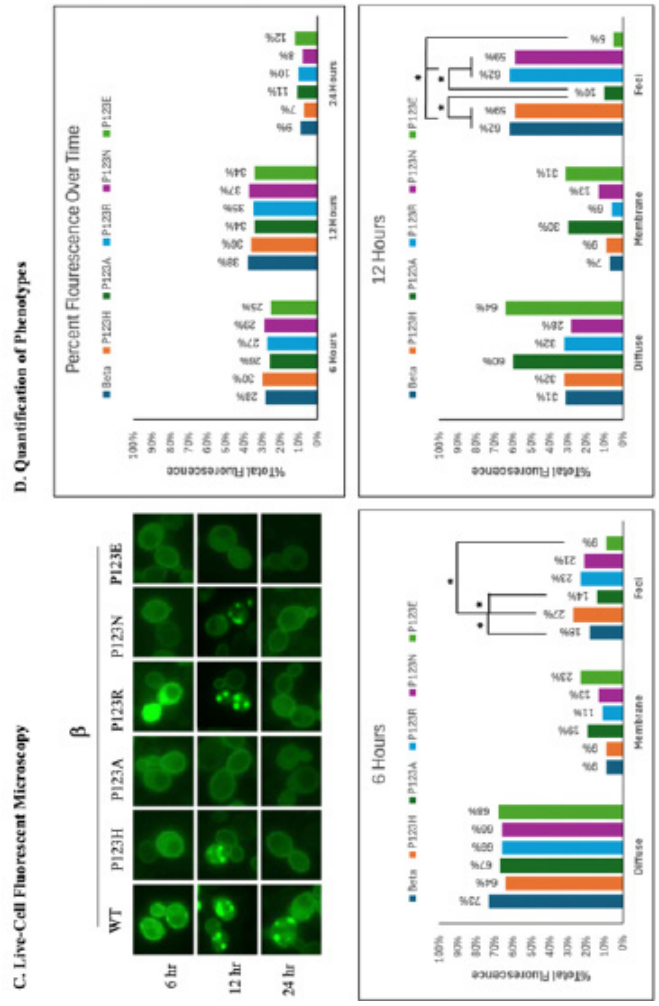

Figure 12: Characterization of P123 substitution mutants in W303
(A) Serial Dilution Spotting. Five-fold serial dilution spotting assay in W303 control yeast strain, expressing βS, P123H-βS, P123R-βS, P123E-βS, P123N-βS, and P123N-βS tagged with GFP. Each sample is spotted in plates containing SC-Ura Glucose (left, not expressing synuclein), and SC-Ura Galactose (right, inducing synuclein expression). The natural mutant P123H-βS was the most toxic out of all mutants compared to βS synuclein. All other mutants were relatively slightly less toxic than βS. (n = 5 each in triplicates).
B) Western Blot. Trials were done at 12 hours after induction of the synuclein tagged with GFP through expressing media (SC-Ura Galactose). Expression was probed using GFP and PGK (loading control) antibodies. No differences in expression were seen across samples. (n = 3).
C) Live-Cell Fluorescent Microscopy. Images were taken 6 hr, 12 hr, and 24 hr after induction of the synuclein through expressing media (SC-Ura Galactose). The images are representative of the dominant phenotypes at these three timepoints for all samples. βS shows aggerates across the 24 hours, only P123H-βS showed aggregation at 12 hours. All other mutants were diffuse throughout the 24 hours. (n = 3).
D) Quantification of Phenotypes. The percentage of cells fluorescing cells was measured at 6, 12 and 24 hours by counting 1000 cells for each synuclein. These counts were analyzed by calculating total percentage of fluorescing, and if the counts passed a threshold of 20%, then they were analyzed using one-way ANOVA with an adjusted a, and Bonferroni post-hoc correction when needed. The phenotypes to classify were cytoplasmic diffuse, membrane bound, and foci (inclusions).

Chapter 3

CHARACTERIZATION OF SYNUCLEIN SWAP MUTANTS IN YEAST
Part of the Gamma swap spottings in this chapter were obtained in collaboration with Leslie Casares '26

Experimental set-up
Nine genetic mutations in αS are linked with both sporadic and familiar forms of early-onset PD. Six of them are conserved in βS. For this reason, I wondered if introducing these swap mutations on them would regulate their aggregation, expression, and toxicity, and to what degree. If they did, it would help identify key amino acids that are critical regulators for their pathogenic potential. In chapter 1, I outlined my success in creating five αS -> βS swap mutants (A18T-βS, A29S-βS, G51D-βS, A53T-βS).
From the literature, I know two βS mutants (V70M and P123H) are linked with DLB patients. If they are inherently toxic to βS, I reasoned that they should also be toxic to αS. My Aim 2 is to introduce the two βS natural mutations into αS and investigate how they would regulate the aggregation, expression, and toxicity of αS. V70 is conserved in the same position in αS but P123 appears as P128 in the longer αS. In chapter 1, I outlined my success in creating both βS -> αS swap mutants (V70M-αS and P128H-αS). I also expanded my Aim 2 and introduced one of the βS natural mutations (V70M) and the genetic mutations of αS onto gS. My reason is I believed that they should make gS be toxic as they do with αS and βS. P123H natural mutation is not conserved in gS. In chapter 1, I outlined my success in creating αS and βS -> gS swap mutants (A18T-gS, A30P-gS, E46K-gS, and V70M-gS).
I characterized these ten successful mutants by assessing their toxicity, localization and expression in both yeast strains, BY4741 and W303.

αS à βS Mutants
βS swap mutants are differentially toxic
Firstly, I analyzed the glucose media plates, where no synuclein is expressed. I concluded that yeast growth was similar, and thus, all samples were equally diluted. For W303, I found that βS-A53T grew similar to βS, whereas the other mutants, βS-A29S, βS-A30P, and βS-G51D grew better than βS, making these three mutants reduce WT toxicity. In particular βS-A30P, grew the best out of all the swap mutants. When looking at the control strain BY4741, I found similar results with βS-A29S, βS-A30P, and βS-G51D that grew better than the βS, but no differences withing these three mutants. And I found that βS-A53T also grew similar to βS (Figure 14A).

βS swap mutants are differentially expressed
When looking at western blot to analyze protein expression (Figure 13B, 14B). The PGK bands, serving as loading control samples, were approximately the same size, indicating a reliable control. In the experimental condition probed with a GFP antibody, bands for all samples weren't the same thickness. aS expressed the most, and thus, why I see the link to higher toxicity. On the other hand, for the βS mutants, A53T-βS expressed the least in both strains. This result shows a decrease in protein expression for this mutant but does not confer a difference in toxicity with WT βS.

A53T-βS in W303 diminished expression after 24 hours
To investigate the link between toxicity and aggregation, I found that at 24 hours for A53T-βS in W303 there was a decrease in protein expression and fluorescence of the cells (Figure 15A, 15B). The yeast remained alive, as seen in the DIC software, but I saw no synuclein expression. Contrary for BY4741, A53T-βS still showed fluorescence at 24 hours. To further investigate the lack of fluorescence at 24 hours, I conducted a Western blot with 24 hours of synuclein induction for both BY4741 and W303 (Figure 15A). I report that for BY4741 after 24 hours, all synucleins were being expressed, surprisingly, with higher expression for A29S-βS, A30P-βS, and G51D-βS. This finding was a surprise because these mutants showed the least toxicity, and thus, I expected to see less expression as compared to the WT forms of the synucleins.
On the other hand, I show that in Western blot I found high expression for A29S-βS, A30P-βS, and G51D-βS, but no expression of A53T-βS – even if the PGK control also was lesser than the other (Figure 15A). Future assessments of these mutants I would like to look into the time point in which expression of the synuclein gets lost for A53T-βS. Furthermore, if the gain of toxicity is the cause of loss of expression, I surprisingly report that A53T-βS in the spotting assays does not show increase toxicity as compared to βS.
For this reason, I conducted fluorescent microscopy at 6, 12, and 16 hours for W303. I report that localization of the swap mutants' protein for A53T-βS is similar to bS, exhibiting inclusions from 12 hours onwards. Live cell imaging unveiled that although cells remained viable at 18 and 24 hours, there was no expression of the synuclein protein, and consequently, no fluorescence was observed (Figure 15B). I used timepoint 16 hours for the aS into βS swap mutants. This lack of fluorescence may be attributed to

the high toxicity of A53T-βS, prompting the yeast to eliminate the inserted plasmid for survival. Alternatively, the surviving cells may not have produced or initiated the production of the protein by the time of imaging.
In contrast, the localization for A29S-βS, A30P-βS, and G51D-βS displayed a distinctive phenotype of cytoplasmic diffusion over 24 hours, typically characterized as a health-associated phenotype (Figure 15C, 16C). I performed quantification for both strains at 6 and 12 hours. I show data at 6 hours in which there was a significant difference in BY4741, $F(5, 12) = 14.15$, $p < .001$, with aS having significantly more foci phenotype as compared to all other mutants, including A53T-βS ($p < 0.001$; Figure 15D, 16D).

For W303, there was also a significant difference, $F(5, 12) = 33.33$, $p < .0001$, aS having significantly more foci phenotype as compared to all other mutants ($p < 0.001$), as well as bS and A53T-βS also presenting more foci as compared to A29S-βS, A30P-βS, and G51D-βS. Even though diffuse was the most prominent phenotype at 6 hours, higher expression of the strain W303 was linked with differences in foci patterns between the WT synucleins, the A53T-βS, and the other swap mutants.
At 12 hours, I noticed these differences, since the most prominent phenotype for aS, bS, and A53T-βS was foci, while for A29S-βS, A30P-βS, and G51D-βS was diffuse. The phenotypes were for both BY4741, $F(5, 12) = 138.92$, $p < .0001$, and W303, $F(5, 12) = 218.12$, $p < .0001$. Surprisingly, only in W303 post-hoc analyses showed A53T-βS having significantly more foci than βS at 12 hours ($p < 0.001$). Based on these results, I am suggesting a strong link between toxicity, aggregation, and expression of the protein.

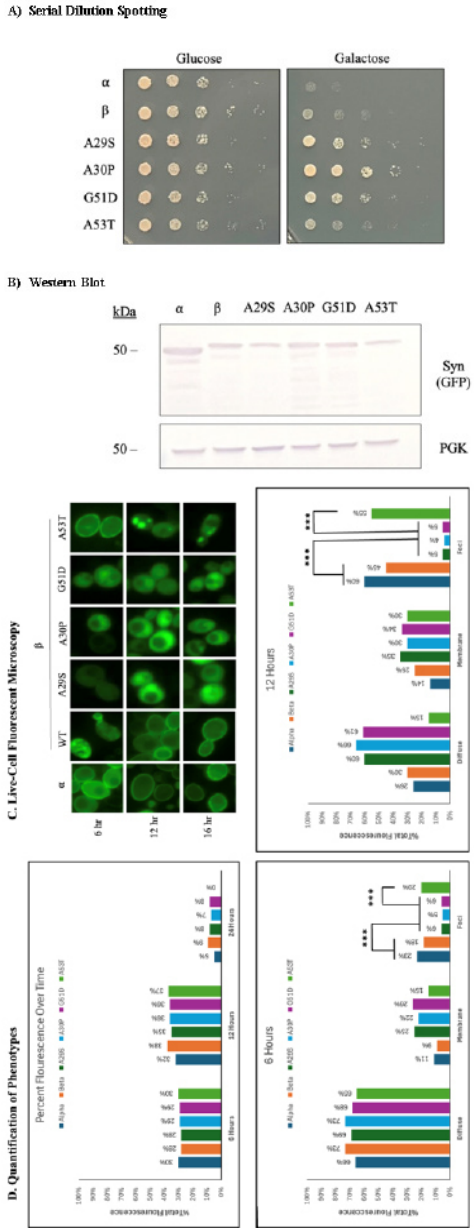

Figure 13. Characterization of Alpha into Beta-Synuclein Swap Mutants
A) Serial Dilution Spotting. Five-fold serial dilution spotting assay in control yeast, W303 expressing αS, A29S-βS, A30P-βS, G51D-βS, A53T-βS, and βS tagged with GFP spotted onto synuclein repressing (SC-Ura glucose) and promoting (SC-Ura galactose) media. (n=5)
B) Western Blot. Western Blot trials at 12 hours of synuclein expression for αS, A29S-βS, A30P-βS, G51D-βS, A53T-βS, and βS. Expression was probed using GFP antibody and PGK antibody as the loading control. (n=3)
C) Live-cell Fluorescent Microscopy. Images showing the dominant phenotypes for samples αS, A29S-βS, A30P-βS, G51D-βS, A53T-βS, and βS over 24 hours for three periods at 6, 12 and 16 hours after synuclein induction in SC-Ura galactose. (n=3)
D) Quantification of phenotypes. The percentage of cells fluorescing cells was measured at 6, 12 and 24 hours by counting 1000 cells for each synuclein. These counts were analyzed by calculating total percentage of fluorescing, and if the counts passed a threshold of 20%, then they were analyzed using one-way ANOVA with an adjusted a, and Bonferroni post-hoc correction when needed. The phenotypes to classify were cytoplasmic diffuse, membrane bound, and foci (inclusions).

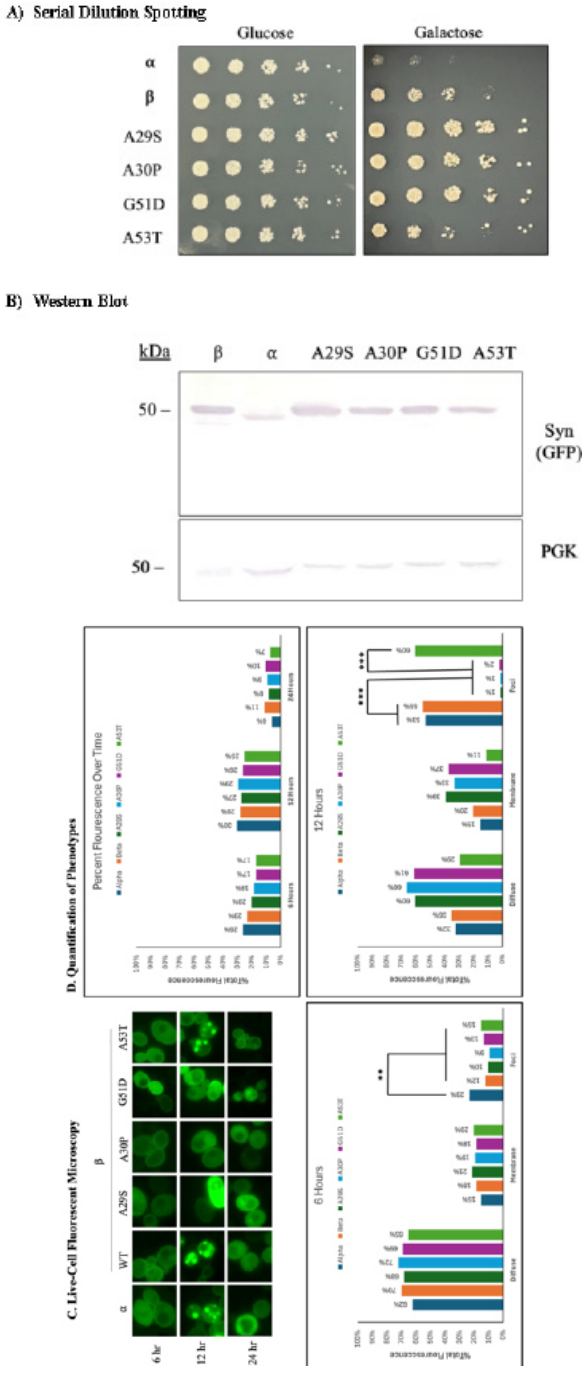

Figure 14. Characterization of Alpha into Beta-Synuclein Swap Mutants
A) Serial Dilution Spotting. Five-fold serial dilution spotting assay in control yeast, BY4741 expressing αS, A29S-βS, A30P-βS, G51D-βS, A53T-βS, and βS tagged with GFP spotted onto synuclein repressing (SC-Ura glucose) and promoting (SC-Ura galactose) media. (n=5)
B) Western Blot. Western Blot trials at 12 hours of synuclein expression for αS, A29S-βS, A30P-βS, G51D-βS, A53T-βS, and βS. Expression was probed using GFP antibody and PGK antibody as the loading control. (n=3)
C) Live-cell Fluorescent Microscopy. Images showing the dominant phenotypes for samples αS, A29S-βS, A30P-βS, G51D-βS, A53T-βS, and βS over 24 hours for three periods at 6, 12 and 16 hours after synuclein induction in SC-Ura galactose. (n=3)
D) Quantification of phenotypes. The percentage of cells fluorescing cells was measured at 6, 12 and 24 hours by counting 1000 cells for each synuclein. These counts were analyzed by calculating total percentage of fluorescing, and if the counts passed a threshold of 20%, then they were analyzed using one-way ANOVA with an adjusted a, and Bonferroni post-hoc correction when needed. The phenotypes to classify were cytoplasmic diffuse, membrane bound, and foci (inclusions).

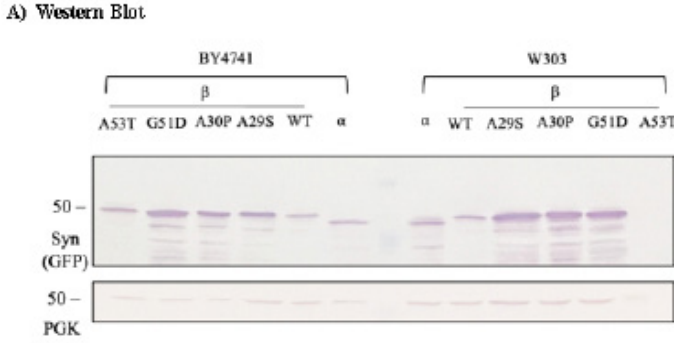

Figure 15. Comparison of Alpha into Beta-Synuclein A53T Swap Mutant for 24 hours
A) Western Blot. Western Blot trials at 24 hours of synuclein expression for αS, A29S-βS, A30P-βS, G51D-βS, A53T-βS, and βS for BY4741 and W303. Expression was probed using GFP antibody and PGK antibody as the loading control. (n=1)
C) Live-cell Fluorescent Microscopy. Images showing A53T-βS in W303 at 24 hours in DIC images (live-cells) and under blue light. (n=3)

βS à αS Mutants
αS swap mutants are differentially toxic
Figures 16A and 17A, depicting 5-fold serial dilution, illustrate that in glucose repressive media, without synuclein induction, yeast growth is similar, indicating an equal number of cells across samples. In the yeast control strains BY4741 and W303, under synuclein induction in galactose, V70M-αS appears as toxic as αS, whereas P128H-αS is as toxic as βS. However, neither of these mutants is more toxic than αS, suggesting that factors other than the change in amino acid contribute to the observed toxicity. Refer to figure 13A for spotting plates in the BY4741 control strain and figure 14A for W303.

αS swap mutants' toxicity linked with expression
Figure 13B (BY4741) and 14B (W303) displays the western blot results used to understand how expression influences toxicity. The PGK bands, serving as loading control samples, were approximately the same size, indicating a reliable control and the same number of cells. In the experimental condition probed with a GFP antibody, bands for V70M-αS and P128H-αS were thicker than those of αS and βS, revealing higher protein expression of the swap mutants.

Toxicity is linked to localization
Fluorescent microscopy at 6, 12, and 24 hours showed that the localization of the swap mutants' protein for V70M-αS is similar to αS, while localization for P128H-αS is more similar to βS for both BY4741 and W303 (Figure 13C, 14C). Both strains exhibit inclusions of protein forming at 12 hours and continuing for 24 hours for V70M-αS and αS, whereas P128H-αS and βS show inclusions at 12 hours and are mostly membrane-bound at 24 hours. Quantification was performed using one-way ANOVA and adjusted $\alpha = 0.0125$ to look at differences between group for aggregation (Figure 13D, 14D). For BY4741 at 6 hours, there was a significant difference between groups, $F(3, 8) = 5.97$, $p < .05$, specifically there was a marginal difference existed between αS and βS ($p = 0.05$), as well as V70M-αS and βS ($p = 0.05$). For these groups, αS and V70M-αS had marginally more foci than βS; no differences were found between any group and P128H-αS. For W303 at 6 hours, there wasn't a significant difference between groups, $F(3, 8) = 1.63$, $p = 0.26$; the most prevalent phenotype was diffuse.
After 12 hours, for BY4741, analysis showed a significant difference of $F(3, 8) = 5.57$, $p < .05$, with Bonferroni post-hoc determining the significant difference was V70M-αS showing more foci phenotype as compared to βS ($p < .05$). No other differences were found. Similarly, for W303 at 12 hours, $F(3, 8) = 17.87$, $p < .001$, having both αS and V70M-αS showing more foci phenotype as compared to βS ($p < .05$). This data suggests a through interpretation of the swaps' toxicities being linked with both aggregation into foci and higher expression, especially for V70M-αS that showed similar parameters to αS as compared to P128H- αS.

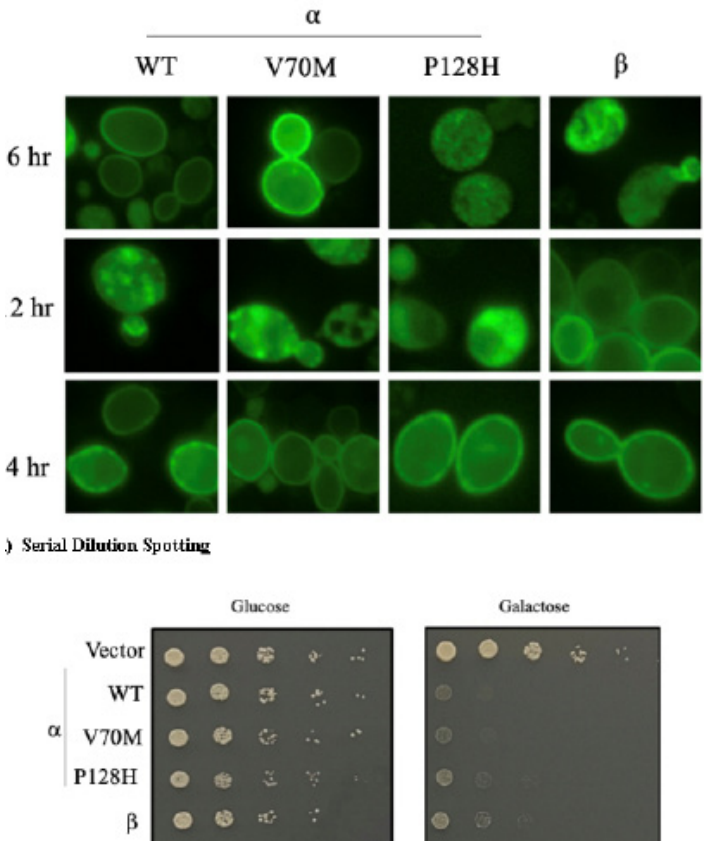

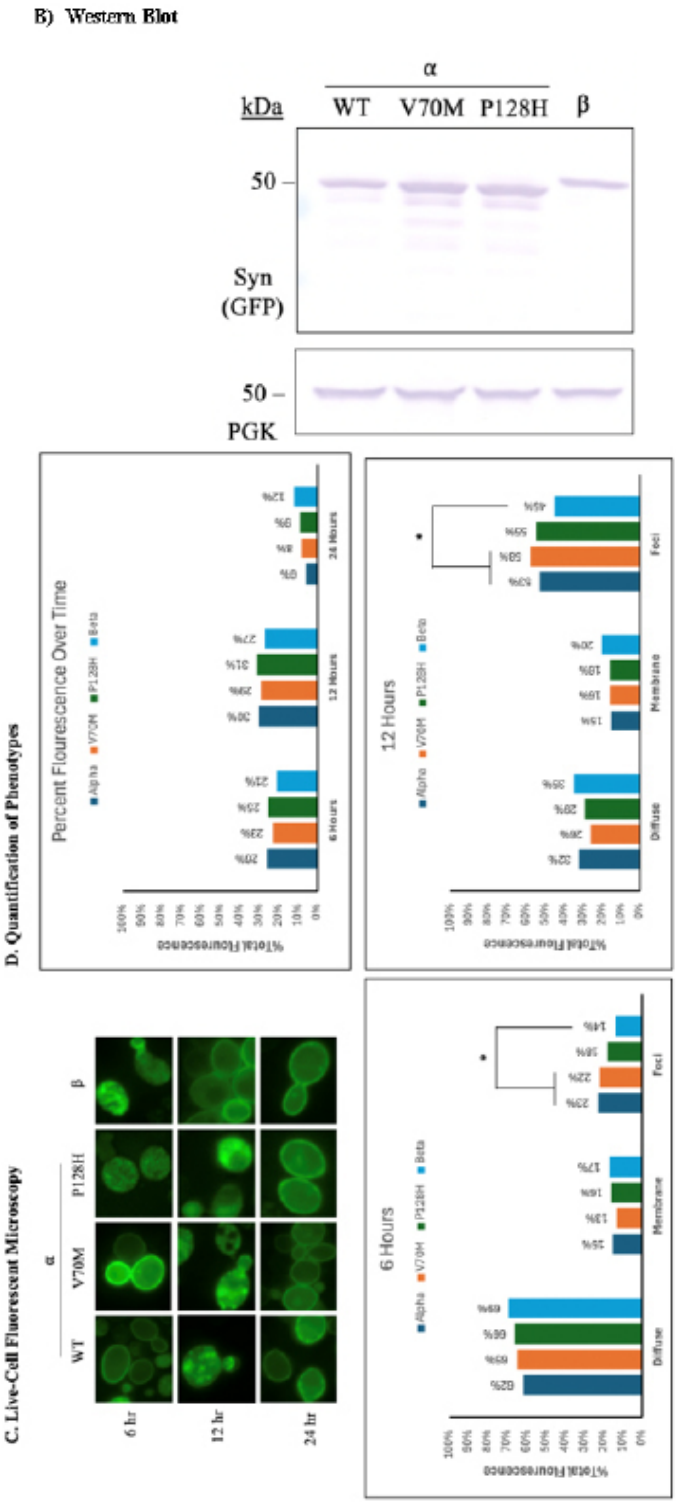

Figure 16. Characterization of Beta into Alpha-Synuclein Swap Mutants
A) Serial Dilution Spotting. Five-fold serial dilution spotting assay in control yeast, BY4741 expressing p426g vector, αS, V70M-αS, P128H-αS and βS tagged with GFP spotted onto synuclein repressing (SC-Ura glucose) and promoting (SC-Ura galactose) media. (n=5) B) Western Blot. Western Blot trials at 12 hours of synuclein expression for αS, V70M-αS, P128H-αS and βS. Expression was probed using GFP antibody and PGK antibody as the loading control. (n=3)
C) Live-cell Fluorescent Microscopy. Images showing the dominant phenotypes for samples αS, V70M-αS, P128H-αS and βS over 24 hours for three periods at 6, 12 and 24 hours after synuclein induction in SC-Ura galactose. (n=3)
D) Quantification of phenotypes. The percentage of cells fluorescing cells was measured at 6, 12 and 24 hours by counting 1000 cells for each synuclein. These counts were analyzed by calculating total percentage of fluorescing, and if the counts passed a threshold of 20%, then they were analyzed using one-way ANOVA with an adjusted a, and Bonferroni post-hoc correction when needed. The phenotypes to classify were cytoplasmic diffuse, membrane bound, and foci (inclusions).

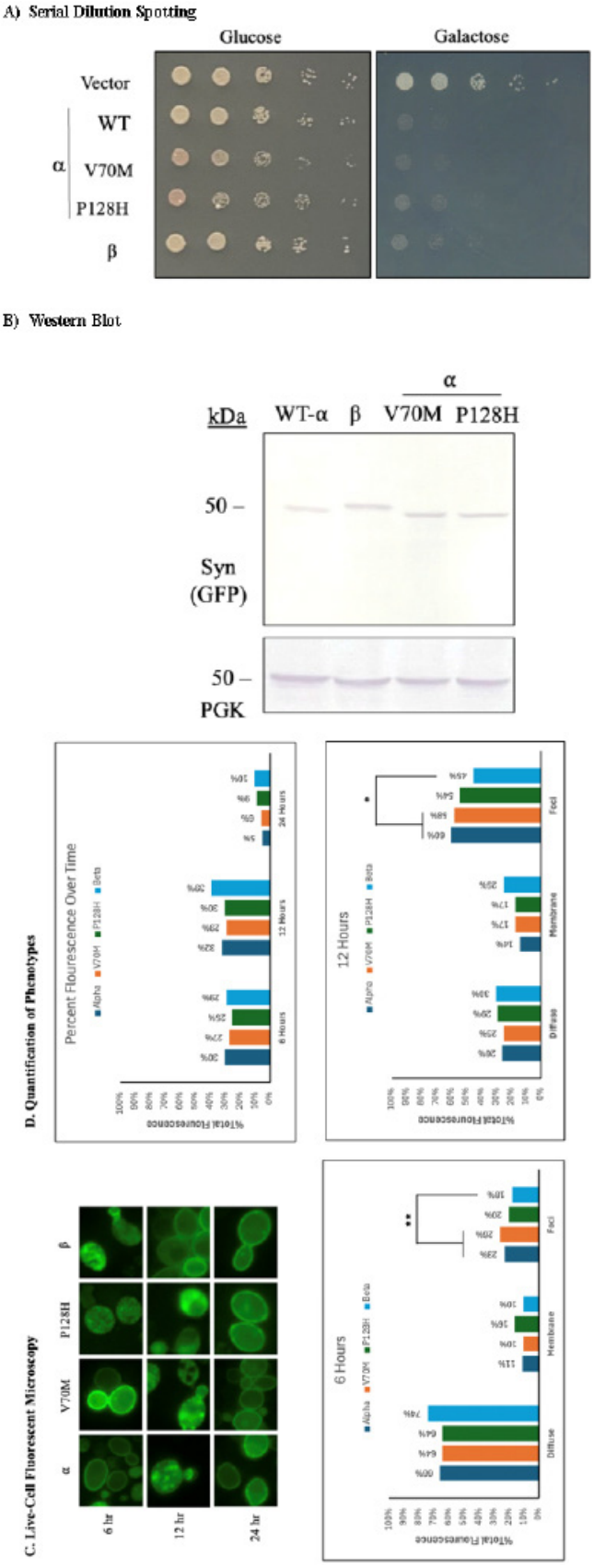

Figure 17. Characterization of Beta into Alpha-Synuclein Swap Mutants
A) Serial Dilution Spotting. Five-fold serial dilution spotting assay in control yeast, W303 expressing p426g vector, αS, V70M-αS, P128H-αS and βS tagged with GFP spotted onto synuclein repressing (SC-Ura glucose) and promoting (SC-Ura galactose) media. (n=5)
B) Western Blot. Western Blot trials at 12 hours of synuclein expression for αS, V70M-αS, P128H-αS and βS. Expression was probed using GFP antibody and PGK antibody as the loading control. (n=3)
C) Live-cell Fluorescent Microscopy. Images showing the dominant phenotypes for samples αS, V70M-αS, P128H-αS and βS over 24 hours for three periods at 6, 12 and 24 hours after synuclein induction in SC-Ura galactose. (n=3)
D) Quantification of phenotypes. The percentage of cells fluorescing cells was measured at 6, 12 and 24 hours by counting 1000 cells for each synuclein. These counts were analyzed by calculating total percentage of fluorescing, and if the counts passed a threshold of 20%, then they were analyzed using one-way ANOVA with an adjusted a, and Bonferroni post-hoc correction when needed. The phenotypes to classify were cytoplasmic diffuse, membrane bound, and foci (inclusions).

αS and βS à gS Swap Mutants

gS swaps do not induce gS toxicity

All swap mutants in gS showed similar growth in the glucose plates. Looking at W303 and BY4741, there was no toxicity induced by the mutations in gS, and no differences in growth with WT gS. They all remained non-toxic for both strains. See data in Figures 18A and 19A for BY4741 and W303, respectively.

Expression and localization are not affected by mutations in gS
Serial dilution spotting showed gS and the swap mutants to be growing the same when synuclein was expressed, and thus, none are toxic (Figure 18A, 19A). I investigate changes in expression using Western blot analysis, and I showed no differences in expression between the gS and the mutants, for either strain (Figure 18B, 19B). Lastly, I conducted microscopy analyzes showing no significant differences in phenotype between the gS and the swap mutants (Figure 18C, 18D, 19C, 19D). They all showed a cytoplasmic diffuse phenotype across 24 hours for both BY4741 and W303. Even though I showed a significant difference between groups on foci phenotype at 6 hours for both BY4741 and W303, $F(6, 14) = 126.3$, $p < 0.0001$, $F(6, 14) = 173.4$, $p < 0.0001$, respectively, the differences showed for higher foci in aS and bS compared to gS and the swaps ($p < 0.0001$ for all). At 12 hours, BY4741 and W303, $F(6, 14) = 234.7$, $p < 0.0001$, $F(6, 14) = 388.5$, $p < 0.0001$, respectively, indicating a significant difference once again between aS and WT-bS compared to gS and the swaps ($p < 0.0001$). Moreover, at 12 hours aS presented also significantly more foci phenotype as compared to WT-b for both strains ($p < 0.0001$). gS swaps lack of toxicity was reflected on their diffuse, health-associated state, phenotype all throughout the 24-hour timepoints.

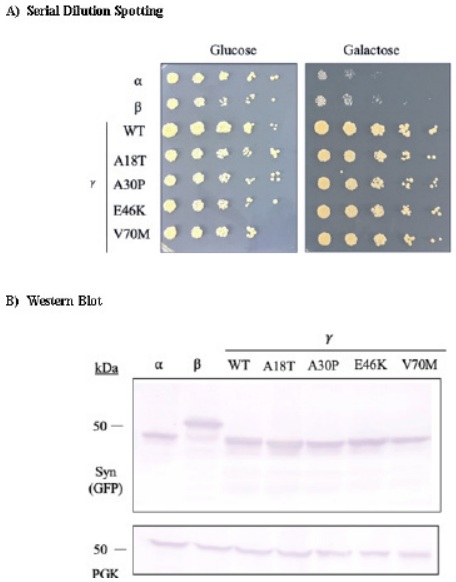

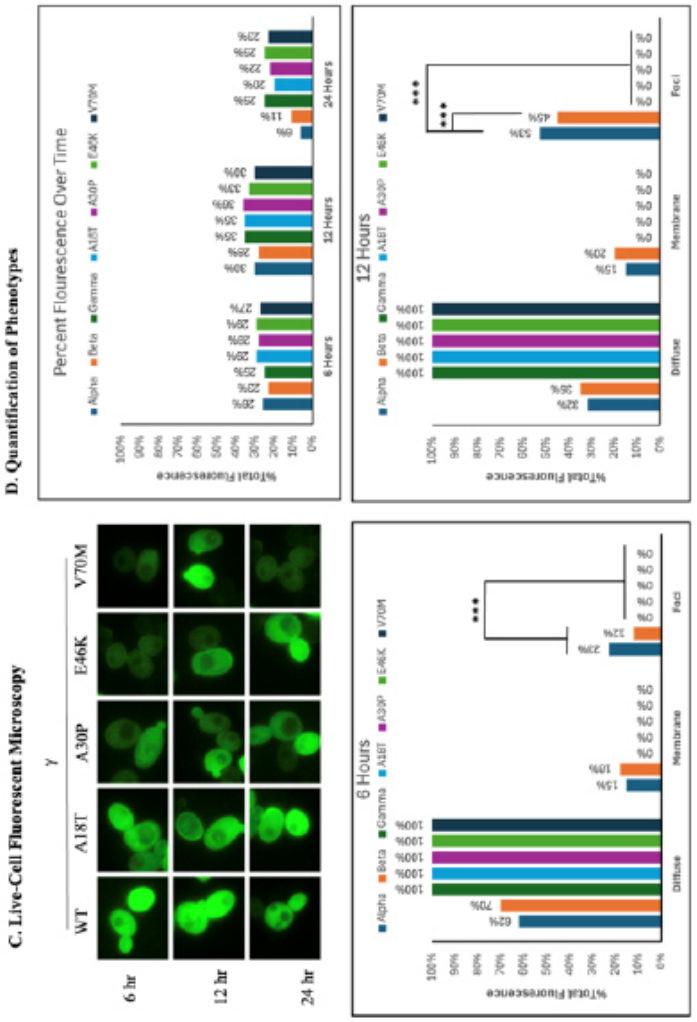

Figure 18. Characterization of Alpha- and Beta-Synuclein into Gamma-Synuclein Swap Mutants
A) Serial Dilution Spotting. Five-fold serial dilution spotting assay in control yeast, BY4741 expressing αS, βS, gS, A18T-gS, A30P-gS, E46K-gS, and V70M-gS tagged with GFP spotted onto synuclein repressing (SC-Ura glucose) and promoting (SC-Ura galactose) media. (n=5)
B) Western Blot. Western Blot trials at 12 hours of synuclein expression for αS, βS, gS, A18T-gS, A30P-gS, E46K-gS, and V70M-gS. Expression was probed using GFP antibody and PGK antibody as the loading control. (n=3)
C) Live-cell Fluorescent Microscopy. Images showing the dominant phenotypes for samples gS, A18T-gS, A30P-gS, E46K-gS, and V70M-gS over 24 hours for three periods at 6, 12 and 24 hours after synuclein induction in SC-Ura galactose. (n=3)
D) Quantification of phenotypes. The percentage of cells fluorescing cells was measured at 6, 12 and 24 hours by counting 1000 cells for each synuclein. These counts were analyzed by calculating total percentage of fluorescing, and if the counts passed a threshold of 20%, then they were analyzed using one-way ANOVA with an adjusted a, and Bonferroni post-hoc correction when needed. The phenotypes to classify were cytoplasmic diffuse, membrane bound, and foci (inclusions).

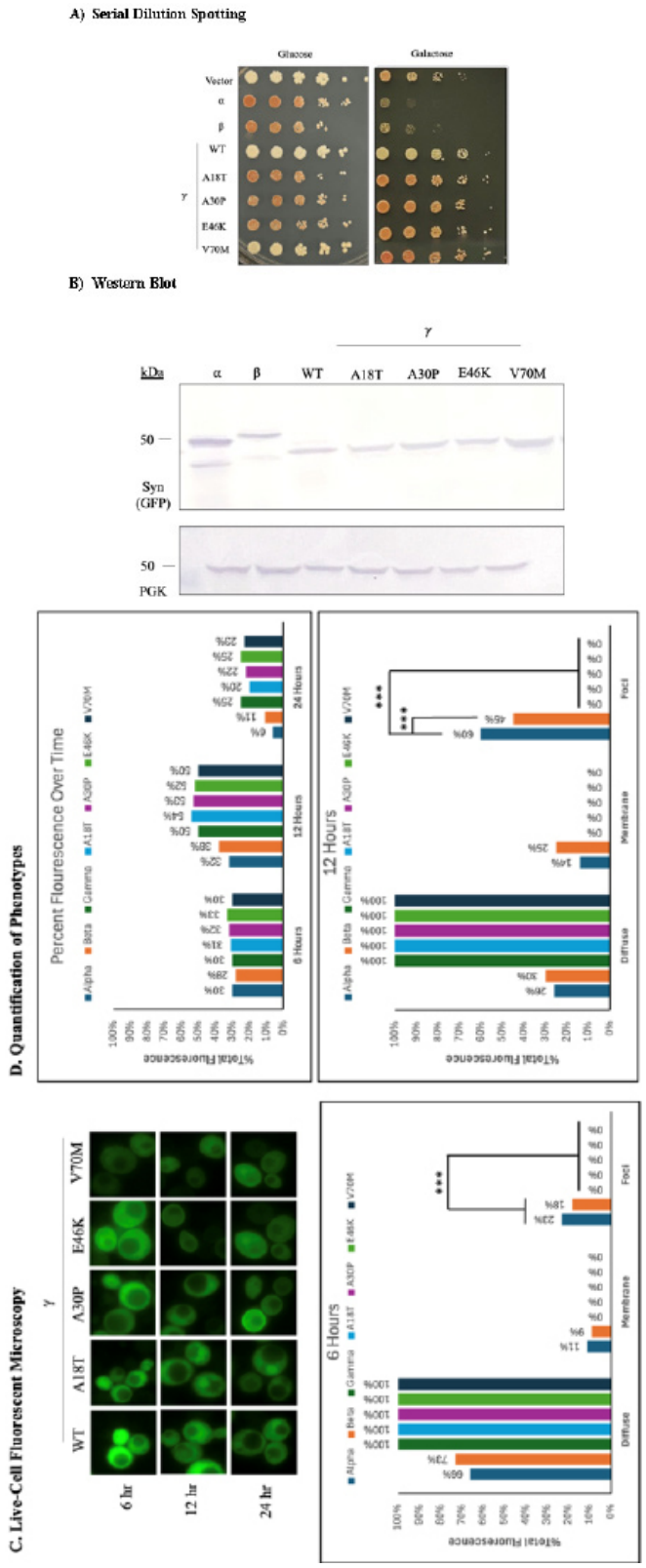

Figure 19. Characterization of Alpha- and Beta-Synuclein into Gamma-Synuclein Swap Mutants

A) Serial Dilution Spotting. Five-fold serial dilution spotting assay in control yeast, W303 expressing vector, αS, βS, gS, A18T-gS, A30P-gS, E46K-gS, and V70M-gS tagged with GFP spotted onto synuclein repressing (SC-Ura glucose) and promoting (SC-Ura galactose) media. (n=5)

B) Western Blot. Western Blot trials at 12 hours of synuclein expression for αS, βS, gS, A18T-gS, A30P-gS, E46K-gS, and V70M-gS. Expression was probed using GFP antibody and PGK antibody as the loading control. (n=3)

C) Live-cell Fluorescent Microscopy. Images showing the dominant phenotypes for samples gS, A18T-gS, A30P-gS, E46K-gS, and V70M-gS over 24 hours for three periods at 6, 12 and 24 hours after synuclein induction in SC-Ura galactose. (n=3)

D) Quantification of phenotypes. The percentage of cells fluorescing cells was measured at 6, 12 and 24 hours by counting 1000 cells for each synuclein. These counts were analyzed by calculating total percentage of fluorescing, and if the counts passed a threshold of 20%, then they were analyzed using one-way ANOVA with an adjusted a, and Bonferroni post-hoc correction when needed. The phenotypes to classify were cytoplasmic diffuse, membrane bound, and foci (inclusions).

Chapter 4

CHARACTERIZATION OF POST-TRANSLATIONAL SITE MUTANTS IN YEAST

Experimental set-up

We know αS toxicity is influenced by a variety of modifications, such as mutations, cellular environments, and post-translational modifications. Because αS is a heavily modified protein, we hypothesized that these post-translational modifications that enhance the well-established α-Synuclein toxicity, could act as conserved toxicity regulators for all synucleins. αS has known identified sited for each covalent modification, for example four nitration sites–Y39, Y125, Y133, and Y136. Using sequence alignment on conserved sites between αS, βS, and gS, I designed post-translational (PT) site mutants. For βS, mutants were created to block acetylation K6R, to mimic nitration Y39F, and to either mimic phosphorylation S118D or block it S118A. For gS, I created mutants to block acetylation K6R and to either block nitration Y39F or mimic it Y39C. The mutant K97R to block SUMOylation is still in progress and gS does not have a conserved site for phosphorylation. γS doesn't conserve any of the phosphorylation sites, and no literature has reported any site to be phosphorylated. A summary of all the mutations can be found in Chapter 1, along with the mutations that are still pending for PTM sites. With seven successful PTM site mutants, I assessed them by looking at toxicity and localization in yeast control strain W303. The other strain and expression were not yet assessed due to time constrains.

Beta-Synuclein Post-translational site mutants do not affect toxicity

On the glucose plates, growth was similar for all synucleins. In the galactose, synuclein-inducing media, I observed that all βS mutants were growing the same as βS (Figure 20A). I did not expect to see no changes for the βS PTM mutants based on how PTM affect αS. In particular, those PTM mutants that we hypothesized to be toxic, such as the K6R, showed no differential toxicity as compared to βS. In this case, we are blocking acetylation that reduces αS toxicity. Similarly, other mutants such as S118A blocking phosphorylation also showed no differences in toxicity, even when phosphorylation is related to enhancing toxicity. The other two, Y39F mimicking nitration and S118D mimicking phosphorylation were expected to show more toxicity than βS, but it did not. As mentioned, phosphorylation is considered a bad regulator, as well as nitration. I found this result puzzling; however, this data is the most preliminary data from my thesis. Therefore, before concluding another factor apart from mutations can influence βS toxicity, more repeats and more assays should be conducted.

Localization patterns of βS PTM site mutants are similar to WT βS

I analyzed the localization patterns of K6R-βS, Y39F-βS, S118A-βS, S118D-βS in comparison to WT βS at 6, 12 and 24 hours (Figure 20B). Diffuse was the most prevalent phenotype at 6 hours for all the synucleins, even though they presented some foci for all samples. After 12 hours, all mutants and wildtype form presented a more prominent foci phenotype, than migrated towards cytoplasmic diffuse after 24 hours. The trials were not quantified due to time constrains, but more assessments need to be done for the localization to draw aggregation conclusions about effects of PTM on bS.

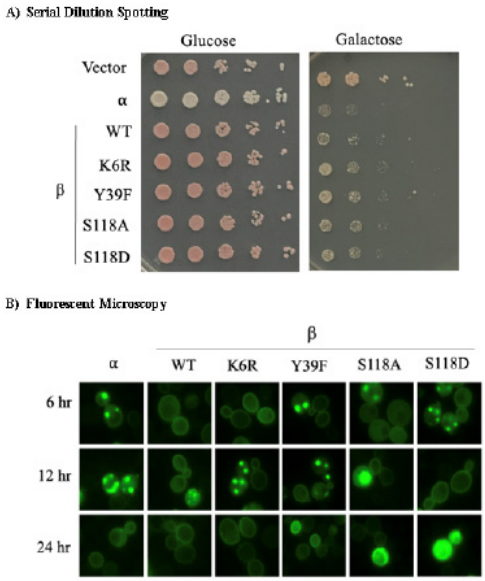

Figure 20. Characterization of PTM Site Mutants in Beta-Synuclein
A) Serial Dilution Spotting. Five-fold serial dilution spotting assay in control yeast, W303 expressing vector, αS, βS, K6R-βS, Y39F-βS, S118A-βS, S118D-βS tagged with GFP spotted onto synuclein repressing (SC-Ura glucose) and promoting (SC-Ura galactose) media. (n=5)
B) Live-cell Fluorescent Microscopy. Images showing the dominant phenotypes for samples gS, K6R-βS, Y39F-βS, S118A-βS, S118D-βS over 24 hours for three periods at 6, 12 and 24 hours after synuclein induction in SC-Ura galactose. (n=3)

g-Synuclein is nontoxic even with post-translational site mutants
After showing same rate of growth in the glucose plates, the experimental plates showed that the mutants K6R-gS, Y39C-gS, and Y39F-gS grew the same as WT gS (Figure 21A). The no differences in growth led me to conclude that regardless of the type of post-translational modification that gS undergoes, it remains nontoxic, as seen from the comparison with the empty control vector. Even though not as surprising as the PTM site mutants for βS, it still remains surprising that two mutants that have opposites effect on aS, do not regulate gS.
Localization patterns of gS PTM site mutants are similar to WT gS
I analyzed the localization patterns of K6R-gS, Y39C-gS, and Y39F-gS in comparison to WT gS at 6, 12 and 24 hours (Figure 21B). Diffuse was the most prevalent phenotype for all timepoints. I did not quantify phenotypes due to time constrains, but no presence of membrane bound, or foci were observed at any timepoint for gS and the PTM site mutants.

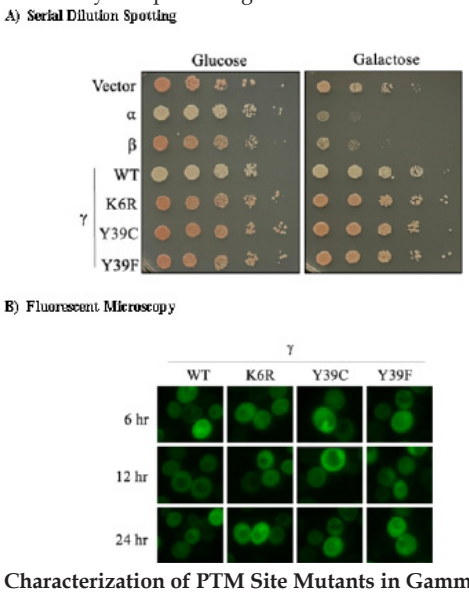

Figure 21. Characterization of PTM Site Mutants in Gamma-Synuclein
A) Serial Dilution Spotting. Five-fold serial dilution spotting assay in control yeast, W303 expressing vector, αS, βS, gS, K6R-gS, Y39C-gS and Y39F-gS, tagged with GFP spotted onto synuclein repressing (SC-Ura glucose) and promoting (SC-Ura galactose) media. (n=5)
B) Live-cell Fluorescent Microscopy. Images showing the dominant phenotypes for samples gS, K6R-gS, Y39C-gS, and Y39F-gS over 24 hours for three periods at 6, 12 and 24 hours after synuclein induction in SC-Ura galactose. (n=3)

Chapter 5

SYNUCLEINS IN ALTERED ENVIRONMENTS
Part of the results in this chapter were obtained in collaboration with Leslie Casares '26

Experimental set-up
A strong link exists between increased nitrative stress and PD pathology (Giasson et al., 2002; Danielson & Andersen, 2008; Stykel & Ryan, 2022). In our lab, several senior theses studied the effect of nitrative stress in different synucleins and their mutants. Emily Ong worked on the α-Synuclein mutants, H50Q, G51D, and A53E, reporting increase in toxicity with high nitrative stress (Ong, Thesis, 2017). Amanda Grassel continued this research by examining newer mutants of α-Synuclein, A18T, A29S, and A53V, demonstrating that elevated nitrative stress affected their toxicity differentially and influenced their localization over 24 hours (Grassel, Thesis, 2023). This work was followed by Tracey Nassuna, who in her thesis, began evaluating the effects of nitration on β, and its mutants. Nassuna reported a differential localization and toxicity for these natural mutants depending on the level of nitration (Nassuna, Thesis, 2023). Therefore, I aimed to continue our work and investigate if gS would also be differentially affected by altered nitrative stress.
Furthermore, other altered cellular environment modifying α-Synuclein's toxicity are glycation and acetylation. Glycation, for instance, heightens α-Synuclein's toxicity by attaching sugar molecules to its lysine residues, hindering its normal degradation and disrupting synaptic transmission (Vicente Miranda et al., 2017). Ultimately αS accumulates in presynaptic neurons. Conversely, acetylation acts protectively against α-Synuclein toxicity by inducing a transient structural change that reduces the formation of toxic aggregates. Previous research by Yoan Ganev in our lab showed that acetylation reduces α-Synuclein toxicity in yeast (Ganev, 2019). To further understand how cellular environments associated with PD regulate synuclein toxicity, I aimed to investigate the effects of acetylation and glycation on αS, βS, and γS.
To carry out this investigation, I introduced the necessary synucleins—αS, βS, βS-V70M, βS-P123H, and γS—along with the vector p426 into yeast strains with cox5aΔ (cytochrome c oxidase subunit 5a) and cox5bΔ (cytochrome c oxidase subunit 5b) knockout mutations to create high and low nitrative stress environments, respectively. Additionally, I introduced these constructs into sirt2Δ and glo1Δ yeast strains to manipulate acetylation levels and glycation, respectively. The sirt2Δ strain lacks the enzyme sirtuin-2, leading to a hyper-acetylation cellular environment, while the glo1Δ strain lacks the gene expressing the enzyme glo1, resulting in a hypo-glycation cellular environment. These strains were obtained from Open Bio Systems. Initially, I compared the knockout strains to the control BY4741 strain, which is well-characterized in our lab for these environments. To evaluate the potential effects of nitration on the synucleins, I conducted two assays: 1) five-fold serial dilution spotting and 2) GFP live-cell fluorescing microscopy.

High nitrative stress aggravates αS, βS, βS-V70M, βS-P123H, and γS toxicity
First, I examined αS and compared the control strain BY4741 to cox5aΔ and cox5bΔ strains as seen in Figure 22A. I found that nitration has a minor influence on αS well-established toxicity. Secondly, I found that βS in the cox5bΔ grew better as compared to the BY4741 control, indicating that low nitration plays a protective role for βS. Thirdly, I saw that γS in the cox5aΔ grew less well as compared to the BY4741 control showing that γS is toxic in a high nitrative stress environment. This finding supports my hypothesis that increasing nitrative stress would exaggerate the toxicity γS. Laslt, I also found that the natural genetic mutants βS-V70M and βS-P123H in cox-5bΔ grew better than BY4741, and βS-P123H particularly more sensitive to toxicity in cox5aΔ. This toxicity pattern suggests low nitration is protective against the natural mutant's toxicity, just as in βS.
Increased nitrative stress affects localization slightly
I evaluated the potential impact of altered nitration on the synucleins by

conducting live-cell fluorescent microscopy at 6, 12, and 24 hours (see Figure 22B). I used this method to investigate whether the observed differences in toxicity in the spotting assays could be linked to nitration-induced changes in localization. While quantification is necessary for assessing phenotypes accurately, my initial observations showed that at 6 hours, only αS exhibited some foci in the cox5aΔ strain, however more diffusely distributed across all strains (Figure 22B). Interestingly, I observed that αS and βS in cox5bΔ showed less aggregates at 12 hours as compared to BY4741. Moreover, I found that across the 24 hours, γS exhibited a diffuse phenotype for all strains. This finding suggests that if γS indeed exhibits toxicity in cox5aΔ, the toxicity is not due to the presence of large visible aggregates as observed in other mutants. I need to conduct more repeats and quantification for βS-V70M and βS-P123H before making a conclusion, but βS-P123H might show less aggregates than BY4741 for cox5bΔ. Other factors, such as protein expression levels, may also contribute to the enhanced toxicity observed for the synucleins.

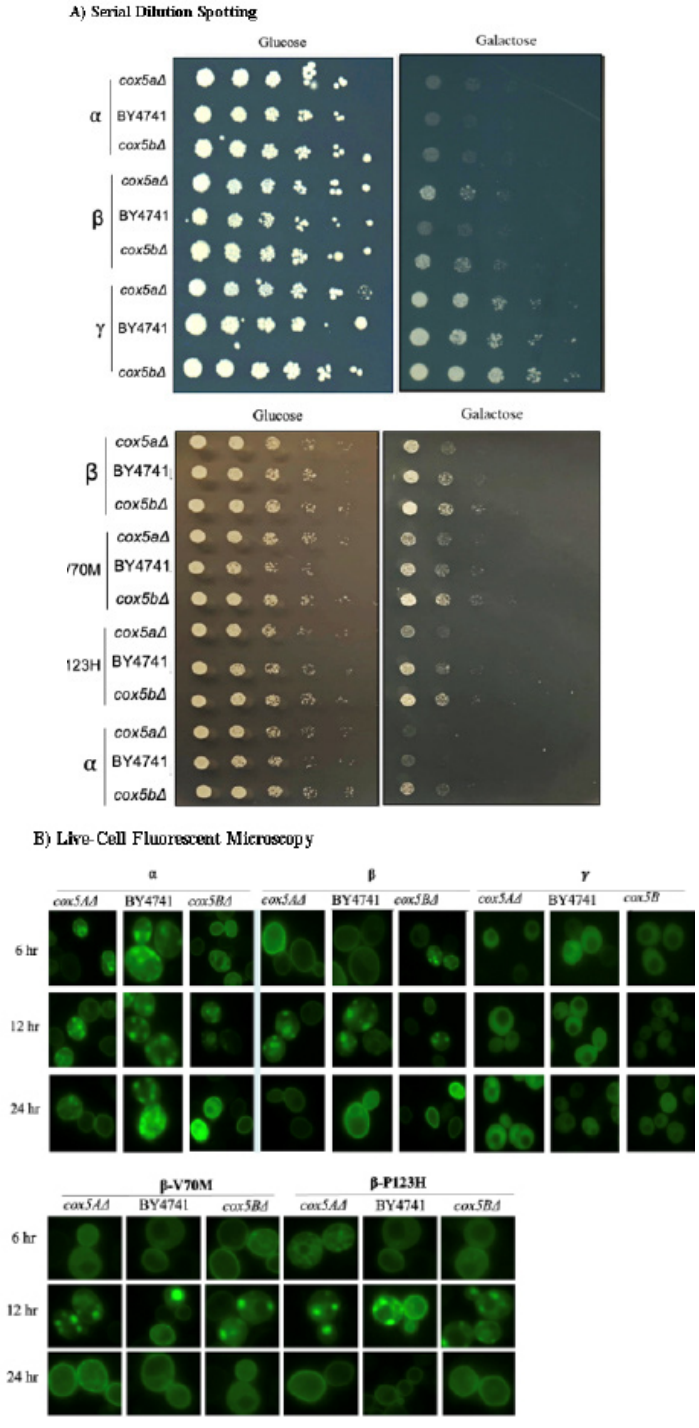

Figure 22. Synucleins and β-Synuclein Mutants in Altered Nitration Environment

A) Five-Fold Serial Dilution Spotting. Two sets of spottings with yeast expressing α-, β-, and g-synucleins in cox5AΔ, (high nitrative stress), BY4741, and cox5BΔ (low nitrative stress). Followed by another set of yeast expressing β-, β-V70M, β-P123H, and α- in same strains. Samples were spotted onto repressing (SC-Ura Glucose) and inducing (SC-Ura Galactose) media. (n = 5)

B) Live-cell Fluorescent Microscopy. Images showing the dominant phenotypes for α-, β-, β-V70M, β-P123H, and g- over 24 hours in cox5aΔ, BY4741, and cox5bΔ. Timepoints are 6, 12 and 24 hours after induction of synuclein expression in SC-Ura galactose. (n=4)

Altered glycation and acetylation do not unlock differential toxicities in synucleins

To further understand the toxicity differences between the synucleins in high acetylation and low glycation environments, I performed serial dilution spottings (Figure 23A). Firstly, I found that the vector's growth on glo1Δ and sirt2Δ was improved as compared to control BY4741, establishing that decreased glycation and increase acetylation make yeast grow better. Secondly, I found that αS and gS grow slightly better in glo1Δ and sirt2Δ suggesting a minor protective role. On the other hand, βS grows better in glo1Δ and sirt2Δ as compared to BY4741, indicating that the altered environments play a protective role, supporting my hypothesis that increasing acetylation and decreasing glycation would protect against the synucleins' toxicity, in some cases (αS and gS) with a minor effect. Additionally, because of time constrains, I didn't assess V70M-β and P123H-β, but for future studies I will perform the same assays on the natural mutants.

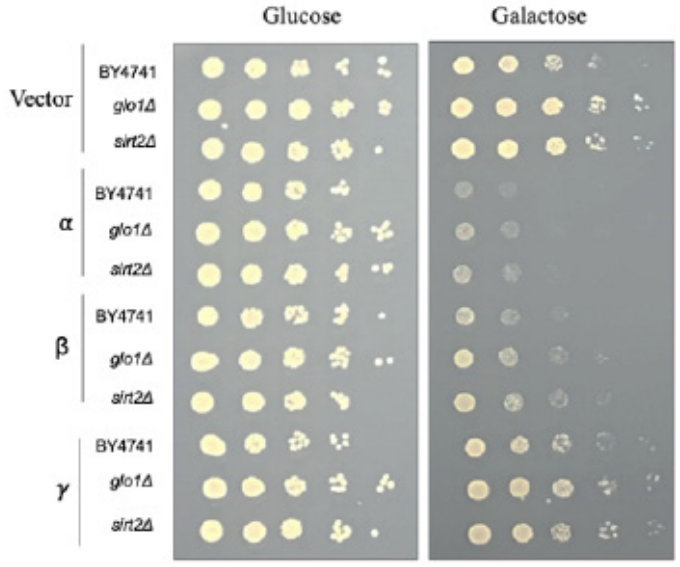

Figure 23. Synucleins in Altered Glycation and Acetylation Environments

A) Five-Fold Serial Dilution Spotting. Two sets of spottings with yeast expressing α-, β-, and g-synucleins in BY4741, glo1Δ (high glycation), and sirt2Δ, (high acetylation). Samples were spotted onto repressing (SC-Ura Glucose) and inducing (SC-Ura Galactose) media. (n = 3)

DISCUSSION

In 1817, James Parkinson provided the first description of PD, labeling it the "Shaking Palsy." This landmark observation led to the identification of aS in Lewy bodies as the underlying pathology not only for PD but also for other synucleinopathies, which became the second most prevalent and debilitating neurological disorders worldwide. Although mutations in aS and βS are responsible for only a fraction of cases, comprehending their role and gS in pathology provides crucial insights into synucleinopathies. My thesis aimed to explore the cellular toxicity, localization, and expression of βS, βS mutants, and gS in previously unexplored conditions. I found: 1) β-Synuclein and mutants are toxic and aggregate in yeast in a

strain dependent manner 2) For β-Synuclein V70M mutant hydrophobicity is key to toxicity 3) For β-Synuclein P123H mutant gain of basic amino acid is key to toxicity and aggregation 4) β-Synuclein familial mutants swapped into α-Synuclein are differentially toxic to a-Synuclein 5) a-Synuclein familial mutants swapped into b-Synuclein differentially affect β-Synuclein toxicity and localization 6) g-Synuclein is nontoxic and cytoplasmically diffuse, even when swapped with a- and β- synuclein natural mutants 7) High nitrative stress makes g-Synuclein and β-Synuclein natural mutants toxic. Decreased glycation and increased acetylation are protective of β-Synuclein's toxicity.

β-Synuclein and mutants are toxic in yeast in a strain dependent manner
My most important thesis finding is that the βS mutants are more toxic than wildtype βS. I hypothesized that these, V70M and P123H, would show more toxicity that wildtype βS considering they are directly linked with patients of DLB. This work was in collaboration with Ryan Osselborn '23 and Tracey Nassuna '23, whose findings support this hypothesis, but only in a strain dependent manner. Osselborn first showed that when tagged with GFP, in both control yeast strains, αS was more toxic than βS and γS was not toxic (See Appendix B). Nassuna followed his work and showed evidence that the βS mutants, V70M and P123H, were more toxic than βS in W303 (See Appendix C). Osselborn '23 also looked at αS, βS, and γS in an emGFP tagged system, but all the synucleins showed no difference and were nontoxic (See Appendix B). We investigated the differences in toxicity between systems and found, through Western blot, that GFP system expressed more protein than emGFP. Therefore, the level of toxicity and aggregation of the synucleins is linked to the expression level of the system.

The observed differences in toxicity, influenced by expression levels, correspond with the literature linking higher expression to worse disease prognosis. Research shows that a triplication in the SNCA gene locus is sufficient to cause earlier disease onset and accelerate progressive symptoms in patients with PD and DLB (Singleton et al., 2003). Furthermore, research shows higher expression of aS leads to higher accumulation of the protein that resides withing the mitochondria complex I, decreasing its function, which is critical for cell survival (Nakamura et al., 2008; Liu et al., 2009). Top of Form
Furthermore, we observed for the GFP and emGFP tagged systems, they have a different kozak sequence. The former one has a yeast kozak sequence, while the latter one a mammalian one. This sequence is upstream to the SNCA/SNCB/SNCG genes that gets transcribed into the RNA and controls the binding of the ribosome to the mRNA for translation. This observation led us to hypothesized that the difference in the sequence affected expression, and thus, we created a new vector with the emGFP tagging and the yeast kozak sequence for all synucleins. Sebastian Gacek's '25 tested this hypothesis and found: 1) aS recovered its toxicity partially, whereas bS remained non-toxic 2) Expression of the synucleins was similar to emGFP system with low expression. Therefore, the exact kozak sequence matters to a minor degree. The difference in the expression is a bonus to the lab because we can study enhancers of toxicity through the low expression system, and repressors of toxicity in the high expression system. See appendix D for results.

For b-Synuclein V70M mutant hydrophobicity is key to toxicity and aggregation

For the substitution mutants, I hypothesized that both the loss and gain are important for βS-V70M. This is to say, I hypothesized that toxicity is driven by a hydrophobic amino acid, based on the evident that both bS – valine - and the natural mutant βS-V70M – methionine - contain a hydrophobic residue at position 70th. One of my most important findings is that hydrophobicity is key for βS-V70M toxicity and aggregation, supporting my hypothesis. In the V70M substitution mutant set-in budding yeast, V70A changed the most in phenotype as it was for the most part foci. Toxicity analyses showed V70A substitution to be the only one that resembled βS and βS-V70M toxicity pattern. This data suggests the amino acid's hydrophobicity is important.
My findings are consistent with in vitro work that examined V70M and P123H mutations and suggested that the bS natural mutants have enhanced membrane-binding affinity as compared to bS, but less than aS (Sharma et al., 2020). The increase on membrane-binding affinity, although not exclusively, it was reported to increase propensity of aggregation for these mutants. Additionally, for V70M, analysis showed the protein undergoes perturbations in the region of the mutation, such as residues S64, L66-G68, and F71–N76 (Sharma et al., 2020). These perturbations could be a result of having methionine with a larger side chain than valine, altering the structure of the protein. Hence, the alteration of the protein's structural conformation is hypothesized to also change the susceptibility of βS-V70M and βS-P123H to aggregation as compared to βS. There are no papers about βS-V70M substitutions; I am the only one who has mutated and characterize them. Therefore, more work and analyzes of each amino acid has to be done before definitive conclusions are made.

For b -Synuclein P123H mutant gain of basic amino acid is key to toxicity
My second most important funding is that gain of the basic and polar residues are key for P123H toxicity. I hypothesized that the loss of proline would lead to the toxicity seen in bS-P123H. Research shows evidence that proline contributes to a larger chain of polyproline II linked to the inhibition of oligomerization and aggregation, providing the protein with stability (Samuel et al., 2000). Because of this, I expected to see the substitution mutants would show similar toxicity as the natural mutant P123H. My research doesn't show this. I reported that only the substitutions P123R and P123N presented same toxicity and aggregation profile as the WT and P123H mutant. For both foci appeared at 6 hours, and it was the most dominant phenotype by 12 hours. This pattern suggests that for the mutant's toxicity the presence of a basic residue is important, both P123H and P123R are basic amino acid residues; and polarity matters at the amino acid 123rd. Furthermore, proline at 123rd amino acid does not seem to play a role in aggregation for bS. This property is evident in the substitution mutants P123A and P123E. Both lost the proline but presented a significantly diffuse phenotype throughout 24 hours as compared to the other mutants. Current literature showcases the importance of proline as the driven factor of toxicity due to the absence of the PPII secondary structure of bS (Janowska & Baum, 2016). Researchers report that the mutation leads to a more flexible unfolded C-terminus, hence the increase in aggregation-prone properties that resemble those of aS, which could still play a role in the toxicity seen for P123R and P123N but wouldn't explain why P123A and P123E did not show toxicity or aggregation. In the case of P123E, the change from proline to glutamic acid, an acidic amino acid, could confer more acidic residues to the already high in acidic residue C-terminus (Vargas & Chandra, 2014). Even P123A, with a hydrophobic amino acid residue – commonly associated to aggregation – no foci were seen, leading to report that hydrophobicity does not matter at this position as much as others for protein aggregation. Furthermore, the gain of the positively charged amino acid histidine, or arginine in the case of the substitution mutant, might indicate for the protein structure that a positive charge joining another negatively charged residue could potentially create new salt bridges. The appearance of new structures, and salt bridges could explain the differences in localization of the protein. For future assessments, I would like to evaluate these properties in other substitution mutants with the other basic amino acid, lysine, other polar amino acids, and glycine. The latter one is important to see how the properties of proline, even though different from glycine (very flexible), matter for the structure and folding of the protein.

Unlike the current studies only looking at P123H, my work is comprehensive of all functional classes of amino acids at position 123rd. Furthermore, my work is done on the mutants' properties in a living organism, yeast. Thus, my work provides strong support that the gain of histidine is key for toxicity; especially the gain of a basic or polar residue make bS toxic.
Similarly, to V70M substitutions, my thesis is the first to do a substitution analysis on P123H, and thus, more thorough analysis of each amino acid is still required to make definitive conclusions about structure and bonding.

β-Synuclein familial mutants swapped into α-Synuclein are differentially toxic to a-Synuclein

My third most important finding is that specific amino acids regulate αS's toxicity and aggregation. I hypothesized that introducing bS mutations into aS would make the latter one more toxic. V70M and P123H are two mutants related to the aggregation and toxicity of bS – a protein not as toxic as aS – then, these would also enhance aS's toxicity providing more support for their role in pathology. To evaluate this hypothesis, I created swap mutants using mutagenesis, and created the variants V70M-αS and P128H-αS following protein alignment and when V and P were con-

served. I reported that the mutants made aS differentially toxic as compared to aS. Firstly, I observed that both V70M-αS and P128H-αS show aS toxic. Secondly, I found that V70M-αS was similarly toxic to aS, while P128H-αS more to WT bS. Even though these findings show evidence for the importance of these sites for localization and toxicity, my hypothesis was partially supported. aS did not become more toxic with the mutations but showed further evidence to say that amino acid V70th is critical for toxicity. When V70 was mutated in aS and bS toxicity and aggregation was influenced. Not surprisingly because aS is already toxic, and not all aS mutations linked with synucleinopathies show more toxicity than aS in yeast. For example, A30P, which was reported to attenuating aggregation and membrane binding of aS (Zhang et al., 2019). As well as, both members from our lab and others reporting A30P cytoplasmic diffuse and not toxic in yeast (Outeiro et al., 2003; Brandis et al., 2006; Sharma et al., 2016). This finding suggests other modifications to the proteins aside from mutation drive toxicity and aggregation, such as altered cellular environments involving covalent modifications or post translational modification.

a-Synuclein familial mutants swapped into b-Synuclein differentially affect b-Synuclein toxicity and localization

My fourth important findings are that mutations of aS when swapped into bS, make the latter one differentially toxic, and thus, A29, A30, G51, and A53 matter and regulate bS toxicity. I hypothesized that these single amino acids could act as conserved toxicity regulators for the synucleins, and would be sufficient to differentially affect bS. My findings showed that when swapping A53T-bS it showed increased aggregation, but not enough to make the swap mutant as toxic as aS.

On the other hand, I observed that A29S-bS, A30P-bS, and G51D-bS have a protective phenotype reducing bS toxicity levels. They also significantly changed bS aggregation as they showed diffuse phenotype across the 24 hours. My hypothesis was not fully supported as neither of the swaps were more toxic bS. These mutations are present in patients, and they should be more toxic, but this finding is not entirely surprising. As mentioned before, αS mutations such as A30P and G51D are nontoxic and decrease aggregation in yeast, as well as in other model organisms for A30P (Zhang et al., 2019). These results allow us to make connections about regulators of toxicity between αS and bS, and possibly identify other cellular factors that are known to modified αS' toxicity and study them on bS. I have a mystery to solve for both, by looking at why is yeast protective against these natural mutations, and figuring out fundamental pathways that play a role in conferring this protective property, so we can then study what happens in neurons.

g-Synuclein is nontoxic, even when swapped with a- and b- synuclein mutants

The following important finding is that aS and bS mutations when swapped into gS, do not make the latter one toxic. I hypothesized that the amino acids in which aS mutants A18T, A30P, E46K and bS V70M are would differentially matter for gS toxicity. My findings do not support my hypothesis. I report that all swap mutants in gS do not make it toxic and do not change localization phenotype. For all mutants the synucleins remained cytoplasmic diffuse across 24 hours, such as in the case of WT gS. This implicates the recipe to make gS is more complexed and different than for aS and bS. One explanation for gS resistance to toxicity comes from the sequence itself. aS and bS have an NAC domain that is commonly linked with aggregation, however, gS does not. In this domain specific amino acid residues participate in the polymerization of the protein toward aggregation forming b-sheets. Moreover, gS also has decreased affinity for phospholipid binding preventing its aggregation.

My aim was to investigate the potential of gS to become toxic, and thus I found that gS also gets post translationally modified. Coexistence of oxidized gS (at methionine 38th) and phosphorylated aS (at serine 129th) are reported in LBs in the amygdala and substantia nigra of DLB, PD, and AD patients (Surgucheva et al., 2014). These findings infer that PTM are also important for gS potential to become toxic and regulate propensity to aggregate. For this reason, I also investigated PTM sites in gS and bS from known sites at aS that regulate its toxicity.

Similarly, to the substitution, the bS, and aS swap mutants, all this work is novel, and thus, no external research exists to compare differences in gS toxicity or aggregation from any other mutations.

Post-translation sites mutants do not regulate bS toxicity and gS potential

My next finding is that bS and gS when mutated for conserved known post-translational sites of aS they are not differentially toxic. This finding does not support my hypothesis that was in the case of bS when blocking the PTM acetylation and SUMOylation, and mimicking nitration and phosphorylation it will increase toxicity, since the former two are environments known to play a protective role in aS toxicity, whereas the latter two to enhance it. Additionally, when blocking nitration and phosphorylation, I expected to see a decrease in bS toxicity. In the case of gS, I expected it to remain nontoxic with mutants that block nitration, while see toxicity when SUMOylation and acetylation were blocked, and nitration mimicked.

My results do not support this hypothesis since for both bS and gS, the mutants did not affect the toxicity, nor the localization of the proteins as compared to their WT form. I selected the sites for the mutants from the conserved sequences with aS, our understanding of its PTM, and research on these PTM on both bS and gS. Furthermore, some sites weren't conserved suggesting these amino acids do not regulate their toxicities, at least not when changing only one amino acid. Previous work in our lab identified that in some cases we need multiple modifications together to give toxicity and aggregation. Yoan Ganev (Thesis, 2019) did this work creating double mutants in aS for PTM, for example with inserting blocking acetylation and phosphorylation all together. He learned that these double modifications are important to drive aS toxicity, and thus, inspired me for future work to create double and triple mutants for PTM on bS and gS.

From the totality of this thesis, the data for PTM sites is the most preliminary data. And thus, before making further definitive conclusions more assays and repeats are needed.

High nitrative stress makes g-Synuclein and β-Synuclein mutants toxic

My final key findings are that high nitrative stress affects all synucleins toxicities, including making gS toxic. I believe that this thesis is the first report to find gS toxicity modulated by nitrative stress in any model. Within the dying neuron, the increasing ROS promotes degeneration by increasing the levels of nitration (Giasson et al., 2000; Hartmann, 2004). Moreover, many studies across model organisms including yeast report that high nitrative stress is involved in Lewy body pathogenesis by inducing aS oligomer formation (Hartmann, 2004). Based on this evidence, I hypothesized that nitrative stress would aggravate bS, bS-V70M, bS-P123H, and gS toxicity and localization. My findings with the help of Leslie Casares '26 support this hypothesis because I report that high nitrative stress, induced through knockout strain cox5aΔ, make WT bS, and the mutants more toxic, with the mutants being more susceptible to changes. Moreover, for the first time gS also showed toxicity. These toxicity patterns seen with the comparison between control strain and high nitrative stress was mitigated for all by a low nitrative stress environment.

These findings are consistent with previous work done in the lab by Tracey Nassuna's senior thesis '23, as well as by Chung et al. (2013) that reported an increase in synuclein toxicity and aggregation by cox5aΔ (high) while a decrease by cox5bΔ (low).

Limitations

Utilizing yeast as a model organism offers significant advantages in unraveling the complex processes of cells. Despite sharing similarities in protein folding and degradation mechanisms with humans, yeast's single-cell nature may restrict its ability to fully elucidate intercellular interactions present in multicellular organisms. This limitation becomes particularly apparent when attempting to understand neuron interactions and synaptic functions that are important for neurodegenerative diseases like PD. Consequently, the translational value of findings from yeast studies may be limited in addressing the complexities of human neurodegeneration, especially when looking at two well understudied proteins such as bS and gS.

In the context of PD, which predominantly affects neurons, yeast fails to replicate the neurodegeneration observed in humans, thereby limiting its suitability for studying disease progression comprehensively. Furthermore, behavioral symptoms characteristic of PD, such as bradykinesia, which is vital for diagnosis, cannot be mirrored in yeast. As a result, insights from yeast studies may not fully capture the behavioral manifestations crucial for understanding the disease in higher organisms.

Moreover, the methodologies employed in yeast studies may impose constraints due to time needed and resources. For this reason, I restricted

my thesis to three assays - GFP-fluorescence microscopy, serial dilution spotting, and Western blotting – which help me capture essential aspects of yeast's response to synucleins, in a limited capacity. However, the last two assays inherently possess qualitative attributes by the way they are conducted in this thesis, introducing subjectivity and hindering the precise quantification of growth rates or the impact of protein expression on toxicity.

Other current studies in the lab

In future studies, I aim to delve deeper into understanding the mechanisms underlying βS-V70M toxicity by conducting an extensive examination of hydrophobicity. Building upon ongoing work within the lab, I would like to generate additional mutants encompassing all hydrophobic amino acids to comprehensively assess their level of hydrophobicity on the impact on synuclein toxicity. Secondly, I would like to investigate the role of basic and polar amino acids in the βS-P123H mutant to elucidate their contribution to mutant toxicity. By systematically altering the degree of basic/polar amino acids within the mutant, I aim to uncover how variations in charge distribution affect synuclein toxicity and localization. Thirdly, I would like to explore the influence of other cellular environments, such as post-translational modifications like SUMOylation and lipid modification, on all synucleins toxicity. Leveraging insights from previous studies demonstrating the protective effects of SUMOylation and acetylation against αS toxicity, through investigating these environments it would elucidate if similar mechanisms apply to βS and its mutants. Lastly, I intend to continue studying mutants that were not obtained during the course of this thesis, including PT sites and two βS swaps. Additionally, I aim to create a mutant for oxidized gS at position M38, further expanding our understanding of synuclein pathology and its implications for neurodegenerative diseases.

By pursuing these future studies, I aim to deepen our understanding of synuclein biology and its role in neurodegeneration.

CONCLUSION

My thesis has provided insights into the characterization and pathological characteristics of bS, b-V70M, b-P123H, and gS through my assessments of substitution mutants in unmodified yeast, swap mutants for all, PTM site mutants, and altered nitrative stress. I found that hydrophobicity is important in V70M, basic and polar amino acids for P123H, and that aS mutations into bS express differential toxicities. Moreover, gS recipe to be toxic could start with high nitrative stress. Furthermore, I confirmed previous findings and I found that localization and toxicity are linked. Together, this thesis has contributed to a deeper understanding of the bS, b-V70M, b-P123H toxicity and what drives it (Figure 25).

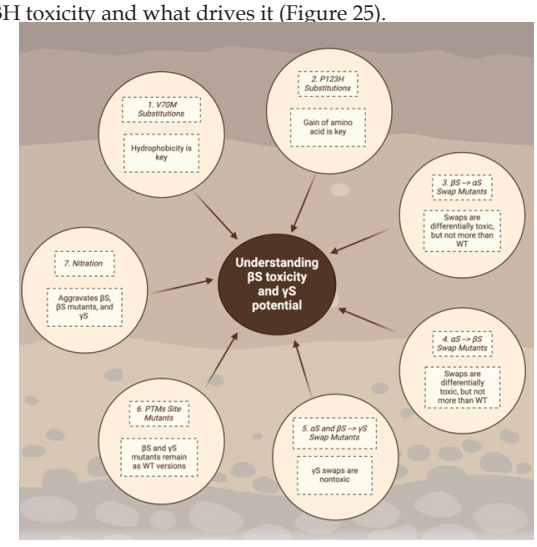

Figure 23: Summary of findings. My investigation yielded seven main findings; 1) Hydrophobicity is key for V70M, 2) Gain of amino acid is key for P123H toxicity and aggregation, 3) βS mutations swapped into αS are differentially toxic, but not more than WT αS 4) aS mutations swapped into bS are differentially toxic, 5) aS and βS mutations do not make gS toxic, 6) PTM sites do not affect βS ynuclein's toxicity and gS remains nontoxic, and 7) nitrative stress make gS toxic.

REFERENCES

Allendoerfer, K. L., Julie Su, L., & Lindquist, S. (2008). Chapter 38—Yeast Cells as a Discovery Platform for Parkinson's Disease and other Protein Misfolding Diseases. In R. Nass & S. Przedborski (Eds.), Parkinson's Disease (pp. 505–536). Academic Press. https://doi.org/10.1016/B978-0-12-374028-1.00038-5

Amberg, D. C., Burke, D. J., & Strathern, J. N. (2006). High-efficiency transformation of yeast. CSH protocols, 2006(1), pdb.prot4145. https://doi.org/10.1101/pdb.prot4145

Anderson, J. P., Walker, D. E., Goldstein, J. M., Laat, R. de, Banducci, K., Caccavello, R. J., Barbour, R., Huang, J., Kling, K., Lee, M., Diep, L., Keim, P. S., Shen, X., Chataway, T., Schlossmacher, M. G., Seubert, P., Schenk, D., Sinha, S., Gai, W. P., & Chilcote, T. J. (2006). Phosphorylation of Ser-129 Is the Dominant Pathological Modification of α-Synuclein in Familial and Sporadic Lewy Body Disease *. Journal of Biological Chemistry, 281(40), 29739–29752. https://doi.org/10.1074/jbc.M600933200

Appel-Cresswell, S., Vilarino-Guell, C., Encarnacion, M., Sherman, H., Yu, I., Shah, B., Weir, D., Thompson, C., Szu-Tu, C., Trinh, J., Aasly, J. O., Rajput, A., Rajput, A. H., Jon Stoessl, A., & Farrer, M. J. (2013). Alpha-Synuclein p.H50Q, a novel pathogenic mutation for Parkinson's disease. Movement Disorders: Official Journal of the Movement Disorder Society, 28(6), 811–813. https://doi.org/10.1002/mds.25421

Bell, R., Thrush, R. J., Castellana-Cruz, M., Oeller, M., Staats, R., Nene, A., Flagmeier, P., Xu, C. K., Satapathy, S., Galvagnion, C., Wilson, M. R., Dobson, C. M., Kumita, J. R., & Vendruscolo, M. (2022). N-Terminal Acetylation of α-Synuclein Slows down Its Aggregation Process and Alters the Morphology of the Resulting Aggregates. Biochemistry, 61(17), 1743–1756. https://doi.org/10.1021/acs.biochem.2c00104

Boyer, D. R., Li, B., Sun, C., Fan, W., Sawaya, M. R., Jiang, L., & Eisenberg, D. S. (2019). Structures of fibrils formed by α-Synuclein hereditary disease mutant H50Q reveal new polymorphs. Nature Structural & Molecular Biology, 26(11), 1044–1052. https://doi.org/10.1038/s41594-019-0322-y

Brandis, K. A., Holmes, I. F., England, S. J., Sharma, N., Kukreja, L., & Deb-Burman, S. K. (2006). α-Synuclein fission yeast model. Journal of Molecular Neuroscience, 28(2), 179–191. https://doi.org/10.1385/JMN:28:2:179

Breckenridge, C. B., Berry, C., Chang, E. T., Jr, R. L. S., & Mandel, J. S. (2016). Association between Parkinson's Disease and Cigarette Smoking, Rural Living, Well-Water Consumption, Farming and Pesticide Use: Systematic Review and Meta-Analysis. PLOS ONE, 11(4), e0151841. https://doi.org/10.1371/journal.pone.0151841

Brenz Verca, M. S., Bahi, A., Boyer, F., Wagner, G. C., & Dreyer, J.-L. (2003). Distribution of alpha- and gamma-Synucleins in the adult rat brain and their modification by high-dose cocaine treatment. The European Journal of Neuroscience, 18(7), 1923–1938. https://doi.org/10.1046/j.1460-9568.2003.02913.x

Brown, J. W. P., Buell, A. K., Michaels, T. C. T., Meisl, G., Carozza, J., Flagmeier, P., Vendruscolo, M., Knowles, T. P. J., Dobson, C. M., & Galvagnion, C. (2016). β-Synuclein suppresses both the initiation and amplification steps of α-Synuclein aggregation via competitive binding to surfaces. Scientific Reports, 6(1), Article 1. https://doi.org/10.1038/srep36010

Burai, R., Ait-Bouziad, N., Chiki, A., & Lashuel, H. A. (2015). Elucidating the Role of Site-Specific Nitration of α-Synuclein in the Pathogenesis

of Parkinson's Disease via Protein Semisynthesis and Mutagenesis. Journal of the American Chemical Society, 137(15), 5041–5052. https://doi.org/10.1021/ja5131726

Burré, J., Sharma, M., & Südhof, T. C. (2018). Cell Biology and Pathophysiology of α-Synuclein. Cold Spring Harbor Perspectives in Medicine, 8(3), a024091. https://doi.org/10.1101/cshperspect.a024091

Burré, J., Vivona, S., Diao, J., Sharma, M., Brunger, A. T., & Südhof, T. C. (2013). Properties of native brain α-Synuclein. Nature, 498(7453), Article 7453. https://doi.org/10.1038/nature12125

Callis, M., Jansen, S., Thiart, R., de Villiers, J. N., Raal, F. J., & Kotze, M. J. (1998). Mutation analysis in familial hypercholesterolemia patients of different ancestries: identification of three novel LDLR gene mutations. Molecular and cellular probes, 12(3), 149–152. https://doi.org/10.1006/mcpr.1998.0164

Catafau, A. M., & Tolosa, E. (2004). Impact of dopamine transporter SPECT using 123I-Ioflupane on diagnosis and management of patients with clinically uncertain parkinsonian syndromes. Movement Disorders, 19(10), 1175–1182. https://doi.org/10.1002/mds.20112

Chandra, S., Chen, X., Rizo, J., Jahn, R., & Südhof, T. C. (2003). A Broken α-Helix in Folded α-Synuclein *. Journal of Biological Chemistry, 278(17), 15313–15318. https://doi.org/10.1074/jbc.M213128200

Choi, W., Zibaee, S., Jakes, R., Serpell, L. C., Davletov, B., Anthony Crowther, R., & Goedert, M. (2004). Mutation E46K increases phospholipid binding and assembly into filaments of human α-Synuclein. FEBS Letters, 576(3), 363–368. https://doi.org/10.1016/j.febslet.2004.09.038

Connor-Robson, N., Peters, O. M., Millership, S., Ninkina, N., & Buchman, V. L. (2016). Combinational losses of synucleins reveal their differential requirements for compensating age-dependent alterations in motor behavior and dopamine metabolism. Neurobiology of Aging, 46, 107–112. https://doi.org/10.1016/j.neurobiolaging.2016.06.020

Cookson, M. R. (2009). α-Synuclein and neuronal cell death. Molecular Neurodegeneration, 4(1), 9. https://doi.org/10.1186/1750-1326-4-9

Corpas, F. J., Chaki, M., Leterrier, M., & Barroso, J. B. (2009). Protein tyrosine nitration: a new challenge in plants. Plant signaling & behavior, 4(10), 920–923. https://doi.org/10.4161/psb.4.10.9466

Danielson, S. R., & Andersen, J. K. (2008). Oxidative and Nitrative Protein Modifications in Parkinson's Disease. Free Radical Biology & Medicine, 44(10), 1787–1794. https://doi.org/10.1016/j.freeradbiomed.2008.03.005

de Oliveira, R. M., Vicente Miranda, H., Francelle, L., Pinho, R., Szegö, É. M., Martinho, R., Munari, F., Lázaro, D. F., Moniot, S., Guerreiro, P., Fonseca, L., Marijanovic, Z., Antas, P., Gerhardt, E., Enguita, F. J., Fauvet, B., Penque, D., Pais, T. F., Tong, Q., … Outeiro, T. F. (2017). The mechanism of sirtuin 2–mediated exacerbation of alpha-Synuclein toxicity in models of Parkinson disease. PLoS Biology, 15(3), e2000374. https://doi.org/10.1371/journal.pbio.2000374

Dettmer, U., Newman, A. J., von Saucken, V. E., Bartels, T., & Selkoe, D. (2015). KTKEGV repeat motifs are key mediators of normal α-Synuclein tetramerization: Their mutation causes excess monomers and neurotoxicity. Proceedings of the National Academy of Sciences, 112(31), 9596–9601. https://doi.org/10.1073/pnas.1505953112

Dickson, D. W. (2012). Parkinson's Disease and Parkinsonism: Neuropathology. Cold Spring Harbor Perspectives in Medicine, 2(8), a009258. https://doi.org/10.1101/cshperspect.a009258

Dikiy, I., & Eliezer, D. (2014). N-terminal Acetylation Stabilizes N-terminal Helicity in Lipid- and Micelle-bound α-Synuclein and Increases Its Affinity for Physiological Membranes *. Journal of Biological Chemistry, 289(6), 3652–3665. https://doi.org/10.1074/jbc.M113.512459

Dorsey, E. R., Sherer, T., Okun, M. S., & Bloem, B. R. (2018). The Emerging Evidence of the Parkinson Pandemic. Journal of Parkinson's Disease, 8(s1), S3–S8. https://doi.org/10.3233/JPD-181474

Eliezer, D., Kutluay, E., Bussell, R., & Browne, G. (2001). Conformational properties of α-Synuclein in its free and lipid-associated states11Edited by P. E. Wright. Journal of Molecular Biology, 307(4), 1061–1073. https://doi.org/10.1006/jmbi.2001.4538

Ellis, C. E., Schwartzberg, P. L., Grider, T. L., Fink, D. W., & Nussbaum, R. L. (2001). α-Synuclein Is Phosphorylated by Members of the Src Family of Protein-tyrosine Kinases *. Journal of Biological Chemistry, 276(6), 3879–3884. https://doi.org/10.1074/jbc.M010316200

Emamzadeh, F. N. (2016). Alpha-Synuclein structure, functions, and interactions. Journal of Research in Medical Sciences: The Official Journal of Isfahan University of Medical Sciences, 21, 29. https://doi.org/10.4103/1735-1995.181989

Fares, M. B., Ait-Bouziad, N., Dikiy, I., Mbefo, M. K., Jovičić, A., Kiely, A., Holton, J. L., Lee, S. J., Gitler, A. D., Eliezer, D., & Lashuel, H. A. (2014). The novel Parkinson's disease linked mutation G51D attenuates in vitro aggregation and membrane binding of α-Synuclein, and enhances its secretion and nuclear localization in cells. Human molecular genetics, 23(17), 4491–4509. https://doi.org/10.1093/hmg/ddu165

Fauvet, B., Mbefo, M. K., Fares, M.-B., Desobry, C., Michael, S., Ardah, M. T., Tsika, E., Coune, P., Prudent, M., Lion, N., Eliezer, D., Moore, D. J., Schneider, B., Aebischer, P., El-Agnaf, O. M., Masliah, E., & Lashuel, H. A. (2012). α-Synuclein in Central Nervous System and from Erythrocytes, Mammalian Cells, and Escherichia coli Exists Predominantly as Disordered Monomer *. Journal of Biological Chemistry, 287(19), 15345–15364. https://doi.org/10.1074/jbc.M111.318949

Fiske, M., Valtierra, S., Solvang, K., Zorniak, M., White, M., Herrera, S., Konnikova, A., Brezinsky, R., & Debburman, S. (2011). Contribution of Alanine-76 and Serine Phosphorylation in α-Synuclein Membrane Association and Aggregation in Yeasts. Parkinson's Disease, 2011, 392180. https://doi.org/10.4061/2011/392180

Flabeau, O., Meissner, W. G., & Tison, F. (2010). Multiple system atrophy: current and future approaches to management. Therapeutic advances in neurological disorders, 3(4), 249–263. https://doi.org/10.1177/1756285610375328

Fredenburg, R. A., Rospigliosi, C., Meray, R. K., Kessler, J. C., Lashuel, H. A., Eliezer, D., & Lansbury, P. T. (2007). The Impact of the E46K Mutation on the Properties of α-Synuclein in Its Monomeric and Oligomeric States. Biochemistry, 46(24), 7107–7118. https://doi.org/10.1021/bi7000246

Fujita, M., Sugama, S., Sekiyama, K., Sekigawa, A., Tsukui, T., Nakai, M., Waragai, M., Takenouchi, T., Takamatsu, Y., Wei, J., Rockenstein, E., LaSpada, A. R., Masliah, E., Inoue, S., & Hashimoto, M. (2010). A β-Synuclein mutation linked to dementia produces neurodegeneration when expressed in mouse brain. Nature Communications, 1(1), Article 1. https://doi.org/10.1038/ncomms1101

Fujiwara, H., Hasegawa, M., Dohmae, N., Kawashima, A., Masliah, E., Goldberg, M. S., Shen, J., Takio, K., & Iwatsubo, T. (2002). α-Synuclein is phosphorylated in synucleinopathy lesions. Nature Cell Biology, 4(2), Article 2. https://doi.org/10.1038/ncb748

Galvin, J. E., Schuck, T. M., Lee, V. M.-Y., & Trojanowski, J. Q. (2001). Differential Expression and Distribution of α-, β-, and γ-Synuclein in the Developing Human Substantia Nigra. Experimental Neurology, 168(2), 347–355. https://doi.org/10.1006/exnr.2000.7615

Galvin, J. E., Uryu, K., Lee, V. M., & Trojanowski, J. Q. (1999). Axon pathology in Parkinson's disease and Lewy body dementia hippocampus contains alpha-, beta-, and gamma-Synuclein. Proceedings of the National Academy of Sciences of the United States of America, 96(23), 13450–13455. https://doi.org/10.1073/pnas.96.23.13450

Ganev, Y. (2019). Combinatorial Impact of α-Synuclein Post-Translational

Modifications in Yeast. Senior thesis (Lake Forest, IL: Lake Forest College).

Giasson, B. I., Duda, J. E., Murray, I. V. J., Chen, Q., Souza, J. M., Hurtig, H. I., Ischiropoulos, H., Trojanowski, J. Q., & -Y. Lee, V. M. (2000). Oxidative Damage Linked to Neurodegeneration by Selective α-Synuclein Nitration in Synucleinopathy Lesions. Science, 290(5493), 985–989. https://doi.org/10.1126/science.290.5493.985

Giasson, B. I., Ischiropoulos, H., Lee, V. M.-Y., & Trojanowski, J. Q. (2002). The relationship between oxidative/nitrative stress and pathological inclusions in Alzheimer's and Parkinson's diseases1, 2 1 2. Free Radical Biology and Medicine, 32(12), 1264–1275. https://doi.org/10.1016/S0891-5849(02)00804-3

Goedert, M., Jakes, R., & Spillantini, M. G. (2017). The Synucleinopathies: Twenty Years On. Journal of Parkinson's Disease, 7(s1), S51–S69. https://doi.org/10.3233/JPD-179005

Goldberg, M. S., & Lansbury Jr, P. T. (2000). Is there a cause-and-effect relationship between α-Synuclein fibrillization and Parkinson's disease? Nature Cell Biology, 2(7), Article 7. https://doi.org/10.1038/35017124

Golebiewska, U., Zurawsky, C., & Scarlata, S. (2014). Defining the Oligomerization State of γ-Synuclein in Solution and in Cells. Biochemistry, 53(2), 293–299. https://doi.org/10.1021/bi401479a

Gómez-Tortosa, E., Newell, K., Irizarry, M. C., Albert, M., Growdon, J. H., & Hyman, B. T. (1999). Clinical and quantitative pathologic correlates of dementia with Lewy bodies. Neurology, 53(6), 1284–1291. https://doi.org/10.1212/wnl.53.6.1284

Gorell, J. M., Johnson, C. C., Rybicki, B. A., Peterson, E. L., Kortsha, G. X., Brown, G. G., & Richardson, R. J. (1997). Occupational exposures to metals as risk factors for Parkinson's disease. Neurology, 48(3), 650–658. https://doi.org/10.1212/WNL.48.3.650

Grassel, A. (2023). Assessment Of Three New α-Synuclein Mutants in Various Parkinson's Disease Environments in A Yeast Model. Senior thesis (Lake Forest, IL: Lake Forest College).

Greenbaum, E. A., Graves, C. L., Mishizen-Eberz, A. J., Lupoli, M. A., Lynch, D. R., Englander, S. W., Axelsen, P. H., & Giasson, B. I. (2005). The E46K Mutation in α-Synuclein Increases Amyloid Fibril Formation *. Journal of Biological Chemistry, 280(9), 7800–7807. https://doi.org/10.1074/jbc.M411638200

Guan, Y., Zhao, X., Liu, F., Yan, S., Wang, Y., Du, C., Cui, X., Li, R., & Zhang, C. X. (2020). Pathogenic Mutations Differentially Regulate Cell-to-Cell Transmission of α-Synuclein. Frontiers in Cellular Neuroscience, 14. https://www.frontiersin.org/articles/10.3389/fncel.2020.00159

Hagihara, H., Fujita, M., Umemori, J., Hashimoto, M., & Miyakawa, T. (2018). Immature-like molecular expression patterns in the hippocampus of a mouse model of dementia with Lewy body-linked mutant β-Synuclein. Molecular Brain, 11(1), 38. https://doi.org/10.1186/s13041-018-0378-3

Hartmann, A. (2004). Postmortem studies in Parkinson's disease. Dialogues Clin. Neurosci. 6, 281-293.

Hassanzadeh, K., Morrone, C., Akhtari, K., Gerhardt, E., Zaccagnini, L., Outeiro, T. F., & Feligioni, M. (2023). Non-SUMOylated alternative spliced isoforms of alpha-Synuclein are more aggregation-prone and toxic. Mechanisms of Ageing and Development, 209, 111759. https://doi.org/10.1016/j.mad.2022.111759

Hayashi, J., & Carver, J. A. (2022a). β-Synuclein: An Enigmatic Protein with Diverse Functionality. Biomolecules, 12(1), 142. https://doi.org/10.3390/biom12010142

Hayashi, J., & Carver, J. A. (2022b). β-Synuclein: An Enigmatic Protein with Diverse Functionality. Biomolecules, 12(1), 142. https://doi.org/10.3390/biom12010142

Hoffman-Zacharska, D., Koziorowski, D., Ross, O. A., Milewski, M., Poznanski, J. A., Jurek, M., Wszolek, Z. K., Soto-Ortolaza, A., Awek, J. A. S., Janik, P., Jamrozik, Z., Potulska-Chromik, A., Jasinska-Myga, B., Opala, G., Krygowska-Wajs, A., Czyzewski, K., Dickson, D. W., Bal, J., & Friedman, A. (2013). Novel A18T and pA29S substitutions in α-Synuclein may be associated with sporadic Parkinson's disease. Parkinsonism & Related Disorders, 19(11), 1057–1060. https://doi.org/10.1016/j.parkreldis.2013.07.011

Hua, H., Xu, L., Wang, J., Jing, J., Luo, T., & Jiang, Y. (2009). Up-regulation of gamma-Synuclein contributes to cancer cell survival under endoplasmic reticulum stress. The Journal of Pathology, 217(4), 507–515. https://doi.org/10.1002/path.2465

Inaba, S., Li, C., Shi, Y. E., Song, D.-Q., Jiang, J.-D., & Liu, J. (2005). Synuclein Gamma Inhibits the Mitotic Checkpoint Function and Promotes Chromosomal Instability of Breast Cancer Cells. Breast Cancer Research and Treatment, 94(1), 25–35. https://doi.org/10.1007/s10549-005-6938-0

Inzelberg, R., Schecthman, E., Paleacu, D., Zach, L., Bonwitt, R., Carasso, R.L. and Nisipeanu, P. (2004), Onset and progression of disease in familial and sporadic Parkinson's disease. Am. J. Med. Genet., 124A, 255-258.

Jakes, R., Spillantini, M. G., & Goedert, M. (1994). Identification of two distinct synucleins from human brain. FEBS Letters, 345(1), 27–32. https://doi.org/10.1016/0014-5793(94)00395-5

Janowska, M. K., & Baum, J. (2016). The loss of inhibitory C-terminal conformations in disease associated P123H β-Synuclein. Protein Science: A Publication of the Protein Society, 25(1), 286–294. https://doi.org/10.1002/pro.2798

Janowska, M. K., & Baum, J. (2016). The loss of inhibitory C-terminal conformations in disease associated P123H β-Synuclein. Protein Science, 25(1), 286–294. https://doi.org/10.1002/pro.2798

Jarrett J. T. (2015). The biosynthesis of thiol- and thioether-containing cofactors and secondary metabolites catalyzed by radical S-adenosylmethionine enzymes. The Journal of biological chemistry, 290(7), 3972–3979. https://doi.org/10.1074/jbc.R114.599308

Jellinger, K. A., Seppi, K., & Wenning, G. K. (2005). Grading of neuropathology in multiple system atrophy: proposal for a novel scale. Movement disorders : official journal of the Movement Disorder Society, 20 Suppl 12, S29–S36. https://doi.org/10.1002/mds.20537

Jensen, P. H., Nielsen, M. S., Jakes, R., Dotti, C. G., & Goedert, M. (1998). Binding of alpha-Synuclein to brain vesicles is abolished by familial Parkinson's disease mutation. The Journal of Biological Chemistry, 273(41), 26292–26294. https://doi.org/10.1074/jbc.273.41.26292

Jiang, A., Handley, R. R., Lehnert, K., & Snell, R. G. (2023). From Pathogenesis to Therapeutics: A Review of 150 Years of Huntington's Disease Research. International journal of molecular sciences, 24(16), 13021. https://doi.org/10.3390/ijms241613021

Jo, E., Fuller, N., Rand, R. P., St George-Hyslop, P., & Fraser, P. E. (2002). Defective membrane interactions of familial Parkinson's disease mutant A30P α-Synuclein11Edited by I. B. Holland. Journal of Molecular Biology, 315(4), 799–807. https://doi.org/10.1006/jmbi.2001.5269

Jo, S., Kim, Y.-J., Park, K. W., Hwang, Y. S., Lee, S. H., Kim, B. J., & Chung, S. J. (2021). Association of NO2 and Other Air Pollution Exposures With the Risk of Parkinson Disease. JAMA Neurology, 78(7), 800–808. https://doi.org/10.1001/jamaneurol.2021.1335

Kasten, M., & Klein, C. (2013). The many faces of alpha-Synuclein mutations. Movement Disorders, 28(6), 697–701. https://doi.org/10.1002/mds.25499

Koga, S., Sekiya, H., Kondru, N., Ross, O. A., & Dickson, D. W. (2021). Neuropathology and molecular diagnosis of Synucleinopathies. Molecular Neurodegeneration, 16(1), 83. https://doi.org/10.1186/s13024-021-00501-z

Konovalova, E. V., Lopacheva, O. M., Grivennikov, I. A., Lebedeva, O. S., Dashinimaev, E. B., Khaspekov, L. G., Fedotova, E. Yu., & Illarioshkin, S. N. (2015). Mutations in the Parkinson's Disease-Associated PARK2 Gene Are Accompanied by Imbalance in Programmed Cell Death Systems. Acta Naturae, 7(4), 146–149.

Konovalova, E. V., Lopacheva, O. M., Grivennikov, I. A., Lebedeva, O. S., Dashinimaev, E. B., Khaspekov, L. G., Fedotova, E. Yu., & Illarioshkin, S. N. (2015). Mutations in the Parkinson's Disease-Associated PARK2 Gene Are Accompanied by Imbalance in Programmed Cell Death Systems. Acta Naturae, 7(4), 146–149.

Krumova, P., Meulmeester, E., Garrido, M., Tirard, M., Hsiao, H.-H., Bossis, G., Urlaub, H., Zweckstetter, M., Kügler, S., Melchior, F., Bähr, M., & Weishaupt, J. H. (2011). SUMOylation inhibits alpha-Synuclein aggregation and toxicity. The Journal of Cell Biology, 194(1), 49–60. https://doi.org/10.1083/jcb.201010117

Lavedan, C. (1998). The synuclein family. Genome Research, 8(9), 871–880. https://doi.org/10.1101/gr.8.9.871

Leitao, A., Bhumkar, A., Hunter, D. J. B., Gambin, Y., & Sierecki, E. (2018). Unveiling a Selective Mechanism for the Inhibition of α-Synuclein Aggregation by β-Synuclein. International Journal of Molecular Sciences, 19(2), Article 2. https://doi.org/10.3390/ijms19020334

Lesage, S., Anheim, M., Letournel, F., Bousset, L., Honoré, A., Rozas, N., Pieri, L., Madiona, K., Dürr, A., Melki, R., Verny, C., Brice, A., & French Parkinson's Disease Genetics Study Group. (2013). G51D α-Synuclein mutation causes a novel parkinsonian-pyramidal syndrome. Annals of Neurology, 73(4), 459–471. https://doi.org/10.1002/ana.23894

Leslie, M. Yeast can live with human genes. (2015). Retrieved October 15, 2023, from https://www.science.org/content/article/yeast-can-live-human-genes

Li, J.-Y., Henning Jensen, P., & Dahlström, A. (2002). Differential localization of alpha-, beta- and gamma-Synucleins in the rat CNS. Neuroscience, 113(2), 463–478. https://doi.org/10.1016/s0306-4522(02)00143-4

Liu G, Zhang C, Yin J, Li X, Cheng F, Li Y, Yang H, Uéda K, Chan P, Yu S 2009. α-Synuclein is differentially expressed in mitochondria from different rat brain regions and dose-dependently down-regulates complex I activity. Neurosci Lett 454: 187–192

Maltsev, A. S., Ying, J., & Bax, A. (2012). Impact of N-Terminal Acetylation of α-Synuclein on Its Random Coil and Lipid Binding Properties. Biochemistry, 51(25), 5004–5013. https://doi.org/10.1021/bi300642h

Martinez, J. L., & Baquero, F. (2000). Mutation frequencies and antibiotic resistance. Antimicrobial agents and chemotherapy, 44(7), 1771–1777. https://doi.org/10.1128/AAC.44.7.1771-1777.2000

McLean, P. J., Kawamata, H., Ribich, S., & Hyman, B. T. (2000). Membrane association and protein conformation of alpha-Synuclein in intact neurons. Effect of Parkinson's disease-linked mutations. The Journal of Biological Chemistry, 275(12), 8812–8816. https://doi.org/10.1074/jbc.275.12.8812

Nakamura K, Nemani VM, Wallender EK, Kaehlcke K, Ott M, Edwards RH 2008. Optical reporters for the conformation of alpha-Synuclein reveal a specific interaction with mitochondria. J Neurosci 28: 12305–12317

Nakamura, T., Yamashita, H., Takahashi, T., & Nakamura, S. (2001). Activated Fyn Phosphorylates α-Synuclein at Tyrosine Residue 125. Biochemical and Biophysical Research Communications, 280(4), 1085–1092. https://doi.org/10.1006/bbrc.2000.4253

Nalls, M. A., Pankratz, N., Lill, C. M., Do, C. B., Hernandez, D. G., Saad, M., DeStefano, A. L., Kara, E., Bras, J., Sharma, M., Schulte, C., Keller, M. F., Arepalli, S., Letson, C., Edsall, C., Stefansson, H., Liu, X., Pliner, H., Lee, J. H., … Singleton, A. B. (2014). Large-scale meta-analysis of genome-wide association data identifies six new risk loci for Parkinson's disease. Nature Genetics, 46(9), Article 9. https://doi.org/10.1038/ng.3043

Nassuna, T. (2023). Evaluation of β-Synuclein Toxicity in a Yeast Model. Senior thesis (Lake Forest, IL: Lake Forest College).

Neitz, J., & Neitz, M. (2011). The genetics of normal and defective color vision. Vision research, 51(7), 633–651. https://doi.org/10.1016/j.visres.2010.12.002

Nelson, D.L. and Cox, M.M. (2017) Lehninger Principles of Biochemistry. 7th Edition, W.H. Freeman, New York, 1328. - References - Scientific Research Publishing.

Ninkina, N., Millership, S. J., Peters, O. M., Connor-Robson, N., Chaprov, K., Kopylov, A. T., Montoya, A., Kramer, H., Withers, D. J., & Buchman, V. L. (2021). β-Synuclein potentiates synaptic vesicle dopamine uptake and rescues dopaminergic neurons from MPTP-induced death in the absence of other synucleins. Journal of Biological Chemistry, 297(6). https://doi.org/10.1016/j.jbc.2021.101375

Nonaka, T., Iwatsubo, T., & Hasegawa, M. (2005). Ubiquitination of α-Synuclein. Biochemistry, 44(1), 361–368. https://doi.org/10.1021/bi0485528

Ohtake, H., Limprasert, P., Fan, Y., Onodera, O., Kakita, A., Takahashi, H., Bonner, L. T., Tsuang, D. W., Murray, I. V. J., Lee, V. M.-Y., Trojanowski, J. Q., Ishikawa, A., Idezuka, J., Murata, M., Toda, T., Bird, T. D., Leverenz, J. B., Tsuji, S., & La Spada, A. R. (2004). β-Synuclein gene alterations in dementia with Lewy bodies. Neurology, 63(5), 805–811.

Okochi, M., Walter, J., Koyama, A., Nakajo, S., Baba, M., Iwatsubo, T., Meijer, L., Kahle, P. J., & Haass, C. (2000). Constitutive Phosphorylation of the Parkinson's Disease Associated α-Synuclein *. Journal of Biological Chemistry, 275(1), 390–397. https://doi.org/10.1074/jbc.275.1.390

Ong, E. (2017). Understanding the nature of toxicity of Parkinson's disease associated α-Synuclein familial mutants (H50Q, G51D, A53E) with yeast models. Senior thesis (Lake Forest, IL: Lake Forest College).

Osselborn, R. (2023). Comparative Evaluation of □-, β-, and □-Synuclein Toxicity Potential in Yeast. Senior project (Lake Forest, IL: Lake Forest College).

Ostrander E. A. (2023). Central dogma. Genome.gov. https://www.genome.gov/genetics-glossary/Central-Dogma

Outeiro, T. F., & Lindquist, S. (2003). Yeast cells provide insight into alpha-Synuclein biology and pathobiology. Science (New York, N.Y.), 302(5651), 1772–1775. https://doi.org/10.1126/science.1090439

Padmaraju, V., Bhaskar, J. J., Prasada Rao, U. J. S., Salimath, P. V., & Rao, K. S. (2011). Role of Advanced Glycation on Aggregation and DNA Binding Properties of α-Synuclein. Journal of Alzheimer's Disease, 24(s2), 211–221. https://doi.org/10.3233/JAD-2011-101965

Pan, Z.-Z., Bruening, W., Giasson, B. I., Lee, V. M.-Y., & Godwin, A. K. (2002). γ-Synuclein Promotes Cancer Cell Survival and Inhibits Stress- and Chemotherapy Drug-induced Apoptosis by Modulating MAPK Pathways *. Journal of Biological Chemistry, 277(38), 35050–35060. https://doi.org/10.1074/jbc.M201650200

Papapetropoulos, T., Johnson, W. G., Lazzarini, A. M., Duvoisin, R. C., Di Iorio, G., Golbe, L. I., & Nussbaum, R. L. (1997). Mutation in the α-Synuclein Gene Identified in Families with Parkinson's Disease. Science, 276(5321), 2045–2047. https://doi.org/10.1126/science.276.5321.2045

Pasanen, P., Myllykangas, L., Siitonen, M., Raunio, A., Kaakkola, S., Lyytinen, J., Tienari, P. J., Pöyhönen, M., & Paetau, A. (2014). Novel α-Synuclein mutation A53E associated with atypical multiple system atrophy and Parkinson's disease-type pathology. Neurobiology of Aging, 35(9), 2180.e1-5. https://doi.org/10.1016/j.neurobiolaging.2014.03.024

Peters, O. M., Millership, S., Shelkovnikova, T. A., Soto, I., Keeling, L., Hann, A., Marsh-Armstrong, N., Buchman, V. L., & Ninkina, N. (2012).

Selective pattern of motor system damage in gamma-Synuclein transgenic mice mirrors the respective pathology in amyotrophic lateral sclerosis. Neurobiology of Disease, 48(1), 124–131. https://doi.org/10.1016/j.nbd.2012.06.016

Polymeropoulos, M. H., Lavedan, C., Leroy, E., Ide, S. E., Dehejia, A., Dutra, A., Pike, B., Root, H., Rubenstein, J., Boyer, R., Stenroos, E. S., Chandrasekharappa, S., Athanassiadou, A.,

Pouchieu, C., Piel, C., Carles, C., Gruber, A., Helmer, C., Tual, S., Marcotullio, E., Lebailly, P., & Baldi, I. (2018). Pesticide use in agriculture and Parkinson's disease in the AGRICAN cohort study. International Journal of Epidemiology, 47(1), 299–310. https://doi.org/10.1093/ije/dyx225

Racette, B. A., Nielsen, S. S., Criswell, S. R., Sheppard, L., Seixas, N., Warden, M. N., & Checkoway, H. (2017). Dose-dependent progression of parkinsonism in manganese-exposed welders. Neurology, 88(4), 344–351. https://doi.org/10.1212/WNL.0000000000003533

Rajmohan, V., & Mohandas, E. (2007). The limbic system. Indian journal of psychiatry, 49(2), 132–139. https://doi.org/10.4103/0019-5545.33264

Ramazi, S., & Zahiri, J. (2021). Post-translational modifications in proteins: Resources, tools and prediction methods. Database: The Journal of Biological Databases and Curation, 2021, baab012. https://doi.org/10.1093/database/baab012

Ritz, B., Lee, P.-C., Hansen, J., Lassen, C. F., Ketzel, M., S, ørensen M., & Raaschou, -Nielsen Ole. (2016). Traffic-Related Air Pollution and Parkinson's Disease in Denmark: A Case–Control Study. Environmental Health Perspectives, 124(3), 351–356. https://doi.org/10.1289/ehp.1409313

Samuel, D., Kumar, T. K., Ganesh, G., Jayaraman, G., Yang, P. W., Chang, M. M., Trivedi, V. D., Wang, S. L., Hwang, K. C., Chang, D. K., & Yu, C. (2000). Proline inhibits aggregation during protein refolding. Protein science : a publication of the Protein Society, 9(2), 344–352. https://doi.org/10.1110/ps.9.2.344

Sano, K., Iwasaki, Y., Yamashita, Y., Irie, K., Hosokawa, M., Satoh, K., & Mishima, K. (2021). Tyrosine 136 phosphorylation of α-synuclein aggregates in the Lewy body dementia brain: Involvement of serine 129 phosphorylation by casein kinase 2. Acta Neuropathologica Communications, 9(1), 182. https://doi.org/10.1186/s40478-021-01281-9

Selkoe D.J., & Lansbury P.J. Jr. (1999). Basic Neurochemistry: Molecular, Cellular and Medical Aspects. (6th edition). Philadelphia: Lippincott-Raven. https://www.ncbi.nlm.nih.gov/books/NBK27944/

Sevcsik, E., Trexler, A. J., Dunn, J. M., & Rhoades, E. (2011). Allostery in a Disordered Protein: Oxidative Modifications to α-Synuclein Act Distally To Regulate Membrane Binding. Journal of the American Chemical Society, 133(18), 7152–7158. https://doi.org/10.1021/ja2009554

Sharma, K., Mehra, S., Sawner, A. S., Markam, P. S., Panigrahi, R., Navalkar, A., Chatterjee, D., Kumar, R., Kadu, P., Patel, K., Ray, S., Kumar, A., & Maji, S. K. (2020). Effect of Disease-Associated P123H and V70M Mutations on β-Synuclein Fibrillation. ACS Chemical Neuroscience, 11(18), 2836–2848. https://doi.org/10.1021/acschemneuro.0c00405

Sharma, M., & Burré, J. (2023). α-Synuclein in synaptic function and dysfunction. Trends in Neurosciences, 46(2), 153–166. https://doi.org/10.1016/j.tins.2022.11.007

Sharma, N., Brandis, K. A., Herrera, S. K., Johnson, B. E., Vaidya, T., Shrestha, R., & DebBurman, S. K. (2006). alpha-Synuclein budding yeast model: Toxicity enhanced by impaired proteasome and oxidative stress. Journal of Molecular Neuroscience: MN, 28(2), 161–178. https://doi.org/10.1385/JMN:28:2:161

Sharma, N., Brandis, K. A., Herrera, S. K., Johnson, B. E., Vaidya, T., Shrestha, R., & Debburman, S. K. (2006). alpha-Synuclein budding yeast model: toxicity enhanced by impaired proteasome and oxidative stress. Journal of Molecular Neuroscience. 28(2), 161–178.

Sharon, R., Goldberg, M. S., Bar-Josef, I., Betensky, R. A., Shen, J., & Selkoe, D. J. (2001). α-Synuclein occurs in lipid-rich high molecular weight complexes, binds fatty acids, and shows homology to the fatty acid-binding proteins. Proceedings of the National Academy of Sciences, 98(16), 9110–9115. https://doi.org/10.1073/pnas.171300598

Sidransky, E., & Lopez, G. (2012). The link between the GBA gene and parkinsonism. The Lancet. Neurology, 11(11), 986–998. https://doi.org/10.1016/S1474-4422(12)70190-4

Sonne, J., Reddy, V., & Beato, M. R. (2023). Neuroanatomy, Substantia Nigra. In StatPearls. StatPearls Publishing. http://www.ncbi.nlm.nih.gov/books/NBK536995/

Statistics | Parkinson's Disease. (n.d.). Parkinson's Foundation. Retrieved October 3, 2023, from https://www.parkinson.org/understanding-parkinsons/statistics

Steinberg M. H. (1998). Pathophysiology of sickle cell disease. Bailliere's clinical haematology, 11(1), 163–184. https://doi.org/10.1016/s0950-3536(98)80074-7

Stokkermans T. J., & Lui F. (2023). Heterochromia. National Library of Medicine. https://www.ncbi.nlm.nih.gov/books/NBK574499/

Stykel, M. G., & Ryan, S. D. (2022). Nitrosative stress in Parkinson's disease. NPJ Parkinson's Disease, 8, 104. https://doi.org/10.1038/s41531-022-00370-3

Surguchev, A. A., & Surguchov, A. (2017). Synucleins and Gene Expression: Ramblers in a Crowd or Cops Regulating Traffic? Frontiers in Molecular Neuroscience, 10. https://www.frontiersin.org/articles/10.3389/fnmol.2017.00224

Surgucheva, I., Newell, K. L., Burns, J., & Surguchov, A. (2014). New α- and γ-Synuclein immunopathological lesions in human brain. Acta Neuropathologica Communications, 2(1), 132. https://doi.org/10.1186/s40478-014-0132-8

Surgucheva, I., Newell, K. L., Burns, J., & Surguchov, A. (2014). New α- and γ-Synuclein immunopathological lesions in human brain. Acta Neuropathologica Communications, 2(1), 132. https://doi.org/10.1186/s40478-014-0132-8

Surgucheva, I., Sharov, V. S., & Surguchov, A. (2012). γ-Synuclein: Seeding of α-Synuclein aggregation and transmission between cells. Biochemistry, 51(23), 4743–4754. https://doi.org/10.1021/bi300478w

Syme, C. D., Blanch, E. W., Holt, C., Jakes, R., Goedert, M., Hecht, L., & Barron, L. D. (2002). A Raman optical activity study of rheomorphism in caseins, synucleins and tau. European Journal of Biochemistry, 269(1), 148–156. https://doi.org/10.1046/j.0014-2956.2001.02633.x

Tangamornsuksan, W., Lohitnavy, O., Sruamsiri, R., Chaiyakunapruk, N., Norman Scholfield, C., Reisfeld, B., & Lohitnavy, M. (2019). Paraquat exposure and Parkinson's disease: A systematic review and meta-analysis. Archives of Environmental & Occupational Health, 74(5), 225–238. https://doi.org/10.1080/19338244.2018.1492894

Tenreiro, S., Rosado-Ramos, R., Gerhardt, E., Favretto, F., Magalhães, F., Popova, B., Becker, S., Zweckstetter, M., Braus, G. H., & Outeiro, T. F. (2016). Yeast reveals similar molecular mechanisms underlying alpha- and beta-Synuclein toxicity. Human Molecular Genetics, 25(2), 275–290. https://doi.org/10.1093/hmg/ddv470

Tuttle, M. D., Comellas, G., Nieuwkoop, A. J., Covell, D. J., Berthold, D. A., Kloepper, K. D., Courtney, J. M., Kim, J. K., Barclay, A. M., Kendall, A., Wan, W., Stubbs, G., Schwieters, C. D., Lee, V. M. Y., George, J. M., & Rienstra, C. M. (2016). Solid-State NMR Structure of a Pathogenic Fibril of Full-Length Human α-Synuclein. Nature Structural & Molecular Biology, 23(5), 409–415. https://doi.org/10.1038/nsmb.3194

Ulmer, T. S., Bax, A., Cole, N. B., & Nussbaum, R. L. (2005). Structure and Dynamics of Micelle-bound Human α-Synuclein *. Journal of Biological Chemistry, 280(10), 9595–9603. https://doi.org/10.1074/jbc.M411805200

Uversky, V. N., Li, J., Souillac, P., Millett, I. S., Doniach, S., Jakes, R., Goedert, M., & Fink, A. L. (2002). Biophysical Properties of the Synucleins and Their Propensities to Fibrillate: INHIBITION OF α-SYNUCLEIN ASSEMBLY BY β- AND γ-SYNUCLEINS *. Journal of Biological Chemistry, 277(14), 11970–11978. https://doi.org/10.1074/jbc.M109541200

Van de Vondel, E., Baatsen, P., Van Elzen, R., Lambeir, A.-M., Keiderling, T. A., Herrebout, W. A., & Johannessen, C. (2018). Vibrational Circular Dichroism Sheds New Light on the Competitive Effects of Crowding and β-Synuclein on the Fibrillation Process of α-Synuclein. Biochemistry, 57(41), 5989–5995. https://doi.org/10.1021/acs.biochem.8b00780

Vargas, K. J., & Chandra, S. S. (2014). Synucleins. In Reference Module in Biomedical Sciences. Elsevier. https://doi.org/10.1016/B978-0-12-801238-3.04785-1

Varkey, J., Isas, J. M., Mizuno, N., Jensen, M. B., Bhatia, V. K., Jao, C. C., Petrlova, J., Voss, J. C., Stamou, D. G., Steven, A. C., & Langen, R. (2010). Membrane Curvature Induction and Tubulation Are Common Features of Synucleins and Apolipoproteins *. Journal of Biological Chemistry, 285(42), 32486–32493. https://doi.org/10.1074/jbc.M110.139576

Wang, W., Perovic, I., Chittuluru, J., Kaganovich, A., Nguyen, L. T. T., Liao, J., Auclair, J. R., Johnson, D., Landeru, A., Simorellis, A. K., Ju, S., Cookson, M. R., Asturias, F. J., Agar, J. N., Webb, B. N., Kang, C., Ringe, D., Petsko, G. A., Pochapsky, T. C., & Hoang, Q. Q. (2011). A soluble α-Synuclein construct forms a dynamic tetramer. Proceedings of the National Academy of Sciences, 108(43), 17797–17802. https://doi.org/10.1073/pnas.1113260108

Wei, J., Fujita, M., Nakai, M., Waragai, M., Watabe, K., Akatsu, H., Rockenstein, E., Masliah, E., & Hashimoto, M. (2007). Enhanced lysosomal pathology caused by beta-Synuclein mutants linked to dementia with Lewy bodies. The Journal of Biological Chemistry, 282(39), 28904–28914. https://doi.org/10.1074/jbc.M703711200

Westphal, C. H., & Chandra, S. S. (2013). Monomeric Synucleins Generate Membrane Curvature *. Journal of Biological Chemistry, 288(3), 1829–1840. https://doi.org/10.1074/jbc.M112.418871

What Is Lewy Body Dementia? Causes, Symptoms, and Treatments. (2021). National Institute on Aging. Retrieved October 3, 2023, from https://www.nia.nih.gov/health/what-lewy-body-dementia-causes-symptoms-and-treatments

Whittaker, H. T., Qui, Y., Bettencourt, C., & Houlden, H. (2017). Multiple system atrophy: Genetic risks and alpha-Synuclein mutations (6:2072). F1000Research. https://doi.org/10.12688/f1000research.12193.1

Wilson, D. M., Cookson, M. R., Van Den Bosch, L., Zetterberg, H., Holtzman, D. M., & Dewachter, I. (2023). Hallmarks of neurodegenerative diseases. Cell, 186(4), 693–714. https://doi.org/10.1016/j.cell.2022.12.032

Wu, Y., Le, W., & Jankovic, J. (2011). Preclinical Biomarkers of Parkinson Disease. Archives of Neurology, 68(1), 22–30. https://doi.org/10.1001/archneurol.2010.321

Zhang, X. M., Anwar, S., Kim, Y., Brown, J., Comte, I., Cai, H., Cai, N. N., Wade-Martins, R., & Szele, F. G. (2019). The A30P α-Synuclein mutation decreases subventricular zone proliferation. Human molecular genetics, 28(14), 2283–2294. https://doi.org/10.1093/hmg/ddz057